REPAIR, EVALUATION, MAINTENANCE, AND REHABILITATION RESEARCH PROGRAM

TECHNICAL REPORT REM-CS-10

DEVELOPMENT OF NONDESTRUCTIVE TESTING SYSTEMS FOR IN SITU EVALUATION OF CONCRETE STRUCTURES

by

Henry T. Thornton, Jr., A. Michel Alexander

Structures Laboratory

DEPARTMENT OF THE ARMY
Waterways Experiment Station, Corps of Engineers
PO Box 631, Vicksburg, Mississippi 39180-0631

December 1987
Final Report

Approved For Public Release; Distribution Unlimited

Prepared for DEPARTMENT OF THE ARMY
US Army Corps of Engineers
Washington, DC 20314-1000

and

DEPARTMENT OF THE INTERIOR
US Bureau of Reclamation
Denver, Colorado 80225

Under Civil Works Research Work Unit 31753

The following two letters used as part of the number designating technical reports of research published under the Repair, Evaluation, Maintenance, and Rehabilitation (REMR) Research Program identify the problem area under which the report was prepared:

	Problem Area		Problem Area
CS	Concrete and Steel Structures	EM	Electrical and Mechanical
GT	Geotechnical	EI	Environmental Impacts
HY	Hydraulics	OM	Operations Management
CO	Coastal		

Destroy this report when no longer needed. Do not return it to the originator.

The findings in this report are not to be construed as an official Department of the Army position unless so designated by other authorized documents.

The contents of this report are not to be used for advertising, publication, or promotional purposes. Citation of trade names does not constitute an official endorsement or approval of the use of such commercial products.

COVER PHOTOS:

TOP — Typical ultrasonic pulse-echo system setup and signal when measuring the thickness of a concrete pavement or floor slab.

BOTTOM — Illustration of acoustic underwater mapping and profiling system operating in a lock chamber.

Unclassified
SECURITY CLASSIFICATION OF THIS PAGE

REPORT DOCUMENTATION PAGE

Form Approved
OMB No 0704-0188
Exp Date Jun 30, 1986

1a REPORT SECURITY CLASSIFICATION
Unclassified

1b RESTRICTIVE MARKINGS

2a SECURITY CLASSIFICATION AUTHORITY

3. DISTRIBUTION/AVAILABILITY OF REPORT
Approved for public release; distribution unlimited

2b. DECLASSIFICATION/DOWNGRADING SCHEDULE

4. PERFORMING ORGANIZATION REPORT NUMBER(S)
Technical Report REMR-CS-10

5. MONITORING ORGANIZATION REPORT NUMBER(S)

6a. NAME OF PERFORMING ORGANIZATION
USAEWES
Structures Laboratory

6b. OFFICE SYMBOL (If applicable)

7a. NAME OF MONITORING ORGANIZATION

6c. ADDRESS (City, State, and ZIP Code)
PO Box 631
Vicksburg, MS 39180-0631

7b. ADDRESS (City, State, and ZIP Code)

8a. NAME OF FUNDING/SPONSORING ORGANIZATION
Department of the Army
US Army Corps of Engineers
Washington, DC 20314-1000
and Department of the Interior
US Bureau of Reclamation
Denver, CO 80225

9. PROCUREMENT INSTRUMENT IDENTIFICATION NUMBER

10. SOURCE OF FUNDING NUMBERS

PROGRAM ELEMENT NO.	PROJECT NO.	TASK NO.	WORK UNIT ACCESSION NO
			CWIS 31753

11. TITLE (Include Security Classification)
Development of Nondestructive Testing Systems for In Situ Evaluation of Concrete Structures

12. PERSONAL AUTHOR(S)
Thornton, Henry T., Jr., and Alexander, A. Michel

13a. TYPE OF REPORT	13b. TIME COVERED	14. DATE OF REPORT (Year, Month, Day)	15. PAGE COUNT
Final report	FROM Apr 1981 TO Jun 1985	December 1987	167

16. SUPPLEMENTARY NOTATION A report of the Concrete and Steel Structures problem area of the Repair, Evaluation, Maintenance, and Rehabilitation (REMR) Research Program. Available from National Technical Information Service, 5285 Port Royal Road, Springfield, VA 22161.

17 COSATI CODES		
FIELD	GROUP	SUB-GROUP

18. SUBJECT TERMS (Continue on reverse if necessary and identify by block number)
Concrete structures — Evaluation
Condition survey — Impact-echo
Dam safety — Nondestructive tests (Continued)

19. ABSTRACT (Continue on reverse if necessary and identify by block number)

The need for additional capability to nondestructively evaluate concrete in large structures is similar for both the US Army Corps of Engineers (CE) and the US Bureau of Reclamation (USBR). In view of this mutual need, the CE and the USBR entered into a cooperative program of research and development designed to increase the nondestructive testing evaluation capabilities of these two organizations, with each agency sharing the program planning and financial support.

Literature reviews were conducted for the five tasks outlined in this investigation, and staff members of organizations known to be engaged in the development of applicable systems or technology were contacted.

An effort was made to develop an ultrasonic pulse-echo system for the investigation and evaluation of the interior of concrete structures. The large pulse-echo transducer (Continued)

20 DISTRIBUTION/AVAILABILITY OF ABSTRACT
☒ UNCLASSIFIED/UNLIMITED ☐ SAME AS RPT ☐ DTIC USERS

21 ABSTRACT SECURITY CLASSIFICATION
Unclassified

22a. NAME OF RESPONSIBLE INDIVIDUAL

22b TELEPHONE (Include Area Code)

22c OFFICE SYMBOL

DD FORM 1473, 84 MAR

83 APR edition may be used until exhausted.
All other editions are obsolete

SECURITY CLASSIFICATION OF THIS PAGE
Unclassified

18. SUBJECT TERMS (Continued).

Pavement thickness	Technology transfer	Ultrasonic pulse-echo
Piezoelectrics	Transducer development	Underwater surveys

19. ABSTRACT (Continued).

fabricated at Ohio State University (OSU) was obtained for study. Experimental transducers were fabricated and bandwidths were altered and optimized. Transducer area and frequency of operation were determined and various piezoelectric materials were studied; acoustic and electrical matching were employed to optimize signal strength and signal-to-noise (S/N) ratio. The final prototype transducers were constructed of lead metaniobate (EC-82) and lead zirconate titanate (PZT-5H). The transducer area and mass was reduced by 90 percent and the S/N ratio was increased by 200 percent when compared with the OSU transducer. The pitch-catch prototype configuration was used to successfully measure the thickness of a 9-1/4-in. concrete test slab with a S/N ratio of 18. The system is presently useful for making thickness measurements on concrete pavements and floor slabs. Limited tests have shown that a metal plate and a plastic pipe can be located in a concrete slab of 9 in. thickness or less. Also, a thickness measurement was made on concrete by generating wide-band acoustic (sonic and ultrasonic) energy by an impact hammer and detecting the echoes with a low Q resonant receiver centered at 180 kHz.

Increased emphasis is being placed on the development of underwater concrete repair techniques. The extent and location of damage must be known in order to determine what steps should be taken to correct the damage and to prepare valid cost estimates. Therefore, a high resolution acoustic mapping system was developed which will provide, without dewatering, an accurate and comprehensive evaluation of top surface wear on horizontal surfaces (such as aprons, sills, lock chamber floors, and stilling basins) where turbulent water flow carrying rocks and debris may have caused erosion or abrasion damage. The results of the mapping system are presented as real-time strip charts showing the absolute relief for each run, three-dimensional surface-relief plots showing composite data from the runs in each area, contour maps of selected areas, and printouts of the individual data point values. The system is designed to operate in 5 to 30 ft of water and produce accuracies of ±2 in. vertically and ±1 ft laterally.

A study was performed to develop engineering guidance to establish a uniform method for evaluating the condition and safety of existing concrete structures. The results of this study are published in a separate report.

Vibration signatures were obtained from various large structures using the impact-resonance technique. Comparative analyses provided indications of the general conditions of the structures. The use of vibration signatures as a field-inspection technique seems feasible.

Mode shapes, resonant frequencies, and damping factors were measured on a prototype concrete wall before and after the wall was subjected to blast loading. Results obtained before and after the blast were compared. Results from damping measurements made on a large dam and on cylinders made of similar concrete were also compared. These comparisons demonstrated that modal characteristics can be used to note changes in the boundary conditions and the elastic modulus of a concrete structure.

PREFACE

The study reported herein was authorized by Headquarters, US Army Corps of Engineers (HQUSACE), under Civil Works Research Work Unit 31753, "Development of Nondestructive Testing Systems for In Situ Evaluation of Concrete Structures." Funds for the conduct of the study were provided through the Concrete Research Program, which is overseen by Mr. Fred A. Anderson, HQUSACE; the Repair, Evaluation, Maintenance, and Rehabilitation (REMR) Research Program, which is overseen by Dr. Tony C. Liu (DAEN-ECE-D), and Messrs. John R. Mikel (DAEN-CW-M), and Bruce L. McCartney (DAEN-CWH-D), all of HQUSACE; and the US Bureau of Reclamation Program Related Engineering and Scientific Studies (PRESS), directed by Dr. Francis G. McLean, Chief, Division of Research and Laboratory Services.

The study was conducted at the US Army Engineer Waterways Experiment Station (WES) during the period April 1981 to June 1985 under the general supervision of Messrs. Bryant Mather, Chief, Structures Laboratory (SL); James T. Ballard, Assistant Chief, SL; and John M. Scanlon, Chief, Concrete Technology Division. Mr. William F. McCleese is REMR Program Manager, and Mr. James E. McDonald is Concrete and Steel Problem Area Leader.

This report was prepared by Messrs. Henry T. Thornton, Jr., the Principal Investigator of this work unit, and A. Michel Alexander.

COL Dwayne G. Lee, CE, is Commander and Director of WES. Dr. Robert W. Whalin is Technical Director.

CONTENTS

CONVERSION FACTORS, NON-SI TO SI (METRIC)
UNITS OF MEASUREMENT

Non-SI units of measurement used in this report can be converted to SI (metric) units as follows:

Multiply	By	To Obtain
degrees (angle)	0.01745329	radians
feet	0.3048	metres
foot-pounds (force)	1.355818	metre-newtons
inches	25.4	millimetres
knots (international)	0.5144444	metres per second
miles (US statute)	1.609347	kilometres
pounds (force)	4.448222	newtons
pounds (mass)	0.4535924	kilograms
square feet	0.09290304	square metres
tons (2,000 pounds, mass)	907.1847	kilograms

DEVELOPMENT OF NONDESTRUCTIVE TESTING SYSTEMS FOR IN SITU EVALUATION OF CONCRETE STRUCTURES

PART I: INTRODUCTION

Background

1. The recent heavy emphasis on the evaluation of existing dams and the shift in policy from new construction to repair and rehabilitation of existing structures have created a need to develop and refine nondestructive testing (NDT) techniques applicable to evaluating the existing conditions of concrete structures. Considerable expense and destruction of a portion of the structure are often incurred in the determination of the parameters necessary to establish the remaining service life, current and future safety, extent of concrete deterioration, and performance of existing structures. The nature and expense of destructive methods of obtaining data often preclude extensive coverage of a structure when it is needed. These undesirable features can be drastically reduced, or eliminated, by developing effective and reliable NDT techniques.

2. The need for additional capability to nondestructively evaluate concrete in large structures is similar for both the US Army Corps of Engineers (CE) and the US Bureau of Reclamation (USBR). In view of this mutual need, the CE and USBR entered into a cooperative program of research and development designed to increase the NDT evaluative capabilities of these two organizations, with each sharing in the program planning and financial support.

Objective

3. The objective of the work unit reported herein was to develop NDT techniques and systems for the assessment of the condition and performance of concrete structures.

Approach

4. The overall approach for the investigation consisted of the following five concurrent tasks:

a. Task I. Develop nondestructive tests to detect the presence, depth, and extent of rebar, cracks, or inferior quality material within concrete structures, and locate voids within (or underneath) concrete structures where only a single surface is accessible.

b. Task II. Screen and investigate systems and technology presently available which might be applicable to mapping and profiling of underwater concrete structures such as stilling basin slabs and lock chamber floors. Systems and technology with developmental potential for application to this task will be evaluated with the ultimate goal of developing a field-testing system.

c. Task III. Develop engineering guidance to establish a uniform method for evaluating the condition and safety of existing concrete structures.

d. Task IV. Assess the use of a structure's vibration signature (obtained by the impact-resonance technique) as a field inspection tool.

e. Task V. Investigate the feasibility of using modal analysis in conjunction with a finite element program as a method for assessing the deterioration, structural integrity, and stability of a concrete structure.

Scope of this Report

5. The research and the development of tests and systems as required by Tasks I through V are described in this report.

PART II: TASK I - NONDESTRUCTIVE TESTING METHODS FOR INTERIOR CONCRETE

6. As stated previously, the objective of Task I was to develop nondestructive tests for (a) detecting the presence, depth, and extent of rebar, cracks, or inferior quality material within concrete structures, and (b) locating voids within, or underneath, concrete structures where only a single surface is accessible.

Background on NDT Methods for Concrete

7. Information on the quality of in-place concrete can be obtained in a number of ways. Nondestructive techniques can be used without destroying or removing concrete. There are two mechanical techniques that are commonly used to test concrete--the Schmidt hammer and the Windsor probe. Techniques incorporating wave propagation principles will be discussed later.

Mechanical techniques

8. Malhotra (1976) presents words of interest about the two mechanical test techniques.

> Weil... and the RILEM* Working Group on Nondestructive Testing and Concrete... have pointed out the need for extreme care in the use of these tests. Frequent calibration and checking of the test hammers are most desirable. The type of cement appears to affect the test results; for example, concrete made with high-alumina cement has given different results from concrete made with portland cement.... It has also been reported by the RILEM Working Group... that in one instance fire-damaged concrete has given a higher estimated strength than comparable undamaged concrete. To correctly interpret the test data, it is desirable to know the mix proportions, type of coarse aggregate used, age, and moisture conditions of concrete under test. Weil... has recommended the removal of soft mortar layers from the surface of concrete before using the impact hammers.
>
> Studies carried out by Weil... and the RILEM Working Group... indicate that the strength of concrete under investigation can be predicted with an accuracy of 20-30 percent by the use of test hammers.

---

* Réunion International des Laboratoires d' Essais et de Recherches sur les Matériaux et les Constructions.

9. Rebound hammer. The rebound hammer, also called the Swiss or Schmidt hammer (see Figure 1), is used to assess the uniformity of concrete in place and to delineate zones or areas of poor quality concrete.

Figure 1. Schmidt rebound hammer and calibration anvil

10. The rebound hammer contains a spring-loaded steel hammer which, when released, strikes a steel plunger in contact with the concrete (ASTM C 805-79/CRD-C 22-80).* The amount of rebound of the plunger is measured on a linear scale attached to the instrument; in effect, the plunger rebounds depending upon the hardness of the material struck.

11. Some advantages of the rebound hammer are that it is portable, easy to use, low in cost-per-test, and can be used quickly to cover a large surface area. The hammer is valuable as a purely qualitative tool.

12. Malhotra (1976) summarizes the limitations of the Schmidt hammer.

> The limitations of the Schmidt hammer are many; these should be recognized and allowances should be made when using the hammer. It cannot be overstressed that this instrument must not be regarded as a substitute for standard compression tests but as a method for determining the

* Test methods cited in this manner are from the American Society for Testing and Materials Annual Book of ASTM Standards and from Department of the Army, Corps of Engineers, Handbook of Concrete and Cement.

> uniformity of concrete in the structures and comparing one concrete against another. Estimation of strength of concrete by the Schmidt hammer within an accuracy of ±15 to ±20 percent may be possible only for specimens cast, cured, and tested under identical conditions as those from which the calibration curves are established. The prediction of strength of structural concrete by using calibration charts based on the laboratory is not recommended.

The user of the Schmidt hammer should make up his own calibration curves for the particular concrete under study.

13. The rebound hammer can be used to good advantage during construction. Stowe (1974) used the hammer to investigate low quality concrete in the new Walter Reed Hospital, Washington, DC. Rebound readings and compressive strength results of cores were sufficient to demonstrate to the contractor that inadequate concrete existed in 22 columns of the first floor. The contractor removed and replaced the 22 columns at an estimated cost of $1.5 million (1974 cost figure). Additional examples of application of the rebound hammer are cited in Grieb (1958), Willetts (1958), Moore (1973), and Victor (1963).

14. Windsor probe. Malhotra (1976) has this to say about the probe:

> The Windsor probe equipment consists of a powder-actuated gun or driver, hardened alloy probes, loaded cartridges, depth gage for measuring penetration of probes, and other related equipment. The probe is driven into the concrete by the firing of a precision powder charge that develops an energy of 575 ft-lb (779.6 N·m).
>
> The Windsor probe is basically a hardness tester and, like other hardness testers, should not be expected to yield absolute values of strength of concrete in a structure. However, like the Schmidt rebound hammer, the probe test provides an excellent means for determining the relative strength of concrete in the same structure or relative strengths in different structures without extensive calibration with specific concretes. The calibration charts provided by the manufacturer do not appear to be satisfactory. It is, therefore, desirable for each user of the Windsor probe to prepare his own calibration charts for the type of concrete under investigation. With change in source of aggregates, new calibration charts become mandatory.

15. The use of the Windsor probe results in damage to the concrete, i.e., the probes must be withdrawn from the concrete and the hole patched.

16. Several laboratory investigations cited in the literature deal with

the evaluation of the Windsor probe for estimating compressive strength of concrete (Gaynor 1969, Malhotra 1970, 1971). Klotz (1972) states that extensive applications of the Windsor probe test system have been made for the determination of in-place concrete strength and in-place quality. The Windsor probe has been used to test reinforced concrete pipe, highway bridge piers, abutments, pavements, and concrete damaged by fire. Klotz concludes that the probe affords a quick and relatively accurate means of ascertaining strength of concrete; he does not define the term "relatively accurate."

Dynamic techniques

17. Ultrasonic velocity through-transmission technique. The ultrasonic pulse velocity method (see Figure 2), ASTM C 597-71/CRD-C 51-72, involves the measurement of the time of travel of electronic/piezoelectric pulsed compressional (longitudinal) waves through a known distance in concrete. From measured time and distance, the pulse velocity through the concrete can be calculated. This system is most effective on structures where two opposite or adjacent surfaces are accessible. Measurements may be made along one surface with the transducers in a side by side configuration, but velocities obtained this way are not always representative of the interior concrete quality. The pulse velocity method is used extensively in the field for determining the

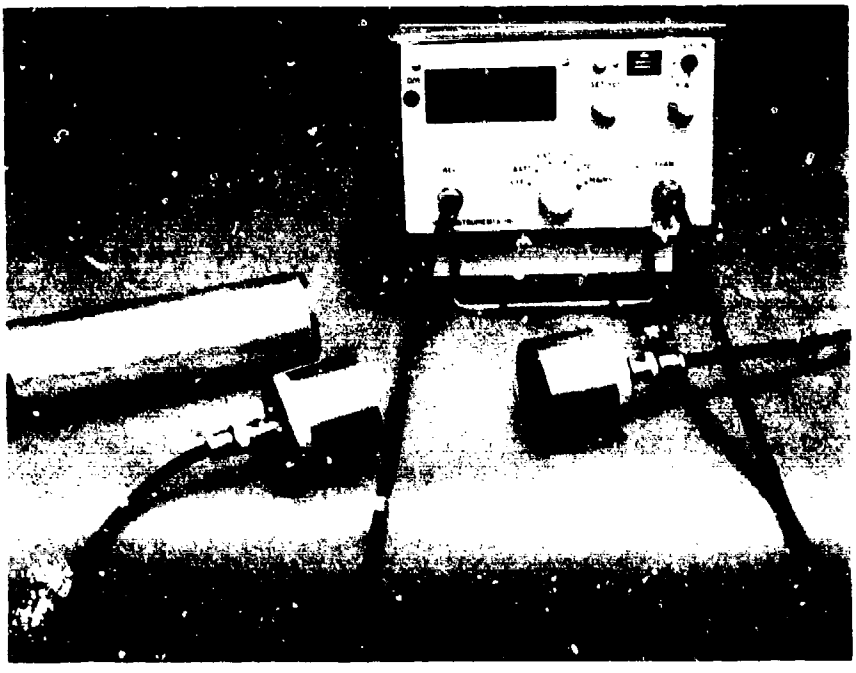

Figure 2. Ultrasonic pulse velocity apparatus

general quality of concrete, locating cracked and inferior concrete, and providing input to condition surveys of concrete structures. The equipment is portable, has sufficient power to penetrate 50 to 70 ft* of good continuous concrete, and has a high data acquisition-to-cost ratio. Standard transducers and those which can be used in boreholes are available and serve to eliminate most problems of access to surfaces, including those underwater. Empirical correlations between pulse velocities and compressive strengths have proved very useful for specific structures and concretes and can be established with limited coring.

18. The ultrasonic through-transmission technique is probably the most widely used method for the nondestructive evaluation of in-place concrete and for providing input for condition surveys of CE structures. Velocity measurements, made through good quality continuous concrete, will normally produce high velocities accompanied by good signal strengths whereas poor quality, or deteriorated concrete, will usually produce decreased velocities and weak signal strength. Concrete of otherwise good quality, but containing cracks, may produce high or low velocities--depending upon the nature and number of cracks--but will almost always produce diminished signal strength. Some engineering judgment is necessary here however as the instrument is not specifically designed to measure signal strength. The ultrasonic pulse velocity method has been used over the years to determine the general condition and quality of concrete, to assess the extent and severity of cracks in concrete, and to delineate areas of deteriorated and/or poor quality concrete.

19. The investigation into the extent of cracking in the downstream gate monolith at Lockport Lock, Illinois Waterway (Stowe et al. 1980), involved a combination of ultrasonic pulse velocity, dye injection, and coring methods. Vertical cracks were visible on each of three exposed vertical faces of a monolith. Velocity measurements were made through sections of this monolith in an attempt to determine the depth of these cracks and whether they joined within the monolith. To facilitate these measurements, a 7-3/4-in.-diam vertical hole was drilled in the monolith. By lowering an omnidirectional borehole transducer into the water-filled hole, it was possible to transmit signals to various points on the vertical faces of the monolith. Results of

---

* A table of factors for converting non-SI units of measurement to SI (metric) units is presented on page 3.

velocity measurements suggested that the visible crack on the downstream face extended deep enough into the concrete to affect velocities 28 to 33 ft from the top of the monolith. Horizontal borings into the downstream face also yielded information which was germane to the interpretation of crack depth.

20. In another part of the structure these types of tests were combined with dyed-water tests in an attempt to trace cracks. The combination of techniques resulted in what was felt to be a reliable and accurate assessment of the location and extent of cracks within the monolith.

21. A similar investigation (Thornton and Glass 1980) was performed at Lock and Dam No. 24 on the Mississippi River where ultrasonic velocity measurements were made through 14 concrete piers which constitute part of the dam structure. Velocity measurements were also made through selected concrete columns that support the service bridge. A condition survey (Stowe and Thornton 1981) which included coring and laboratory testing of concrete was performed as a follow-up.

22. An investigation of larger scale was performed to determine the condition of the Lake Superior Regulatory Structure, Sault Ste. Marie, Michigan. Ultrasonic velocity measurements provided data on the condition of the metal tainter gates, operating machinery, and concrete piers of the structure and its foundation (Thornton et al. 1981).

23. Resonant frequency. Thornton (1977) states that the resonant frequency method (CRD-C 18-59) involves determination of natural frequencies of vibration in concrete specimens. Frequencies of vibration are then utilized to determine various physical properties of the specimens. These properties include dynamic Young's moduli of elasticity and rigidity (shear modulus) and Poisson's ratio. The resonant frequency method is used almost exclusively in the laboratory, and at the US Army Engineer Waterways Experiment Station (WES) it is used extensively for detecting changes in the dynamic moduli of test specimens undergoing accelerated freezing-and-thawing tests. It is also used as a monitor for the progress of deterioration of bars in sulfate resistance tests. In 1981, Alexander reported the results of work on the development of the resonant frequency technique as a nondestructive method for evaluation of concrete structures in place and in real time. The continuation of this work is a part of Task IV of the study reported herein.

24. Dynamic deflection. The dynamic deflection method of NDT applies a sine wave repetitive force or oscillatory load to a slablike or continuous

system (such as floor slabs or pavement) and measures the deflection produced in the system. By evaluating the deflection measurements, the shape of the deflection basin can be determined. The dynamic deflection method is a very practical and useful tool for the evaluation of highway and airport runway pavements, as well as other types of flat slab concrete construction. The evaluation is not limited to the quality or condition of the structural member but can be extended into such areas as assessing support parameters and joint efficiency and determining extent or degree of crack damage.

25. The WES directed an investigation in which this method was used to locate void areas beneath a concrete-lined river channel after the channel had been dewatered. The concrete lining consisted of a 6-in.-thick, V-shaped reinforced concrete slab with 1V on 6H side slopes. Certain portions of the concrete lining were undermined in the late stages of construction when water in the diversion channel overtopped its banks and flowed into the channel. The dynamic deflection method was used to delineate the undermined slabs so that replacement could be accomplished at minimum cost. By correlating the results of deflection measurements with the results of limited coring, a procedure was developed whereby voids with depths as small as 1/2 in. could be detected. Application of the results of this investigation enabled the sponsor to realize substantial cost savings.

26. Acoustic emission. When materials are subjected to stresses which cause them to be strained beyond their elastic limit, localized deformations will occur. The occurrence of these deformations in the forms of dislocation movement or microcrack growth results in the release of stored strain energy. The release of this energy causes the propagation of rapid elastic waves throughout the material. These elastic waves can be detected as small displacements by sensors placed on the surface of the material. It is therefore conceivable that this method could be used as an early warning signal to indicate the start of mechanical failure within a structure.

27. This method has been used extensively to monitor the in-service behavior of pressure vessels to indicate the presence and growth of fatigue cracks and to monitor the response of systems to preservice load tests. Although some work was done as early as the 1950's by L'Hermite (1962), and some later data have been published by Green (1970), Malhotra (1972), and Mlakar, Walker, and Sullivan (1981), the application of acoustic emission

techniques to the evaluation of concrete structures is very new. Malhotra (1976) states:

> The acoustic emission methods are still in their infancy. The equipment, though available commercially, is very expensive, and proper test methods have yet to be developed. Furthermore, observations can be made only during a period of increasing deformation and stress, and this method cannot be used for individual or comparative measurements of concrete in a static condition of loading. However, this technique has potential for nondestructive evaluation of loading levels in structures. It may be possible to monitor large structural members to locate the origin of cracking and the zones of maximum deterioration. However, at the present state of development, the cost of equipment prohibits the use of this technique for the above type of investigation and limits its use to the testing of laboratory specimens only.

28. Radar. Certain types of radar have been used to evaluate the condition of concrete up to 30 in. in depth. Radar can differentiate between serviceable concrete and deteriorated concrete. The deterioration can be in the form of delaminations, microcracks, and structural cracks. Radar can also detect material changes and locate where these changes occur (Alongi, Cantor, and Alongi 1982).

29. The ability of radar to identify the condition of concrete above water has been established. For instance, radar was used to detect voids in pavements in the 1970s (Lundien 1972). Field studies also show excellent reproducibility (Cantor and Kneeter 1982, Cantor 1984). Other laboratory and field experiments showed the possibility of identification and detection of buried containers by radar (Lord, Koerner, and Freestone 1982; Bowders, Koerner, and Lord 1982).

30. In 1982, a team from the US Army Cold Regions Research and Engineering Laboratory (CRREL) visited Plattsburgh Air Force Base to inspect a cavity which had been found under the airfield pavement. Twenty-eight cavities were detected and mapped using an impulse radar system (Kovacs and Morey 1983).

31. Most of the developments in the use of radar for the evaluation of concrete were taking place during the same period in which the WES-USBR's NDT development effort was getting under way. With the exception of the work by Lundien (1972), none of this work was reported until 1982. At this time,

state-of-the-art radar equipment was very expensive and it was uncertain whether the use of radar for the evaluation of concrete was practical. Concrete is placed in environments of varying moisture conditions and moisture interferes with electromagnetic waves where interpretation of results is concerned. However, investigations into the use of radar for inspection of concrete will continue at WES.

Other methods

32. There are other nondestructive methods available which have not been widely used to gather data on in situ concrete structures. These methods include: radioactive, nuclear, magnetic and electrical methods, and microwave-absorption techniques. Malhotra (1976) describes these methods in detail. Clifton et al. (1982) provides another source which contains descriptions, applications, and limitations of some of these NDT methods.

Acoustic Pulse-Echo

Background

33. After review of the literature and evaluation of the information available on methods which should be considered for achieving the objective defined in Task I, it was decided that the development of an acoustic pulse-echo (reflection technique) system should be the major effort. There was a real need for a nondestructive system for detecting and defining voids and discontinuities in and underneath concrete structures. Situations arose frequently that called for the capability to obtain data on a concrete structure with only one accessible surface. These situations did not lend themselves to inspection and determination of problem parameters by use of "through-transmission," as described in the previous section on ultrasonic pulse velocity.

34. There is no commercially available ultrasonic pulse-echo system for concrete structure evaluation. Eight years of research at Ohio State University (OSU) (Mailer et al. 1970), four years of research at the Illinois Institute of Technology (Howkins 1968), and a program on NDT research at WES (Alexander 1981) have shown that the development of equipment for ultrasonic pulse-echo measurements in concrete is feasible. These programs, along with this joint WES-USBR NDT R&D (Research & Development) program, have significantly increased the state-of-the-art knowledge and expertise in this very

difficult area of scientific endeavor. A field-worthy ultrasonic NDT pulse-echo system would greatly enhance the capability to evaluate the condition of concrete structures.

35. The piezoelectric (pressure-electric) effect was discovered in 1880 by Pierre and Jacques Curie. (This was the same family who made the famous discovery of radium 20 years earlier.) A group of artificial materials called ferroelectrics was discovered to be piezoelectric by Valasek in 1921. Barium titanate, a ceramic and ferroelectric, was used extensively in ultrasonics until the discovery of lead zirconate titanate (PZT). "PZT" is a registered trademark by the Vernitron Piezoelectric Division. PZT was discovered by Jaffee in 1955. This briefly covers the history of materials that will emit a voltage when pressure is applied, and vice versa. Piezoelectric materials are the best sources for the production of ultrasonic energy. They also make the best detection devices.

36. Sokolov of Russia in 1929 first suggested the use of ultrasonic waves to find defects in metal objects. He "sounded out" specimens to find those with faults. Almost simultaneously Firestone of the United States and Sproule of England developed the first flaw detector for metals in 1942. Firestone applied the principles of the sonic depth finder, well known from ship locating and depth sounding at sea (Krautkramer and Krautkramer 1977).

37. Bradfield (1948) developed an electroacoustic rod transducer in 1948 that enabled him to make a thickness measurement on a 2-in. slab of concrete. Later, he built a double transducer (pitch-catch) pulse-echo system of 100-kHz barium titanate piezoceramics that enabled him to make thickness measurements of greater magnitude (Bradfield and Woodroffe 1953). Bradfield modified this system by using PZT and variable angle wedges to direct the beam more efficiently. He was able to measure the thickness of a slab of concrete 18 in. thick, although noise from surface waves was a problem and the signal-to-noise (S/N) ratio was low (Bradfield and Gatfield 1964).

38. In 1968, Howkins measured the thickness of a 10-in. slab with a 100-kHz double transducer system of PZT rod elements epoxied into a lucite disc. He, too, recognized the presence of unwanted surface waves and recommended a larger diameter transducer. His work was very helpful in this investigation. Howkins (1968) also built a 40-in. rod transducer and used a nonresonant condenser microphone to pick up the echo from a small ball bearing (BB) shot from a BB gun onto the end of the rod; thus, enabling him to

determine the thickness of the slab.

39. Golis built an 18-in.-diam ring transducer (doughnut shaped) for measuring pavement thickness. Again, the surface wave energy prevented flaw measurements, but the S/N ratio was sufficient to measure pavement thickness within about 2 or 3 percent. The system used lithium sulfate for the receiver. Barium titanate was used initially for the transmitter and later PZT (Golis et al. 1966), Golis 1968, Mailer et al. 1970, and Mailer 1972). A concentrated effort by the OSU team was made to document its work that permitted others to follow up with less effort. Two of the four reports referenced above contain over 200 pages of theory and experimental work.

40. Canfield was successful in measuring the thickness of a 5-in. slab with 80-kHz PZT transducers but was also plagued with the problem of interfering surface waves (Canfield and Moore 1967). Claytor measured the thickness of a refractory concrete slab 12 in. thick using 250-kHz PZT elements with a liquid buffer between the ceramic and the concrete to reduce surface wave energy. An excellent state-of-the-art review of acoustic inspection principles that can be applied to concrete is given in his report (Claytor and Ellingson 1983). Telephone conversations with Howkins, McMaster, Golis, Canfield, and Claytor revealed that only Claytor has recently been involved in ultrasonic pulse-echo measurements in concrete. The reports referenced here describe the complex scientific endeavor to develop ultrasonic pulse-echo in concrete. The heterogeneous nature of concrete complicates the development of pulse-echo for use in this material. Many people have mistakenly assumed that the well established technique of ultrasonic pulse-echo in homogeneous materials can be immediately applied to concrete. This is not the case.

41. As mentioned, the heterogeneous nature of concrete complicates the use of ultrasonic pulse-echo as an evaluative tool for concrete structures. Many factors had to be studied and evaluated before gaining an understanding of the physics of the propagation of ultrasonic waves in concrete. Much time was required to find and study reference material, prepare laboratory equipment, and obtain piezoelectric materials (one piezoelectric manufacturer took one year to fabricate some special piezoelectric elements).

42. The laws of optics of reflection, refraction, and diffraction had to be reviewed and, in some cases, learned for the first time. These laws of optics apply also to ultrasonics. It was only at the time that this research program was ending that some of the ideas came into better focus. Although

significant progress was made with the development of a new transducer, some ideas will not be put into practice until work is resumed. WES's plans are to continue improving the development of the pulse-echo technique as new funds are obtained. The authors have been challenged by this program and have a desire to improve the system in hopes of detecting the presence of flaws and cracks in conjunction with thickness measurements of concrete.

Attenuation

43. Energy losses in concrete are significant. Because of aggregate dimensions (up to 1-3/4 in.) that correspond to the wavelength, ultrasonic attenuation is a problem (Bradfield and Woodroffe 1964). Penetration distances will be reduced if the frequency is increased to obtain better resolution. Also, reflections due to scattering from aggregate-paste interfaces will increase with an increase in frequency. Concrete with a velocity of 14,600 ft/sec will have a wavelength of 1.5 in. for a frequency of 100 kHz. Three main sources of energy attenuation in concrete are: grains, matrix, and porosity. The mechanism of scattering causes more attenuation than absorption (energy turning to heat). Spreading loss due to beam divergence is another problem and is not considered under the definition of attenuation. For example, a plane wave would not show any signal loss if the attenuation in the concrete was zero since the beam has no divergence. A spherical wave with no attenuation would decrease in proportion to the inverse of the distance from the source due to large beam divergence.

44. But, back to attenuation. It can be seen that flaw detection in concrete will be more difficult than that in mortar. The scattered energy from various grain sizes and interfaces in concrete can be higher than the energy of reflections from small cracks and could therefore prevent detection. If the wavelength is increased, both factors will decrease; if the wavelength is decreased, both factors will increase. Neither option is suitable. It may require a minimum dimension for flaws in order that they be detectable. At the present state-of-the-art the best that can be accomplished is to measure back wall reflections and reflections from large discontinuties which return high energy.

45. When energy is lost by absorption, it can be detected by amplification. With scattering, however, amplification only serves to increase the noise level with the signal level. Attenuation increases exponentially with distance. This is more significant than the simple linear inverse relationship

with distance that occurs with spreading. The signal level at a distance of 2X will be much less than one-half of that seen at a distance of X . The basic problem in developing ultrasonic pulse-echo for concrete is overcoming the effects of the heterogeneous material. Higher pulse power is the first obvious solution to part of the problem. Golis modified a Sperry pulser to deliver twice the voltage normally needed for piezoelectric loads (Golis et al. 1966). This reference offers more information on energy loss mechanism such as attenuation, impedance mismatch at single interfaces (Figure 3), and

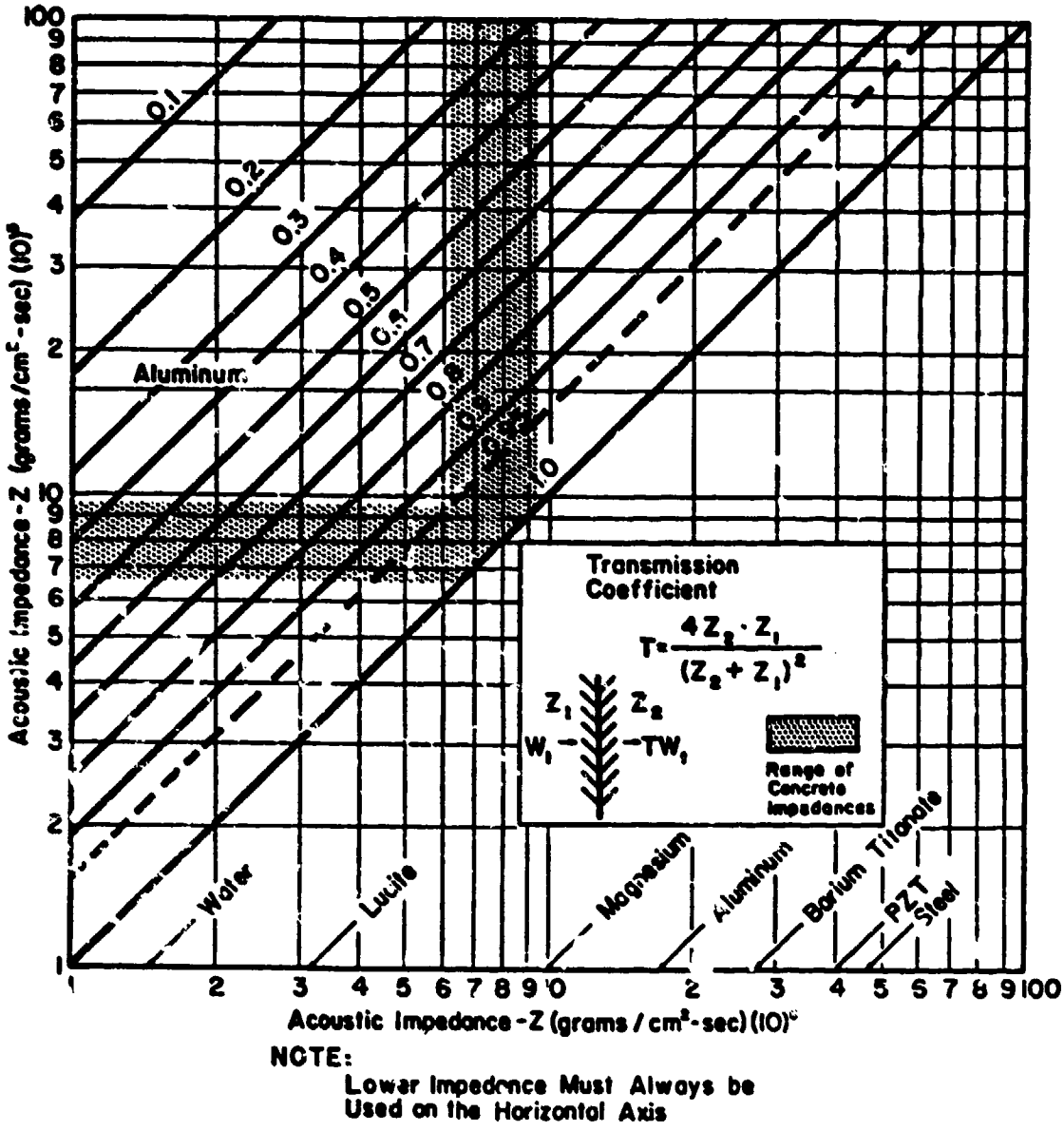

Figure 3. Acoustic impedance-Z (grams/cm^2 · sec) (10)^5 (Golis et al. 1966)

surface roughness. Also, refer to the textbook by Krautkramer and Krautkramer (1977).

Thin film interference

46. The problem of energy loss for a single interface was mentioned in the previous section. Next, the double interface problem is considered. As ultrasonic energy is passed through thin films, interference effects are produced. Because the faceplate of a transducer cannot be in true ultrasonic contact with the concrete surface due to surface roughness, a liquid couplant must be used to fill air gaps and provide a transmission path with a medium having an acoustic impedance that matches the concrete and faceplate more closely than air. In effect two interfaces are created with the transducer faceplate in contact with the top surface of the couplant and the concrete is in contact with the bottom surface of the couplant. Although the couplant will produce interferences, they will not be as disrupting as those produced by air. The thin film interference produced by air can be clearly seen with the through-transmission measurements. Without using a couplant, the attenuation of energy is highly significant.

47. There are three special cases of thin film thickness mentioned in the literature (Kinsler and Frey 1962):

Case a. Layer much thinner than wavelength, $t << \lambda$.

Case b. Half-wavelength layer, $t = \lambda/2$.

Case c. Quarter-wavelength layer, $t = \lambda/4$.

Note that this discussion applies only to thicknesses less than a wavelength and, also, in the case of ultrasonic pulse echo, the acoustic impedance of the faceplate, coupling media and concrete will all be different. Figure 4 shows the transmission characteristics of thin sections.

48. It has been determined that maximum transmission will occur for a thickness close to zero (Case a) and also for a half-wavelength (Case b). Maximum transmission is then equal to the transmission coefficient for a single interface condition for these two cases. See equation in Figure 3. From Figure 4, it is seen that the poorest transmission occurs for a layer with a quarter-wavelength thickness. Plexiglass causes less interference than aluminum. There is another interesting case with the quarter-wavelength layer. Instead of interference occurring as the graphs shows, 100 percent transmission will occur when the coupling media has an acoustic impedance equal to the geometric mean of the impedances of the media on either side of the thin film.

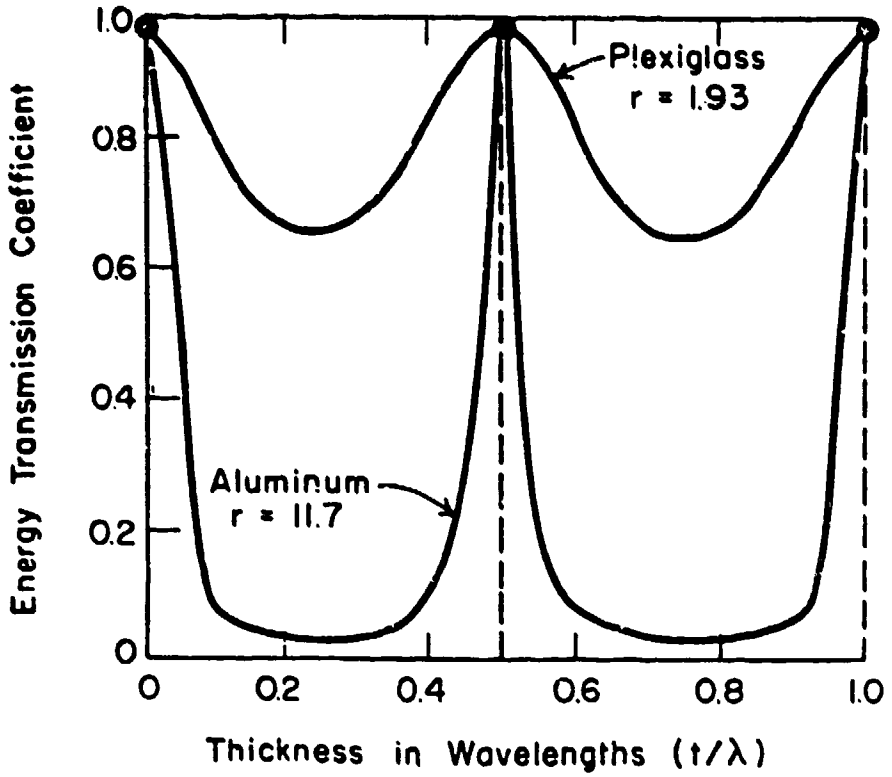

Figure 4. Transmission through thin sections

This condition does not occur, however, for concrete testing. In concrete testing only Case a is attempted. That is, one tries to obtain a layer as thin as possible by using a low viscosity fluid and by rotating the transducer back and forth with 30 or 40 lb of force applied to the transducer to squeeze out the air and excess fluid. One only has to observe the received signal on the oscilloscope to note the improvement in reception. The interference effects of thin sections were developed assuming continuous waves. Since ultrasonic pulse-echo involves pulsed waves (band of frequencies) rather than continuous waves (single frequency) the effects mentioned for the $\lambda/4$ and $\lambda/2$ cases only occur for the center frequency of the pulse. Canfield (1967) obtained confusing results when he tried to build a quarter-wavelength resonating transducer with pulsed excitation. He could only match the center frequency of the resonating transducer. The band of frequencies that compose the pulse contain a wide range of wavelengths that do not match the single frequency of Cases b and c. When the coupling media is much less in dimensions than any of the wavelengths in the band of frequencies that are components of the pulse then Case a is satisfied. The pulse is then transmitted without interference and without distortion.

Diffraction

49. The concept of diffraction (Sears and Zemansky 1957) must be considered if one is to understand the generation of surface waves. Even when one uses the straight-line representations of geometric optics to determine the sound beam profile of a plane wave passing through some aperture, it is not sufficient to explain the complex sound beam in the near field and the divergence of the far field with secondary lobes of acoustic energy. It has been found useful to use a concept called Huygens principle to explain diffraction. At any point on the wave front of the plane wave mentioned above, one can visualize a small elementary wave that spreads out in a spherical pattern. Graphically, one can trace the locus of points that reinforce when the wavelengths are in phase, and points that cancel when the wavelengths are out of phase. This concept has been found sufficient to describe the interference rings in the near field as explained in paragraph 51. When the ratio of the diameter of the acoustic source to the wavelength is small ($D/\lambda \approx 1$), the sound beam lacks directivity (direction). Mode conversion and the generation of surface waves are produced when rays of energy refract into the concrete with large angles. Therefore, spurious energy is reduced considerably when the D/λ ratio is large ($D/\lambda \geq 15$ to 20). Any wave produced other than the longitudinal mode will be spurious and unwanted. Mode conversion produces shear waves and combinations of longitudinal and shear waves arriving at varying times. By maintaining a large D/λ ratio and hence small angles of refraction a pure longitudinal mode is approached.

50. The near field and far field are important characteristics for ultrasonic transducers. They are also known, respectively, as the Fresnel zone and Fraunhofer zone in ultrasonic textbooks (Heuter and Bolt 1955). These fields can only be described by diffraction phenomena which come into play when wavelengths approach the dimensions of test pieces. Unlike refraction and reflection which occur in straight lines and can be understood with geometric optics, when small wavelengths are present, the wave nature of ultrasonics must be considered rather than thinking of small bundles of energy moving in straight lines.

51. Diffraction theory for a piston radiating in an infinite baffle (Figure 5) has been studied and described by Hueter and Bolt (1955). Although the results are not strictly the case for the various transducers described in this report, the general results are applicable. Derivations are made with

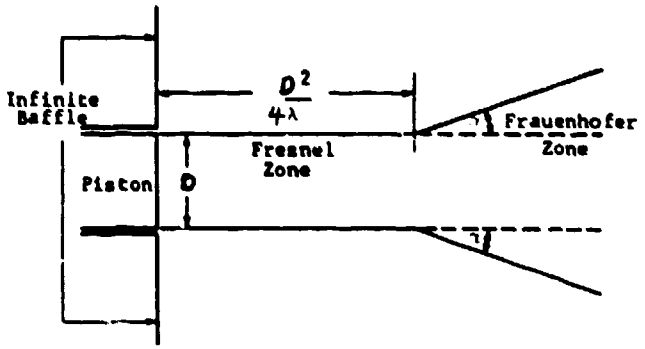

Figure 5. Diffraction theory for a piston radiating in an infinite baffle (Hueter and Bolt 1955)

continuous waves rather than pulses. In the near field the beam is parallel and has the same area as the transducer. The following equation yields the length of the near field.

$$N = \frac{D^2 - \lambda^2}{4\lambda} \qquad (1)$$

where

D = diameter of transducer, M

λ = wavelength of energy, M

The near field contains patterns that produce rings of interference. They resemble bull's eyes with alternate rings of maximum intensity and alternate rings of minimum intensity (see Figure 6 (Krautkramer and Krautkramer 1977)).

52. If one could imagine moving a receiver down the axis of the transducer, a minimum would be detected at N/2 and a maximum at N . Other points between the face of the transducer and the end of the near field (N) while still on the axis, would be represented by the following graph (Figure 7). A natural focus occurs at a = N as the pressure would be double the mean pressure observed at the surface of the transducer.

53. Figure 8 shows the sound pattern in the far field. Once past the near field, the intensity will slowly decrease (never going null as in the near field) with a rate determined by the angle of divergence.

$$\sin \sigma = \frac{1.22\ \lambda}{D} \text{ circular transducer} \qquad (2)$$

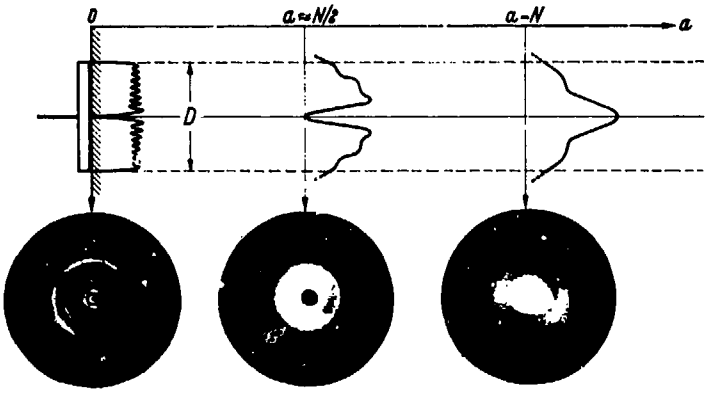

Figure 6. Near-field in front of an ideal piston oscillator or behind a circular diaphragm in a plane wave with distributions of the acoustic pressure along sections spaced a = 0, N/2, and N, for D/λ = 16, with correlated photographed simulated images of the beam cross-section (Krautkramer and Krautkramer 1977)

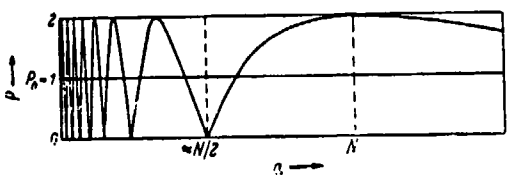

Figure 7. Acoustic pressure on the axis of a piston oscillator

where

σ = half angle of beam divergence

D = diameter of transducer

λ = wavelength

54. For a rectangular transducer, the 1.22 is replaced by 1.0 and the diameter is replaced by D_1 or D_2, which refers to the length of either side of the transducer. At a distance of 3N from the transducer, the pressure is back down to the mean pressure and from there decreases as the beam widens and loses intensity.

55. As noted, the ratio of D/λ determines the radiation pattern and, therefore, how the acoustic energy is introduced into the concrete. The following diagram (Figure 9) shows the radiation pattern for various D/λ ratios.

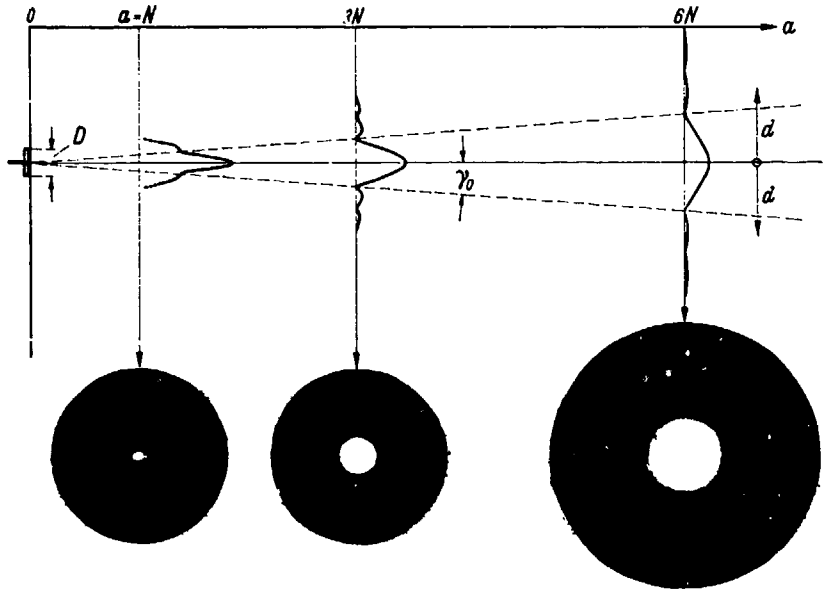

Figure 8. Transition from near to far field with acoustic pressure distributions in cross section as shown

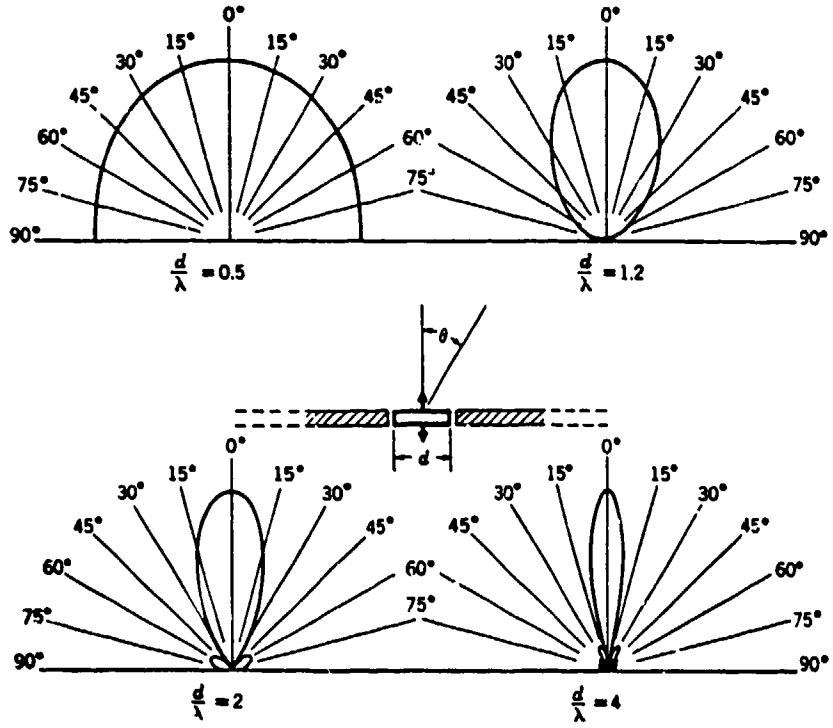

Figure 9. Beam patterns for circular piston (Hueter and Bolt 1955)

56. The key to reducing the presence of spurious modes that interfere with the interpretation of longitudinal reflections is in the diameter/wavelength (D/λ) ratio of the transducer. Metal flaw detectors which operate with a minimum of interference have a D/λ ratio of 5 to 25. A large ratio (>5) produces a sound beam with low divergence. The higher the ratio, the more closely the beam approaches a collimated pattern where the sound rays become parallel.

57. As discussed in paragraph 43, the large grain size in concrete imposes an upper frequency limit. A couple of investigations suggest 200 kHz as an upper frequency limit for a transducer for concrete (Howkins 1968; Bradfield and Woodroffe 1953). A typical transducer frequency for metal ultrasonic units might be 2 mHz. This is a ratio of 10 for the two frequencies. Assuming that the velocities are about the same in concrete and metal, this means that the wavelength in concrete is also about 10 times larger than that in metal. Therefore, the diameter of the transducer for concrete must be roughly 10 times larger than the transducer for metal in order that the D/λ ratio be maintained for the two materials. If the diameter of the transducer for metal is 0.75 in., then the diameter of the transducer for concrete will be about 7.5 in. Because it is expensive to manufacture large pieces of ceramic and impossible to find nonstandard shapes and sizes, a mosaic transducer must be constructed from smaller pieces. Various sizes of rods, discs, plates, and other standard shapes are available. A mosaic, if constructed correctly, will perform as a one-piece ceramic.

58. Various ultrasonic phenomena can influence the development of an ultrasonic pulse-echo system for concrete (refer to Golis (1966) and Mailer (1970) for more detail on each phenomenon). Reflection occurs when a wave encounters an abrupt change in the acoustic impedance, such as a change in the type of medium. Refraction occurs when waves encounter another material with a different sound velocity. The wave assumes a new direction given by the angle of refraction (Snell's law). Critical angles can be determined beyond which no transmitted or reflected beam of a stated velocity can exist. Mode conversion takes place at interfaces where reflection and refraction occur. Energy can exist as a combination of longitudinal, shear, and surface wave energy. When a plane wave of infinite cross section passes through an aperture, the emerging beam diverges and also has nonplanar wave fronts. These effects result from wave interference (or diffraction) as in optics.

Similarly, like the beam pattern from a transducer of finite area a reflection from a small discontinuity will have a diffraction pattern.

59. Attenuation consists of energy losses in a material that is independent of beam spread, field effects, transducer couplant mismatch, transducer loading, or sample geometry. In such materials, an attenuation increase is usually accompanied by a noticeable rise in random reflections or noise from scattering surfaces, probably caused by larger grain faces, excessive porosity, or numerous inclusions. These interfering reflections usually limit the upper frequency that is practical for testing a given material.

60. Numerous factors affect a successful measurement in pulse-echo, as noted above. These concepts are fully explained in various ultrasonic publications such as Krautkramer and Krautkramer (1977). Like most physical problems, a few factors will be significant and most will be of ordinary importance. However, one small but necessary factor can prevent the reception of discernible echoes if it is ignored or neglected.

61. A number of concepts that fall under the heading of energy loss mechanisms are mentioned. As it may be impossible to totally cover all the mechanisms on the first prototype transducer, one can overdesign the power output of the transducer and introduce enough energy to receive detectable echoes. The OSU team made use of this idea. Also, to hold in check diffraction problems (and hence surface waves) they opted for an excessively large diameter transducer. Reflections at concrete-transducer interfaces and high standing wave ratios between cable and transducer can be helped by matching acoustical and electrical impedances. Refraction effects can be advantageous by directing the energy from transmitter to concrete and back to receiver by angled transducers. Unwanted shear wave energy can be eliminated by creating critical angles with angle transducers to curb the effects of mode conversion.

62. As can be seen by the earlier explanation of the near- and far-fields, pulse-echo measurements in the near field can be confusing. That length is referred to as the zone of confusion in the literature. Therefore, it is best to measure outside the near field. Probably, the ideal near-field length would be just short of the thickness desired to be measured.

Electromechanical properties of piezoelectric elements

63. Table 1 shows the constants that relate the properties of various piezoelectric materials (Krautkramer and Krautkramer 1977). Two of the most

Table 1

Constants of Some Piezoelectric Materials (Krautkramer and Krautkramer 1977)

Constant	Unit of Measure	Piezoelectric Material: Lead Zirconate-titanate	Barium Titanate	Lead Meta-niobate	Lithium Sulfate	Quartz	Lithium Niobate
Density q	g/cm^3	7.5	5.4	6.2	2.06	2.65	4.64
Acoustic velocity c	m/s	4000	5100	3300	5460	5740	7320
Acoustic impedance Z	$10^5 g/cm^2 \times s$	30	27	20.5	11.2	15.2	34
Resonance frequency f_r of a plate 1 mm thick	MHz	2.0	2.55	1.65	2.73	2.87	3.66
Critical temperature	°C	190 to 350	120	>400	130	576	1210
Dielectric constant ϵ_r		400 to 4000	1000	300	10.3	4.5	30
Internal damping coefficient d		1.008 to 1.2	1.000	1.3		1.00003	
Electromechanical coefficient of coupling k_{33} for thickness oscillation		0.6 to 0.7	0.45	0.4	0.38	0.1	0.2
Coefficient of coupling k_p for radial oscillations (interfering oscillations)		0.5 to 0.6	0.3	0.07	0	0.1	
Piezoelectric modulus d_{33} for thickness oscillation	10^{-12} m/V	150 to 593	125 to 190	85	15	2.3	6
Piezoelectric pressure constant g_{33}	10^{-3} Vm/N	20 to 40	14 to 21	32	156	57	23
Piezoelectric constant of deformation k_{33}	10^9 V/m	1.8 to 4.6	1.1 to 1.6	1.9	8.2	4.9	6.7

important constants are the transmitting constant (d_{33}) and the receiving constant (g_{33}) (Bacon 1961). Subscript 3 always refers to the poling direction of the piezoelectric ceramic. The first subscript means the electrodes are perpendicular to axis 3. The second subscript means that the strain or stress occurs along axis 3. This represents a longitudinal mode of operation.

64. Table 1 shows that PZT has the largest output displacement (d_{33}) for a given excitation voltage. It ranges from 150 to 593 $\times 10^{-12}$ m/V. The following equation (Krautkramer and Krautkramer 1977) determines the displacement developed from a given voltage:

$$\Delta th = Vd_{33} \tag{3}$$

where

Δth = change in thickness, m

V = excitation voltage, V

d_{33} = transmitting constant, m/V

Barium titanate has the second largest d_{33} constant.

65. The piezoelectric material having the best receiving constant (g_{33}) is lithium sulfate with a value of 156 $\times 10^{-3}$ Vm/N. The output voltage V from this receiver is as follows (Krautkramer and Krautkramer 1977):

$$V = th\ \sigma\ g_{33} \tag{4}$$

where

th = thickness, m

σ = acoustic pressure, N/m^2

g_{33} = receiving constant (Vm/N)

For a single transducer element where the element is both the transmitter and receiver, the highest loop gain can be obtained from PZT. It would be directly proportional to the product of d and g . However, if separate elements are used for the transmitter and receiver, then PZT would be the best transmitter and lithium sulfate the best receiver--if nothing other than gain is considered.

66. The electromechanical coupling coefficient represents the efficiency of conversion of mechanical energy to electrical and vice versa. The coupling coefficient is related to the transmitter constant d and the receiver

constant g by the following equation (Gulton Industries 1980):

$$k_{33}^2 = Y_{33} d_{33} g_{33} \tag{5}$$

where Y = Young's modulus, N/m^2. A high loop gain can be recognized quickly by noting that the value of the coupling coefficient k_{33} is related to the product of d_{33} and g_{33}. As can be seen in Table 1, PZT has the largest coupling coefficient (in the range of 0.6 to 0.7).

67. Another important piezoelectric property is the acoustic impedance. To obtain the highest transmission coefficient through interfaces, the impedance of the crystal should be close to that of the test piece. Table 1 shows that the impedance of lithium sulfate is very close to that of concrete. Concrete ranges from 6 to 9 × 10^5 gm/cm^2 × s and lithium sulfate is about 11 × 10^5 gm/cm^2 × s. When the impedances differ by large amounts, transmission can be improved by inserting a third material between the crystal and the concrete, the third material should have an impedance equal to the geometric mean of the other two materials (Carlin 1960). Aluminum has an impedance roughly equal to the geometric mean of PZT and concrete. Aluminum is 17 × 10^5 gm/cm^2 × s and PZT is 30 × 10^5 gm/cm^2 × s.

$$Z_A = \sqrt{Z_p Z_c}$$

$$Z_c = \frac{Z_A^2}{Z_p} = \frac{(17)^2}{30} \tag{6}$$

$$Z_c = 9.6$$

where

Z_A = aluminum impedance
Z_p = PZT impedance
Z_c = concrete impedance
Z = $(gm/cm^2 \cdot sec) \times 10^5$

As can be seen in Table 1, the acoustic impedance is the product of the density and acoustic velocity.

68. The resonant frequency f of a given crystal is determined by the use of the following equation (Krautkramer and Krautkramer 1977).

$$f = \frac{c}{2\ell} \tag{7}$$

where

f = frequency Hz

c = acoustic velocity, m/s

ℓ = length, m

In Table 1 a thickness of 1 mm is assumed and the resonant frequency is given for each of the piezoelectric materials. Lead metaniobate has the lowest resonant frequency, because it has the lowest velocity. Lithium niobate has the highest resonant frequency, because it has the highest velocity. This is not a significant factor for ultrasonic pulse-echo development for concrete, as the crystal thickness will be large enough so that the crystal will not be fragile. Even for operation at 200 kHz, which would be a high frequency for concrete, the thickness of lead metaniobate would be almost 1/3 in.

69. The mechanical Q should be low (1-3) to reduce ring time and to obtain good resolution in pulse-echo measurements. See paragraph 82 for a definition of Q. PZT-4 is used for high Q operation--such as through transmission measurement--whereas PZT-5 would be used for pulse-echo measurements where a broad bandwidth signal is necessary (Table 2). Even then, PZT-5 would require damping to reduce the Q from its value of 65-75 down to 1-3. Lead metaniobate has a Q of 10-15 which would require very little external damping. Quartz has a Q of about 50,000!

70. Another important concept is the relative dielectric constant. The constant is given as a factor which is related to the permittivity of free space. The permittivity of free space is 8.85×10^{-12} farads/m, and a relative dielectric constant of 4,000 means that it is 4,000 times as high as that of free space. The higher the dielectric constant of a given piezoelectric material, the higher is its capacitance. Quartz has a low capacitance and PZT has a high capacitance, as seen in Table 1.

71. The capacitance c of a crystal is determined from the following equation:

Table 2

Typical Electromechanical Properties (Vernitron Piezoelectric Division, no date)

	Multiplying Factor	PZT-4	PZT-5A	PZT-5H	PZT-8	PZT-7A
Coupling Coefficients						
k_{33}		0.70	0.71	0.75	0.64	0.66
Piezoelectric Constants						
d_{33}	10^{-12}	285	374	593	225	150
g_{33}	10^{-3}	24.9	24.8	19.7	25.4	39.9
Free Dielectric Constants						
K_3	-	1,300	1,700	3,400	1,000	425
Elastic Constants Short Circuit						
$1/s^E_{33} = Y^E_{33}$	10^{10}	6.6	5.3	4.8	7.4	7.2
Density	-	7,600	7,700	7,500	7,600	7,600
Mechanical Q	-	500	75	65	1,000	600
Curie Point	-	325°C	365°C	195°C	300°C	350°C

NOTE: d = resulting strain/applied field in metres per volt.
g = resulting field/applied stress in volt-metres per newton.
1/s = Y in newtons per metre.
Density is in kilograms per cubic metre.

$$C = \frac{K_3 \epsilon_o A}{th} \qquad (8)$$

where

K_3 = relative dielectric coefficient
ϵ_o = permittivity of free space, 8.85×10^{-12} farads/m
A = area of crystal, m^2
th = thickness of crystal, m

A large capacitance means that the impedance (capacitive reactance) is low as shown by the following equation.

$$X_c = \frac{1}{\omega c} \tag{9}$$

where

X_c = capacitive reactance (ohms)
c = capacitance (farads)
ω = frequency (Hz)

A low impedance is useful for delivering large amounts of energy into the crystal when used as a transmitter. Less voltage is required to produce a given amount of energy from PZT than from Quartz. Very little precaution against arcing is needed for crystals with a large dielectric constant. As an example, two electrodes brought close to each other may arc, but if a dielectric such as a piece of glass is inserted between the electrodes, the voltage can be increased without flashover occurring. More energy can be supplied to PZT with untuned (broadband) pulsers than with tuned (narrowband) pulsers. Most commercial ultrasonic pulse-echo units are tuned pulsers which have a high output impedance. This works well for quartz and other crystals having similar dielectric constants. However, PZT requires untuned pulsers such as capacitor discharge units (shock excitation) to produce higher energy pulses. Untuned pulsers have a low output impedance which matches the impedance of the crystal, allowing maximum transfer of energy to the crystal. A pulser with a gated sine wave output would be a tuned pulser.

72. Table 2 shows some of the electromechanical properties of PZT (Vernitron Bulletin). The relationships between some of the constants are illustrated with two equations. The first is (Gulton Industries 1980) the following:

$$d_{33} = K_3 \varepsilon_o g_{33} \tag{10}$$

Take the data for PZT-7A as an example.

$$d_{33} = (425)8.85 \times 10^{-12}(39.9 \times 10^{-3})$$
$$d_{33} = 150 \times 10^{-12}$$

The calculated value agrees with the value given in the table. The second equation (Gulton Industries 1980) is:

$$d_{33} = k_{33} \frac{\varepsilon_o K_3}{Y_{33}^E}$$

$$d_{33} = 0.66 \frac{8.85 \times 10^{-12}(425)}{7.2 \times 10^{10}} \qquad (11)$$

$$d_{33} = 150 \times 10^{-12}$$

and again the calculated value agrees with the value given for PZT-7A in Table 2.

73. The ideal piezoelectric material for constructing a transducer for ultrasonic pulse-echo in concrete would have a high transmitting coefficient (d_{33}) like that of PZT-5H. It would have a large receiving coefficient (g_{33}) like that of lithium sulfate. The material would have a low mechanical Q of 1 to 3 with an acoustic impedance value in the range of concrete (6 to 9 gm/$cm^2 \cdot s$). It would have a high dielectric constant like that of PZT-5H and low mode conversion with a transverse coupling coefficient that is low like lithium sulfate. PZT and quartz create interference due to the large effects of mode conversion. Obviously, no single piezoelectric material exists that exhibits all of the desired properties. However, because transducer development is the most important factor in solving the problem of ultrasonic pulse-echo measurements in concrete, these properties are important.

Matching electrical impedances

74. Not only is it important to match acoustic impedances of the piezoelectric transducers to the concrete, but also it is important that the electrical impedances of the transducers match the electrical impedances of the receiving and transmitting circuitry. Electrical matching of impedances is important to obtain maximum efficiency from a transmitter or receiver (Walker and Lumb 1964). When the bandwidth has been increased (Q lowered) by an external backing member, the sensitivity has also been reduced from that of an air-backed element. However, some of that sensitivity can be regained,

without degrading the bandwidth, by tuning out the reactance of the static capacitance of the transducer with the addition of an inductor. The electrical resonance of the inductor and capacitor is tuned to the mechanical resonance of the crystal (Vernitron Piezoelectric Division, no date).

> The shunt static capacitance generally is undesirable, whether the device is designed for operation at resonance or for broadband, below resonance operation. In electrically driven devices, it shunts the driving amplifier or other signal source requiring that the source be capable of supplying extra current. In the case of mechanically driven devices, the static capacitance acts as a load on the active part of the transducer, reducing the electrical output.
>
> In non-resonant devices, not much can be done about the shunt capacitance, except choose a piezoelectric material having maximum activity. In resonant devices, however, the static capacitance may be "neutralized" by employing a shunt or series inductor chosen to resonate with the static capacitance at the operating frequency. This is illustrated in Figure 10.

75. The input impedance of the crystal is determined by the following equation:

$$X_c = \frac{1}{2\pi fc} \qquad (12)$$

where

X_c = capacitive reactance, ohms

f = frequency of crystal, Hz

c = capacitance of the crystal, farads

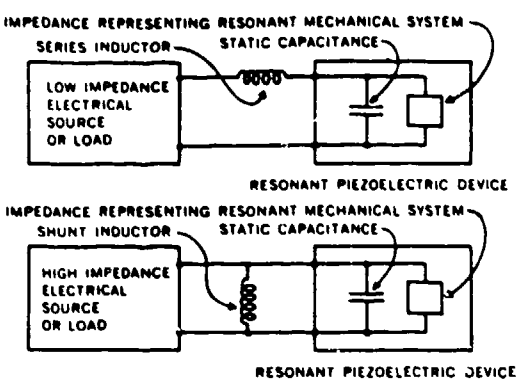

Figure 10. Resonant piezoelectric device with static capacitance "neutralized" by inductor- (Vernitron Piezoelectric Division, no date)

The capacitance can be measured with an impedance bridge or calculated with the following equation:

$$C = \frac{K_3 \varepsilon_o A}{th} \tag{13}$$

where

K_3 = dielectric constant of crystal

ε_o = permittivity of free space, farads/meter

A = area of crystal, m^2

th = thickness of crystal, m

76. Impedance matching is achieved with an inductor, once the inductance is calculated with the following equation. At resonance the inductive reactance is equal to the capacitive reactance.

$$L = \frac{X_c}{2\pi f} \tag{14}$$

where

L = inductance of coil, henries

77. When a single transducer is used for transmitting and receiving, optimal matching is not possible as the pulser has a different output impedance than the receiving amplifier would have. However, where a separate transmitter and receiver transducer are used, optimal matching is possible in both cases (Krautkramer and Krautkramer 1977).

78. The addition of an inductor across the piezoelectric transducer tuned to the appropriate thickness mode oscillations is also useful to avoid undue excitation of the lateral ringing of the transducer elements (Bradfield 1948).

Bandwidth measurements and ringing

79. It is necessary that bandwidth measurements be made in the process of constructing a transducer. The bandwidth will change from its undampened condition in air. As elements are bonded together into a mosaic in various series or parallel combinations, the bandwidth will change. Other factors that alter the bandwidth are: the addition of external damping, the installation of the piezoelectric elements into a housing, the associated

electrical impedance placed on the transducer by the cable, various transmitting and receiving circuitry, and the mechanical loading of the test specimen.

80. Evaluation of the characteristics of the piezoelectric resonator is dependent upon accurate measurements of the physical and dielectric properties and impedance of the element or resonator. While the measurements of capacitance and dissipation factor are relatively simple, the evaluation of the critical frequencies must be carefully performed. The recommended test circuit for determining the critical frequencies and impedances of the piezoelectric resonator is shown in Figure 11 (EDO Western, no date).

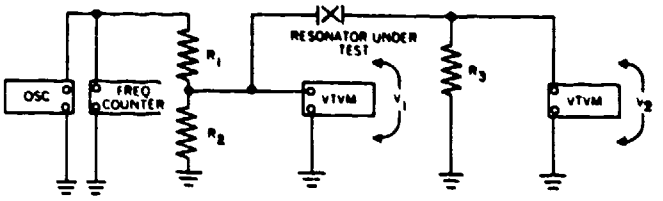

Figure 11. Typical circuit for making bandwidth measurements (EDO Western, no date)

81. A sweep oscillator was used in the actual bandwidth measurements. The frequency counter is only used when operating at a constant frequency. The sweep oscillator used is capable of providing a sweep voltage for the oscilloscope that is proportional to the output frequency of the oscillator. By repeating the sweep at a suitable repetition rate, a continuous bandwidth curve is displayed on the oscilloscope. The sweep rate must be lowered when the transducer has a high quality factor (Q) (see paragraph 82). A high Q transducer requires a definite amount of time for the amplitude to build up to maximum near resonance. If the Q of the transducer is 10, it will take 10 cycles of excitation to build up to 96 percent of the full amplitude. A Q of 100 will require 100 cycles and so on. The vertical axis represents the reciprocal of impedance or admittance. VTVM#2 (Vacuum Tube Volt Meter) was substituted with the oscilloscope and VTVM#1 could be removed after initial setup as the oscillator generated a constant voltage with frequency.

82. Figure 12 shows a bandwidth measurement made on a PZT (C5500) rod element, 1 in. in length and 1/2 in. in diameter. The horizontal axis is scaled at 10 kHz/cm starting at zero. The frequency constant of the cylinder

was 56 kHz × in. With a 1-in. length, the crystal had a longitudinal resonance at 56 kHz. The photograph shows that the undamped crystal has a sharp Q. This means that the energy is contained within a narrow bandwidth of frequencies. The equation for computing the quality factor Q is:

$$Q = \frac{f_r}{f_2 - f_1} \tag{15}$$

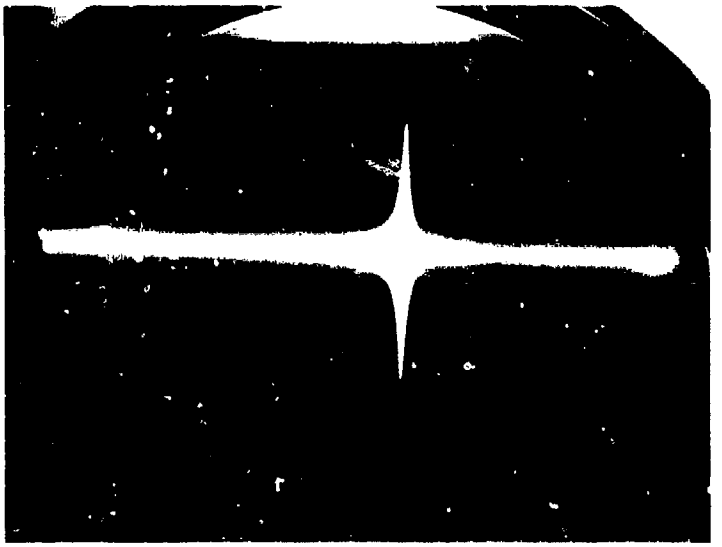

Figure 12. Bandwidth measurement on a PZT (C5500) rod element. Resonance occurs at 56 kHz

where

f_r = resonant frequency

f_2, f_1 = frequencies above and below resonance where amplitude is down by a factor of $1/\sqrt{2}$ (-3dB)

A rough calculation of Q from this measurement follows:

$$Q = \frac{56{,}000 \text{ Hz}}{2{,}000 \text{ Hz}} = 28 \tag{16}$$

According to paragraph 119, the time required QT_o for the crystal to ring down to 4 percent of its original amplitude would be 500 μsec $\left(28 \times \frac{1}{56{,}000}\right)$. Obviously, a transmitter or receiver with a 500 μsec ring-down time could not be used to measure an echo through a 9-in. slab (102 μsec round trip) as it would still be ringing and obscure the reception of the reflected signal.

This example was used as an illustration to point out the need for having a damped receiver and transmitter.

83. Notice how the bandwidth measurement, on a piezoelectric rod element, is clean and free of spurious modes (Figure 12). The radial mode is above 100 kHz and is outside the scale shown on the photograph. However, the large separation in frequency is ideally suited for filtering out the radial mode. A mosaic transducer could be constructed with a number of these point sources to form a flat radiator with directivity (Howkins 1968). The higher frequency radial mode could be reduced, or eliminated, with low pass filtering and by embedding the rod elements in a disc or plate made of tungsten-loaded epoxy. The frequency constant of PZT-C5500 is 56 kHz in. in the longitudinal direction and 78 kHz in. in the radial direction. This means that the interfering mode would be three times as high in frequency as the desired mode for a 1-in.-long, 1/2-in.-diam rod element. Also, the concrete itself would act as a low pass filter, since attenuation is very high when the wavelength of the input signal is equal to, or smaller than, the dimensions of the aggregate.

Impact-echo measurements

84. One important aspect of ultrasonic pulse-echo using impacts is understanding the frequency spectra of various continuous waves and transient signals. Any signal can be represented by the sum of various sine waves with different frequency, amplitude, and phase. A pure tone is a sinusoidal wave of infinite duration, and its representation in the frequency domain is a single spectral line at the frequency $f = 1/T$. In Figure 13, a complex harmonic tone is shown made up of the sum of a fundamental frequency and one harmonic (Hewlett-Packard 1981). This is a signal of infinite duration (continuous wave). There are two ways to look at signals, both of which give different understanding--in the time domain and in the frequency domain. Figure 14a, b illustrates the two views of the same thing. Information is neither gained nor lost--it is only represented differently.

85. A general principle observed is that signals which are broad in one domain are narrow in the other. Figure 14c illustrates the two narrow spectral lines resulting from the two sine wave components making up the complex harmonic tone. Figure 15 shows one square wave signal of continuous duration and three transient signals of finite duration (Heuter and Bolt 1955). As mentioned, the square wave of continuous duration has a spectrum that occurs

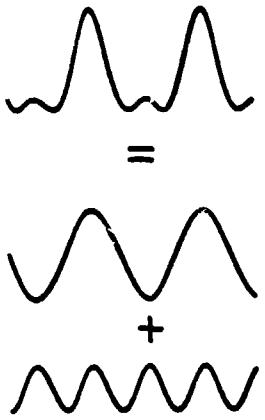

Figure 13. Any real waveform can be produced by adding sine waves together (Hewlett-Packard 1981)

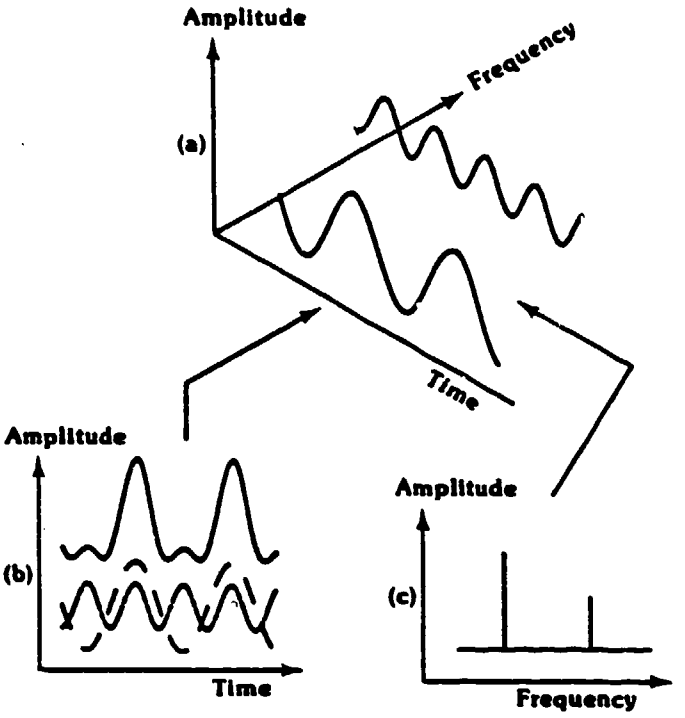

Figure 14. The relationship between the time and frequency domains, (a) three-dimensional coordinates showing time, frequency, and amplitude, (b) time-domain view, and (c) frequency-domain view (Hewlett-Packard 1981)

at discrete frequencies with narrow lines of amplitude. However, the opposite of that is true with the next three signals of short duration in the time domain. Each of these signals develop spectra that are of continuous-band character. The impact waveform generated from a hammer is very similar to the single square pulse shown in Figure 15b. The spectrum will dip to a minimum at a frequency equal to the reciprocal of the pulse width duration. It will then produce a spectrum that resembles the locus of a bouncing ball, with dips occurring at integral multiples of the fundamental. It can be seen that most of the energy is concentrated at the low frequencies which causes vibration signals that can interfere with the ultrasonic echoes. It then is necessary to use a filter to reject vibration noise. Because a sharp load-pulse

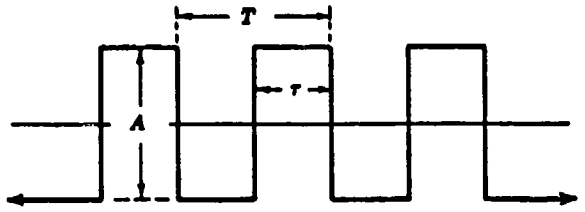

a. Square Wave

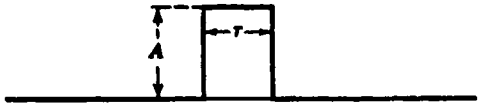

b. Single Square Pulse

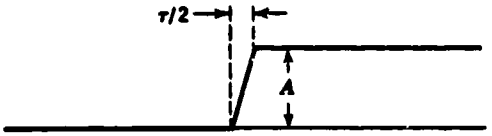

c. Single Step

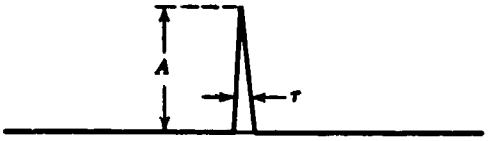

d. Single Spike

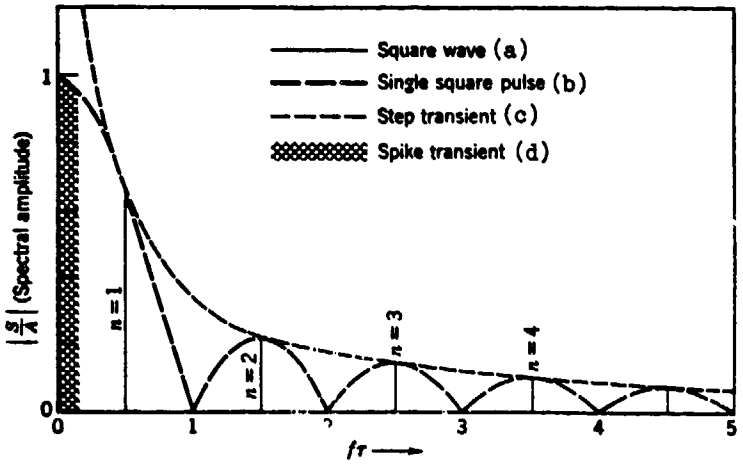

Figure 15. When time signals are narrow, the frequency spectrum is wide (continuous-band); when the time domain is wide, the frequency domain yields discrete and narrow lines of energy (Hueter and Bolt 1955)

develops energy up to infinite frequencies, there is enough energy present, at lower frequencies, to excite resonances in a piezoceramic up to a few 100,000 Hz. Figure 16 shows the load signal in the time domain and its respective energy content in the frequency domain (Hewlett-Packard 1981). As mentioned, the shorter the pulse is in the time domain, the broader the spectrum in the frequency domain.

86. A primary effort was made to determine the state-of-the-art of damping piezoelectric materials to prevent ringing. It was found that transducer companies were reluctant to discuss the type of material and techniques used to obtain various bandwidths and sensitivities of piezoelectric elements as this was proprietary information. A number of investigators have done research on damping piezoceramics with epoxy-loaded backings to obtain desired

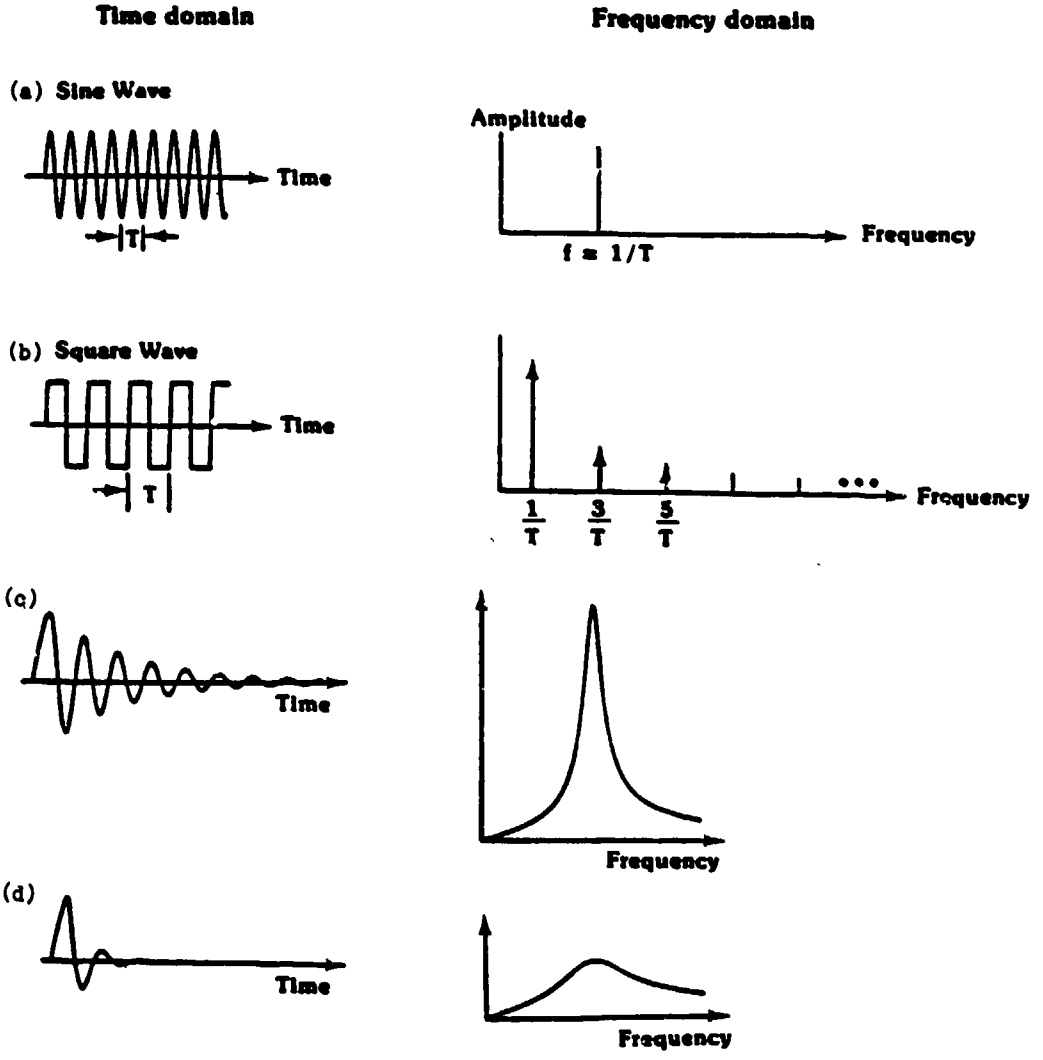

Figure 16. Frequency spectrum example (Hewlett-Packard 1981)

bandwidths (Kossoff 1966; Washington 1961; and Lutsch 1961). A mixture of epoxy and tungsten powder will produce a good acoustic impedance match with that of PZT. This match will produce a minimum of reflection at the PZT/backing interface and allow most of the energy leaving the back face of the crystal to enter into the backing. If the pulse reflects back into the crystal, it will cause ringing. Lutsch also used rubber powder in the backing to increase the attenuation and reduce reflections from the back end of the backing. Washington found that a mixture of 2:1 by weight of tungsten:epoxy gave a good backing. Increasing the amount of tungsten above this produced marginal improvements. Kossoff found that a quarter wavelength layer matched to the load and a low impedance backing that was also a quarter wavelength thick gave the best bandwidth, with reduced sensitivity. He worked with PZT-7A.

87. There are mainly three different ways to damp a transducer. First, a Hopkinson's bar that has a long backing behind the transmitted pulse can be used. This serves to delay the echo from the end of the bar until echoes have been received from the concrete. Second, a shorter backing can be used. This backing matches the crystal in impedance, but yet has high attenuation properties to dissipate the energy leaving the back face of the crystal and to eliminate the standing waves in the backing. This same idea is used with electrical cables in transmission-line calculations for electrical power problems. And finally, the third technique involves using a quarter wavelength backing that does not compromise the sensitivity of the transducer as much but gives a wider bandwidth. Canfield and Moore (1967) tried to use the third technique to measure thickness of concrete but had limited success. The purpose then is to terminate the back face of a crystal in its characteristic impedance. By definition the characteristic impedance of a material is the impedance required to eliminate reflections. As in electrical cables, an infinite length is not required for a backing to eliminate standing waves.

88. To accurately reproduce transients with an undamped (resonant) transducer, make sure that the natural period of the transducer is much lower than the width of the pulse being measured so that operation occurs in the broadband portion of the frequency response curve and the transducer does not resonate. With one-half sine or triangular transients, the transducer's natural period should be less than one-fifth the pulse duration (Stein 1964) for faithful reproduction.

89. This becomes much more critical with short square transients like

one produced by sharp impacts from a Schmidt hammer. A typical impact waveform is shown in Figure 17. The trace is load versus time. The width of the pulse is 70 μsec. Since the curve is the result of an impact on a metal load cell housing the actual pulse width of an impact directly on the softer concrete surface would create a wider pulse. However, the rise time is still sharp when the hammer impacts the concrete directly.

90. With these sharp impact pulses the rise time of the pulse becomes the determining criteria rather than the pulse width. If the rise time is short in comparison with the pulse width, as much as 100 percent overshoot is present (caused by subsequent excitation of the transducer natural period).

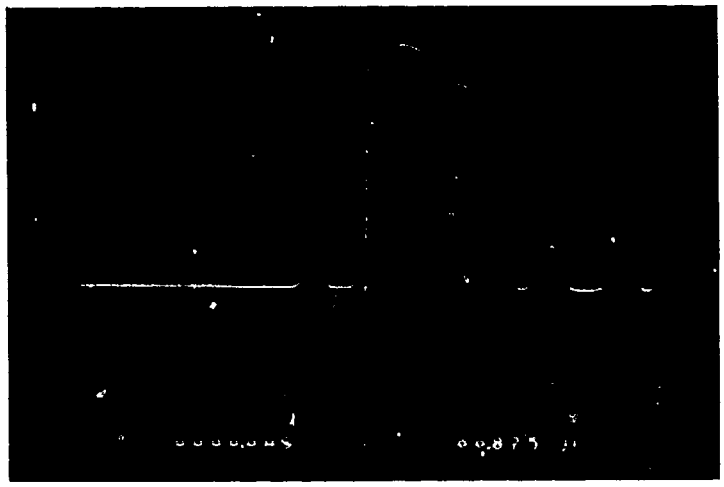

Figure 17. Typical load pulse produced from impact on concrete with a Schmidt hammer

If filtering is not used to clear the ringing, then it is desirable that the transducer have a natural period of one-third the rise time, or less. If it took 5 μsec for a 70-μsec width pulse to rise, then one would need a transducer with a natural period of five-thirds μsec, or less, to accurately resemble the pulse without ringing and overshooting. That corresponds to a frequency of 600 kHz.

91. So, in summary, a much shorter natural period is required for the transducer to reproduce a rectangular pulse than a sine pulse. Or, the resonant frequency of the transducer must be much higher to reproduce rectangular waves than to reproduce sine wave pulses.

92. At the beginning of this research program, the main emphasis was on damping a piezoelectric element. The problem of ringing in the transducer was

responsible for obscuring the arrival of echoes. If one transducer was being used for the transmitter and receiver, it was necessary for the ringing in the transducer to stop before the echo arrived so the transducer could respond as a receiver. The problem seemed to be a matter of reducing the mechanical quality factor Q without excessively sacrificing the sensitivity of the transducer.

93. Jones (1962) reports that due to the difficult problems in damping low frequency transducers (~100 kHz), it was impossible to operate a common transmitter-receiver system in concrete measurements as it is so common with higher frequency measurements on metal. Because the task of developing a damped transmitter with large power output seemed to be a difficult task, it was decided to introduce the energy by impact. Previous tests with impact measurements on concrete piles (Alexander 1980) revealed the presence of strong sonic energy and also ultrasonic energy. Impacts with short pulse widths would be introduced into the concrete and a damped broadband receiver would be developed instead of a low Q resonant transducer to detect the echoes.

94. Bradfield (1948) measured the thickness of a 1-in. and a 2-in. slab of concrete using a magneto striction rod. A small coil was used around the rod to induce a short mechanical pulse of about 12-μsec width. Another coil around the 1/4-in.-diam rod was used as a pickup coil. Although the system had poor sensitivity, it did solve the ringing problem. Two acoustic pulses will be generated, traveling in opposite directions from the coil, when the coil is electrically excited. See paragraph 87. The rod was 2 ft 6 in. long, and it delayed the pulse that left the back end of the transmitter coil long enough for the front end pulse to be reflected from the back wall of the concrete and received at the pickup coil before the other pulse was received from the reflection off the back end of the nickel rod. The rod was further encased in sponge rubber to help dissipate the pulse of energy traveling to the back end of the rod. Another serious loss of energy occurred at the interface of the rod and concrete due to the large acoustic impedance mismatch (see Figure 3).

95. Howkins (1968) also used a 40-in. steel rod with the top end case hardened to receive a small ball bearing (BB) from an air gun. He was able to produce a pulse as short as 10 μsec. He used a condenser microphone (ultramicrometer) as a receiver. The receiver was designed for the low acoustic impedance of air and, therefore, presented a serious mismatch with that of

concrete. The system was subject to noise as the sensitivity of the microphone was very low. However, Howkins was able to measure the thickness of a 10-in. slab of concrete.

96. Figure 18 shows the first transducer built at WES. It was a steel rod 7 ft long and 1/2 in. in diameter. A 1/2-in.-diam PZT element, about 1/16 in. thick and initially resonant at 1.2 mHz, was bonded with silver epoxy to the lower end of the rod. A short piece of rod 1-1/2 in. long was bonded to the front face of the crystal. It took 840 μsec for a pulse to travel from the piezoceramic to the top of the rod and back to the crystal. This allowed enough time to get a number of echoes from the 9-in.-thick slab shown in the photograph. The two-way travel time in the slab was 102 μsec. The energy was

Figure 18. PZT-steel rod transducer (7 ft by 1/2 in.)

introduced into the slab with a Schmidt hammer. Initially, to increase the high frequency content a piece of 1/4-in.-thick steel was bonded to the surface of the concrete and the impact was made on the plate. The sonic pulse-echo measurement is shown in Figure 19. The horizontal time base is scaled at 50 μsec/cm. At least three echoes can be seen at 100, 200, and 300 μsec. The top of the waveform is flattened as the input amplifier is being overdriven

Figure 19. Sonic echoes from concrete slab measured with steel rod transducer, impact made on a steel plate

because of the high acoustic energy from the hammer. This Hopkinson's bar demonstrates that measurements can be made when a sensitive broadband receiver is available. However, the long rod is not practical for field work and would probably never be feasible for detecting flaws. In Figure 20, a pulse-echo measurement is shown where an impact was made directly on concrete, without the steel plate. The horizontal scale is 20 μsec/cm and the arrival time is roughly 100 μsec. The rise time is obviously too slow for accurate thickness measurements.

97. The load-pulse from the hammer does not necessarily match with the longitudinal mode of resonance of the concrete. The width of the load pulse (contact time) would have to be equal to 1/2 the period (T) of the longitudinal resonance in the concrete. The amplitude of the echo would maximize if the hammer matched the concrete as explained. It is necessary that the contact time of the hammer be equal to or less than 1/2 T of the concrete to properly resolve echoes in the time domain.

98. Another rod transducer was built (Figure 21). It also consisted of a PZT element resonant at 1.2 mHz, before damping. The acoustic impedance of aluminum is closer to concrete than steel, and it was hoped this aluminum rod might improve measurements. Also, the rod was only about 3 ft long as compared with the steel rod of 7 ft. No significant improvement was noted.

Figure 20. Sonic echoes from concrete slab with steel rod transducer, impact directly on concrete

Figure 21. Aluminum rod transducer with PZT element

99. Next, a mosaic of PZT elements taken from a James Electronics transducer was used with a backing of epoxy mixed with lead powder. The idea was to terminate the back side of the crystal in its own characteristic impedance with the damping of lead being high enough to totally prevent reflections. This would allow the transducer to be short in length and field-worthy. Here, the idea was to match the backing with the PZT in its acoustic impedance

so that the transmission coefficient was high at this interface. Once all the energy was introduced into the backing without reflections at the interface, it was hoped that enough lead was added to the back of the crystal to dissipate the energy before reflections could come from the back side of the backing and return to the crystal (see paragraph 94). Bandwidth curves are shown of the mosaic before and after damping (see Figures 22 and 23).

100. Both horizontal scales run from 0 to 100 kHz. Obviously, the damping was successful (as far as the response being flat) throughout the range of interest. However, the sensitivity was reduced considerably by the damping and (more than was necessary) as the lead/epoxy backing produced a partially shorted path for the output voltage where the ceramic crystals were molded into the backing. Early experiments had shown that a larger grain combined with epoxy still had high insulation properties. This was not the case with small sized lead powder. The lead powder used in the backing would pass a 100 mesh sieve (150 μm openings). The transducer is shown in Figure 24. The thickness measurement on the 9-in. slab is shown in Figure 25. A low pass filter was used to pass frequencies below 10 kHz. The horizontal scale is 20 μsec/cm with arrival time at roughly 100 μsec.

101. At this point it was felt that measurements of the impact pulse lacked the necessary rise time and sensitivity for the accuracy needed in pulse-echo measurements in concrete. Too much of the energy was in the sonic range rather than the ultrasonic range. In other words, a much shorter pulse was needed with higher intensity. An air pistol that shot steel ball bearings (BB's) was obtained. The small projectiles were fired onto a steel plate epoxied to the surface of the concrete. Successful measurements were made on a 3-in.-thick slab using the steel rod transducer (referred to earlier). However, even though the pulse was about 20 μsec wide, the measurements lacked sufficient accuracy.

102. The idea of using a resonant ultrasonic receiver, rather than a nonresonant one, was then considered. In the effort to develop a broadband receiver that would accurately reproduce the shape of the load-pulse, it was temporarily forgotten that some ringing might be acceptable for shorter wavelengths. In fact, the greatest sensitivity of a ceramic exists at resonance. The ringtime need only be less than the time between echoes. Since an impact consists of broadband energy, it was thought that the higher frequency components from an impact could be used to excite a damped but narrow band

Figure 22. Bandwidth of a PZT mosaic transducer, undamped

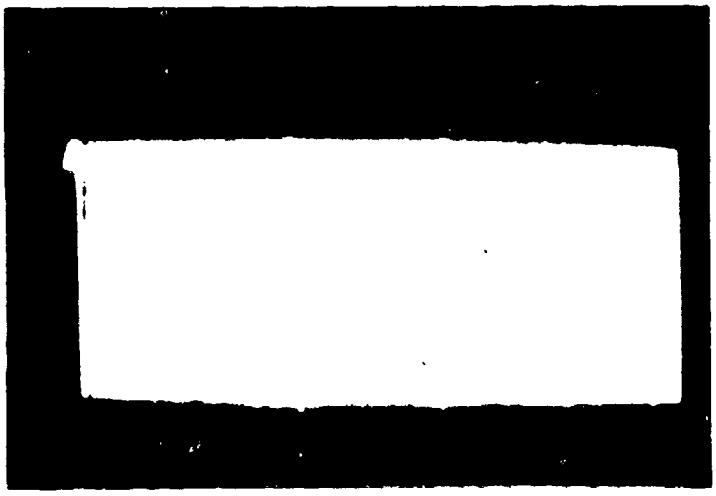

Figure 23. Bandwidth of a PZT mosaic transducer, damped

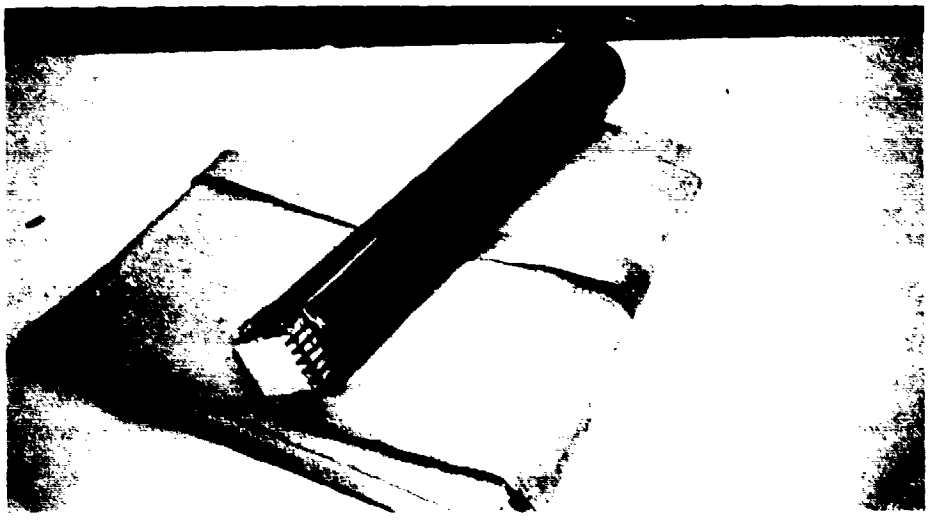

Figure 24. PZT mosaic transducer with epoxy/ lead backing

receiver in the ultrasonic range. The low frequency, large amplitude, compressional load-pulse could be filtered out of the composite signal as it

Figure 25. Thickness measurement on concrete slab with lead-backed PZT transducer

would be noise for all practical purposes. Various undamped transducers were then tested. Almost all of the time, the resonance of the transducer was so low in amplitude that it could not be seen in the presence of the lower frequency impact pulse. By using a high pass filter with cutoff above the lower frequencies that make up the load pulse spectrum (but, below the resonance of the crystal) the resonance was observed.

103. A number of PZT (C5500) ceramic elements were purchased for that purpose. The elements were 1/4 in. in diameter and 1/4 in. in length. The undamped natural frequency was about 200 kHz. A backing of tungsten-loaded epoxy was used for matching and damping. A 1/4-in. faceplate of aluminum was installed on the front face of the crystal. A small wire was soldered to the silver electrodes on the back side, and a thin foil of brass was cemented with silver epoxy between the aluminum and front electrode of the crystal. The ground end was tied to this foil. The bandwidth measurements of the undamped and damped ceramic are shown in Figures 26 and 27.

104. The first horizontal scale is 50 kHz/cm with resonance at about 190 kHz. The second trace is scaled at 36 kHz/cm and the main resonance has been reduced to 180 kHz with a much lower Q. Numerous spurious modes are present in the trace due to high mode conversion of PZT (see paragraph 73).

105. Again, measurements were made of the 9-in. slab using the L-6 Schmidt hammer directly on the concrete (Figure 28). Horizontal scale is 50 μsec/cm.

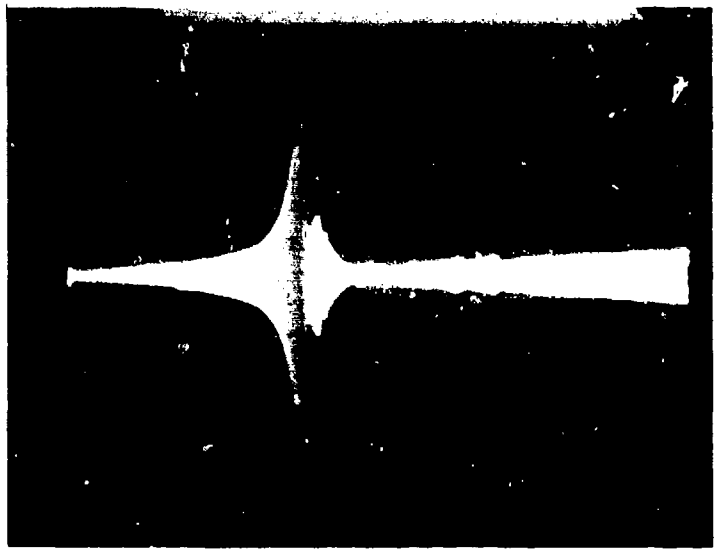

Figure 26. Bandwidth measurement of undamped PZT (C5500) element (1/4 in. diam and 1/4 in. length)

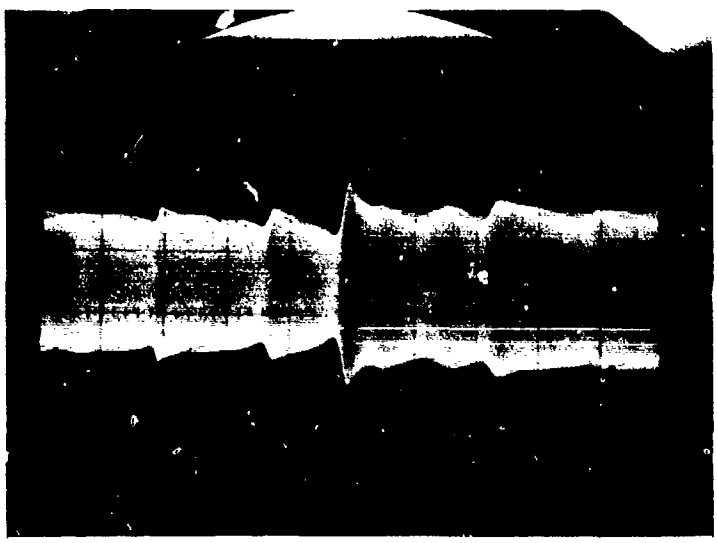

Figure 27. Bandwidth measurement of damped PZT (C5500) element

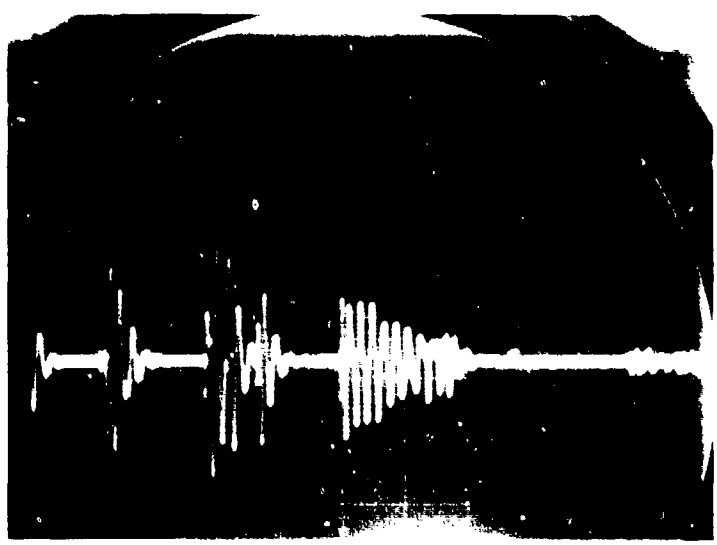

Figure 28. Pulse-echo measurements on 9-in. slab and PZT (C5500) transducer

106. Disregarding the first pulse (trigger of trace may be delayed from beginning of impact), each succeeding pulse is roughly 100 μsec apart. However, the response from a second impact would not always duplicate the previous one. Results were somewhat confusing at this stage, but future investigation should reveal the source of confusion. It appears that surface waves are not producing a problem even though diffraction theory says that a small area impact has no directivity in the beam profile. Transducer theory states that the pulse width of the impact (~70 μsec) should be one-half of the period of the natural frequency of the crystal to produce maximum excitation (Stein 1964). This would mean that it would be most efficient for a crystal having a resonance at 7,150 Hz $\left[f = \frac{1}{2(70\ \mu\text{sec})}\right]$. This crystal resonates at around 110 kHz which is 15 times the optimum frequency from the hammer. Spectrum analysis tests on the Schmidt hammer show the impact frequency content to follow the "bouncing ball" spectrum of a rectangular pulse (see the negative-going rectangular pulse in Figure 29 and the corresponding frequency spectrum in Figure 30).

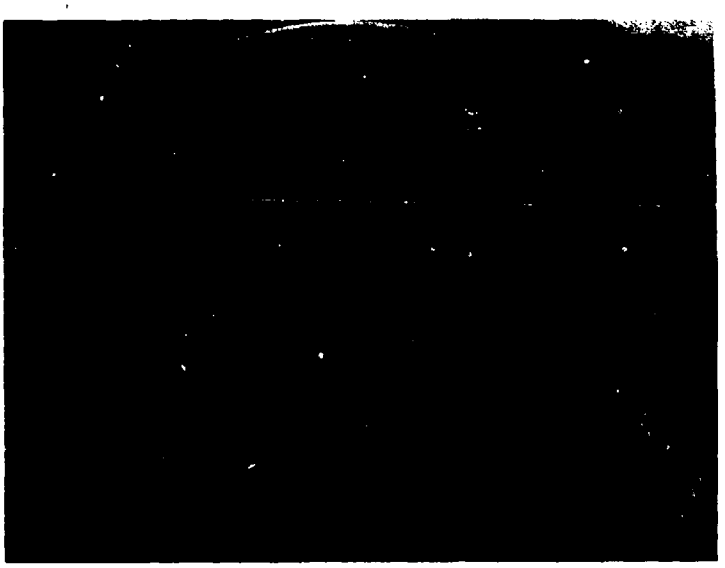

Figure 29. Rectangular pulse from an electronic pulse generator (similar to load pulse from Schmidt hammer)

107. The width of the pulse is 100 μsec from an electronic pulse generator. The first null of the frequency content curve is at $1/T = 10$ kHz ; the second null at 20 kHz and so forth. However, the frequency of the optimum energy is from 0 to 5 kHz. The next main peak would be at 15 kHz, then 25 kHz,

Figure 30. Spectrum of rectangular pulse from an electronic pulse generator

and so on. We can see that there is a component of energy up at higher frequencies that can be used to resonate a crystal. Not only will the broadband spectrum of energy from a Schmidt hammer excite the fundamental resonant frequency of a crystal 15 times higher in frequency than the optimum hammer frequency, but one could use a crystal having a fundamental resonance of 5,000 Hz $\left[\frac{1}{2}\ (100\ \mu\text{sec})\right]$ and only pass the fifteenth harmonic. This may be as efficient as the previous example.

108. With only limited investigation, it would seem that two of the main concerns of impact measurements are not a problem: (a) that a small transmitter area will create surface waves that will interfere with detection; and (b) that a sharp impact will not produce sufficiently high frequency energy to introduce ultrasonic energy into the concrete, near 200 kHz. Some disadvantages are that the spherical wave created will generate other interfering waves through mode conversion and also that a larger area of concrete will receive (and reflect) energy rather than a smaller desirable area just under the hammer.

109. Limited tests were made on determining the thickness of a concrete slab with an impact-resonant technique. Previously continuous wave measurements had been made in the time domain (Muenow 196). However these latter tests involved analysis in the frequency domain. The received signal was displayed with a frequency analyzer. In this test the longitudinal resonance in the thickness direction was detected with a broadband pickup, i.e., a pickup that was broadband in the range of the particular resonance of interest.

Figure 31 shows a resonance at 4200 Hz. The horizontal axis is scaled at 1 kHz/cm. The concrete slab tested was 1.5 ft thick, and was backed by soil. The energy was introduced with a Schmidt rebound hammer and the reverberations were detected with an accelerometer. The equation describing the relationship is:

$$v = 2 f \ell \tag{17}$$

where

v = concrete velocity (13,020 ft/sec)

f = frequency of resonance

ℓ = thickness, ft

The above measurement gave a thickness of 1.55 ft. The velocity used in the calculation was determined on a concrete wall adjacent to the concrete slab which was measured with a through-transmission type ultrasonic pulse velocity instrument.

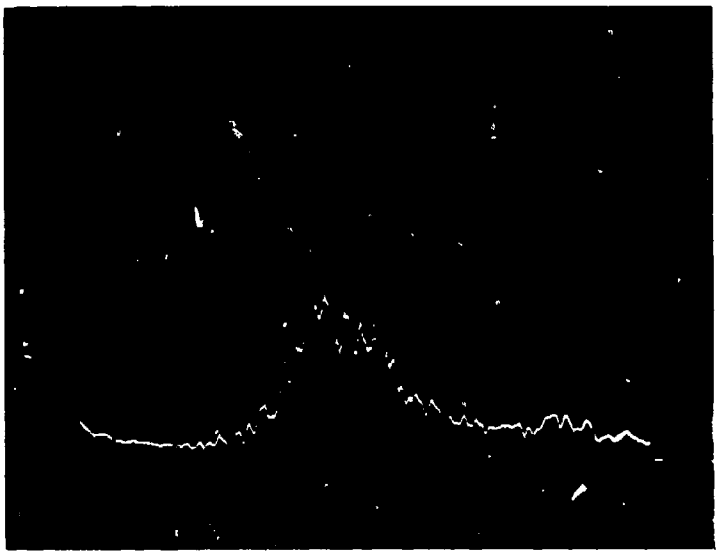

Figure 31. Response spectrum from a 1.5-ft-thick concrete slab from an impact with a concrete rebound hammer

110. Since the area of the hammer tip is small, the distribution of the energy introduced into the concrete would spread out in a hemispherical pattern with no directivity. It would be considered a point source. When energy enters an interface at angles other than normal, mode conversion takes place and other waves are produced (such as shear waves and Rayleigh waves). These combine with the longitudinal wave to create unwanted resonances, which

probably produce the broad band of energy displayed. However, the desired longitudinal resonance seems to dominate.

111. Since significant noise is centered around the resonance, the measurement could be difficult in another situation. The back wall echo would have to be improved considerably before flaw detection measurements could be made with confidence. Signal processing might improve the thickness measurements, and it is possible that a large concentration of small peaks might indicate the scatter that could be produced by deteriorated concrete. Also a more sensitive broadband pickup should be used to improve the signal to noise ratio. Although this test demonstrates that thickness measurements can be made in the sonic range it will require an ultrasonic measurement to obtain sufficient resolution for thicknesses of 1 ft or less.

112. This concluded the work with mechanical excitation (impacts). Attention was then turned to electrical excitation of piezoelectric crystals.

Restoration and modification of OSU transducer

113. WES recently received a transducer from the Pennsylvania State Highway Department that was in need of repair. This was one of the experimental transmitters built by OSU. The transducer housing is 18 in. in diameter with a 5-in.-diam hole in the center to accommodate a receiver. Two lithium sulfate receivers were also obtained, but the wear-plate surfaces were cracked and worn and as lithium sulfate is hydroscopic, the crystals had been damaged by moisture. The receivers were abandoned as they could not be repaired.

114. Contamination and loose connections in the ground circuit were causing arcing inside the transmitter and a signal that jittered about on the oscilloscope. Also, the 200-kHz resonance that the transducer was designed to produce was absent on the scope trace; however, a strong 40-kHz resonance was present. The transducer was dissembled, and the electrical connections and the method of ultrasonic coupling were modified. The aluminum foil that was in contact with the 14-PZT (C5400) elements was replaced with a copper foil and was bonded to the crystals with Loctite 326 to improve the ultrasonic coupling. Previously, stopcock grease had been used by OSU to couple the foil to the crystals. The grease tended to pick up dust and contamination and increased the likelihood of arc-over. Loctite 326 produces a very thin adhesive layer and does not electrically insulate the foil from the PZT electrode.

115. After restoration of the transducer, a 180-kHz resonance was present but obscured by the 40-kHz resonance previously mentioned. The set-up for the measurement of the thickness of a 9.25-in. slab is shown in Figure 32. The transmitter was excited by a gated sine wave pulse, as shown in Figure 33.

116. An electronic pulse generator was used to produce a rectangular pulse shown in the bottom of the trace. The width of this pulse determined the number of sine wave pulses emitted by the sine wave generator. This gated sine wave pulse was then amplified by a power amplifier used to drive the transmitter. A damped PZT-7A broadband receiver was used to receive the echo (see paragraph 134). The measurement is shown in Figure 34. Here, the 40-kHz resonance is strong and appears to arrive at roughly the expected time of 122 μsec. The horizontal time base is 50 μsec/cm. The pulse-echo time in the slab is 102 μsec with 20 μsec of system zero time making the total of 122 sec. However, a measurement made on a 2-ft-thick slab revealed that the received signal also arrived at about the same time as that shown above.

117. By using a filter in the high pass mode with cutoff at 100 kHz, the following signal was obtained (Figure 35). Resonance was approximately 180 kHz. The arrival time of 120 μsec, or so, is correct, but the onset of the received signal is much weaker than a few cycles later. The horizontal time base is 50 μsec/cm.

118. This small onset is due to the time required for a resonant circuit to reach full amplitude when the electrical Q is high. A highly resonant system (High Q) can only absorb energy slowly and conversely; a highly resonant system will ring for a longer time when the excitation is removed (Stein 1964).

119. The following statement from Acoustical Society of America (1959) further explains the action of the high Q OSU transducer.

> The term Q is also significant in describing the transient behavior of a singly resonant system which is less than critically damped ($Q > 0.5$), either mechanical or electrical. If the frequency of the force or voltage coincides with the natural frequency of the system, ($f_o = 1/T_o$), it takes Q cycles, or a total time QT_o, for the velocity or current to build up to 96 percent of its final (steady-state) value. Similarly, if the force or voltage is cut off, it takes Q cycles for the velocity or current to decay to 4 percent of its value at the time of the cut-off. Thus, Q is a measure of the duration of the transient and is used in specifying the build-up or decay time of the system under pulsed excitation conditions.

Figure 32. Thickness measurement (using OSU transducer)

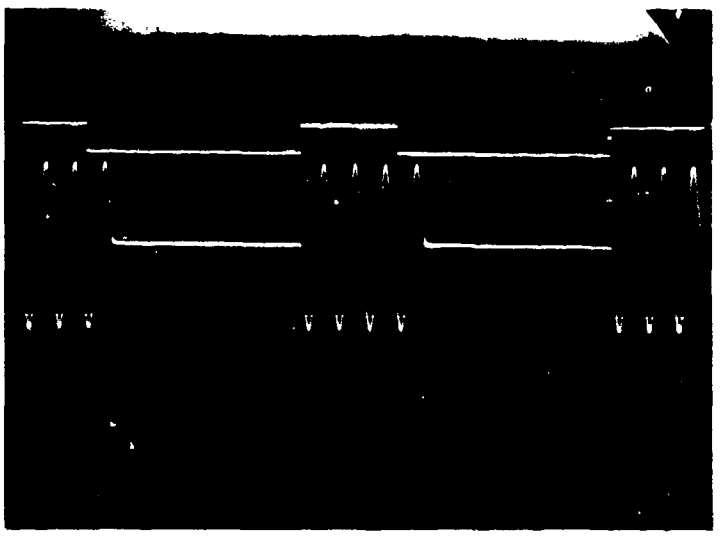

Figure 33. 200-kHz gated sine wave from oscillator (width controlled by rectangular pulse from pulse generator, 10 μsec/cm)

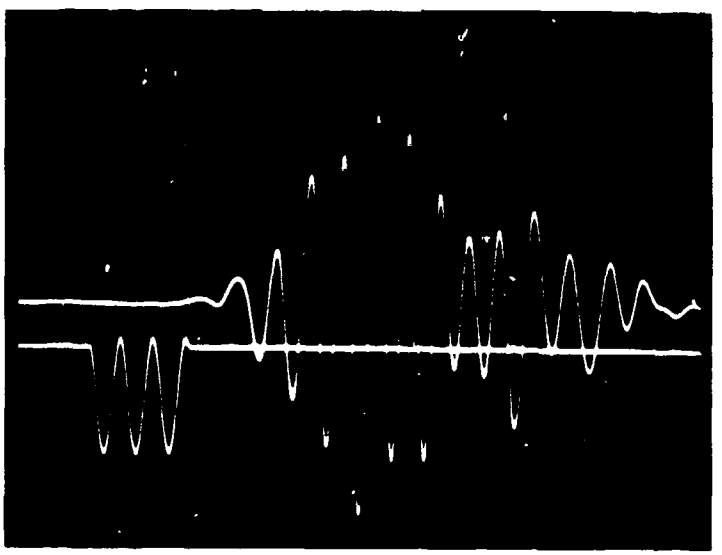

Figure 34. OSU transmitter excited by 40-kHz gated sine wave pulse and received by broadband PZT-7A transducer (50 μsec/cm)

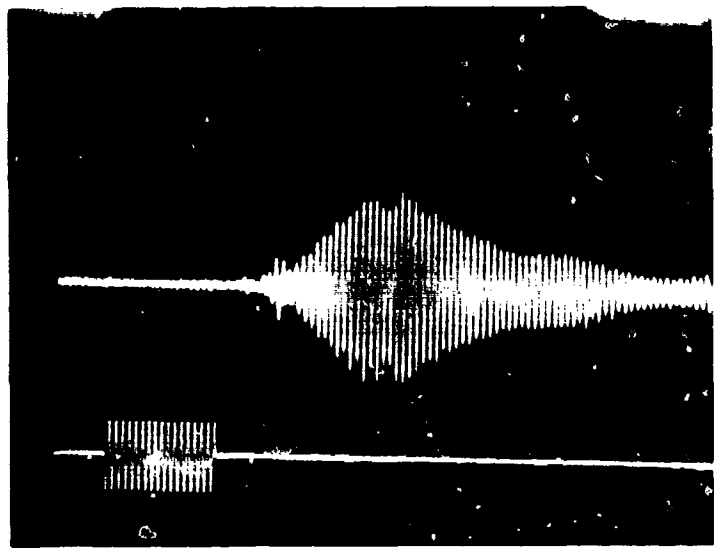

Figure 35. OSU transmitter excited by 180-kHz gated sine wave pulse with filtering and received by PZT-7A transducer (50 μsec/cm)

It appears from Figure 35 that about 17 cycles were required for the received signal to peak. So a time of (17) $\frac{1}{180,000}(QT_o)$, or 95 μsec, where $f_o = \frac{1}{T_o}$ was required to reach full amplitude. It also means that the transducer has a Q of about 17.

120. Shock excitation is necessary to get a sharp onset for the received signal. In other words, it is better to use an untuned pulser to excite the transmitter than a tuned pulser (see paragraph 71).

121. Considering this, measurements were then made with a pulser of the shock variety. A sharp capacitor discharge voltage of negative 600 V is applied to the transducer in about 1 μsec which then decays in an exponential pattern. Figure 36 shows the pulse-echo signal as received on the 9-in.-thick slab.

122. The onset of the received pulse is sharper, but the surface wave energy is also larger with the untuned pulser. Because a shock pulse consists of a band of excitation frequencies (many of them lower than the frequency of the wanted resonance), other modes of vibration in the lateral direction are excited. As already mentioned, lower frequencies produce energy with a larger angle of divergence which automatically (by the principle of diffraction) generates surface waves. The S/N ratio is about 4. Figure 37 shows a bandwidth measurement for one piezoelectric element of the large diameter OSU transducer.

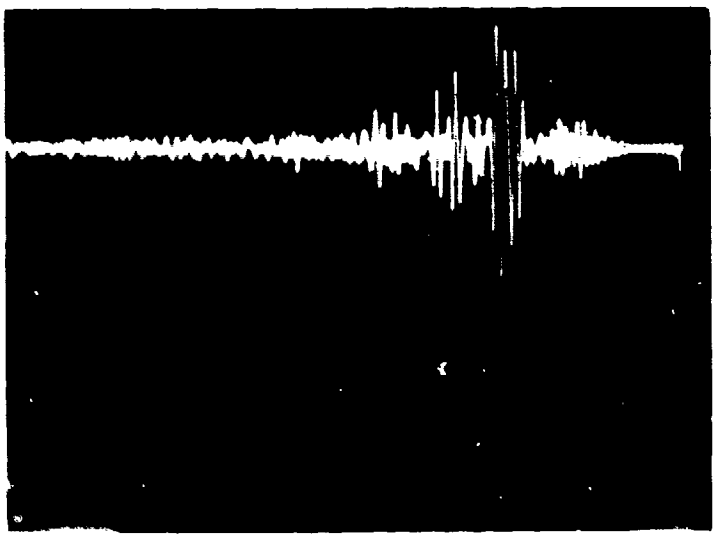

Figure 36. Received signal when OSU transducer is excited with a sharp capacitor discharge pulse (50 μsec/cm)

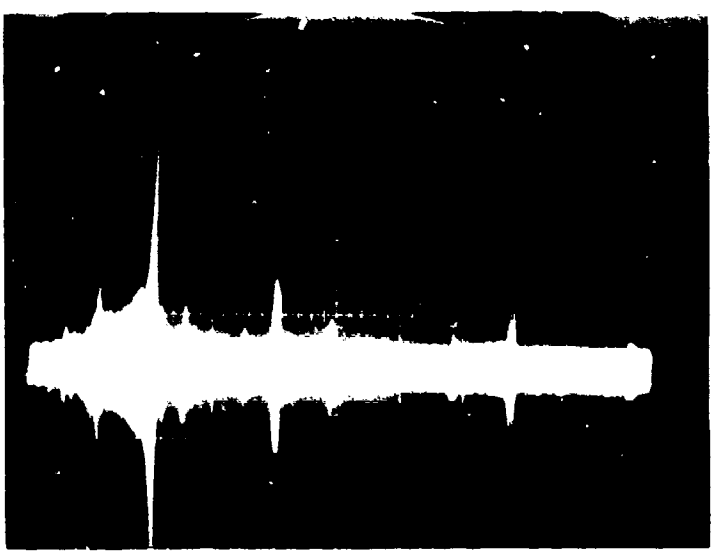

Figure 37. Bandwidth measurement of one PZT undamped wedge element from OSU transducer (1 mHz)

123. The resonance near 200 kHz is clear, with numerous spurious resonances above and below 200 kHz. The frequency axis is 100 kHz/cm and goes from 0 to 1 mHz. The following bandwidth curve (Figure 38) is 10 kHz/cm and goes from 0 to 100 kHz. Each PZT wedge is shaped like the following diagram (Figure 39). Fifteen wedges placed adjacent to each other will form a doughnut with an outside diameter of 16 in. and an inside diameter of 6 in. The transducer, however, is composed of 14 elements arranged in a ring each

Figure 38. Bandwidth measurement expanded over 0- to 100-kHz range. Mode conversion is very pronounced. Demonstrates need of a filter to eliminate extraneous resonances

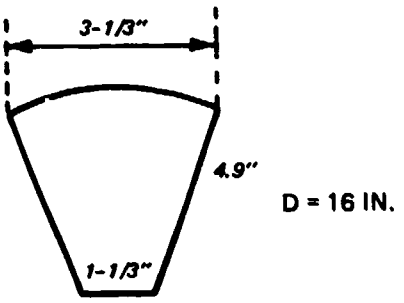

Figure 39. PZT wedge

separated by about 1/4 in. along the outside circumference. The housing is 18 in. in diameter with a 5 in. hole in the center.

124. The capacitance of the mosaic after reassembly was 0.1065 μf with a dissipation factor of 0.0005. This agreed with the calculated capacitance of the mosaic (0.126 μf) quite closely. This was down about 10 percent from the capacitance at construction, but the PZT elements (Channel 5400) were 14 years old. A representative of Channel Industries said this aging was typical. Measurement of the capacitance with an impedance bridge is a good way to test the quality of the piezoelectric element, and the dissipation factor will test for leakage paths or power loss in the ceramic.

125. The length of the near field for an 18-in.-diam transducer with a frequency of 180 kHz in 15,000-ft/sec concrete is 6.7 ft (see Equation 1). Mailer (1972) states that he measured the length of the near field to be 1-2/3 ft (20 in.). This is the correct length if the transducer was operating at approximately 40 kHz. By using a high pass filter, this would have eliminated this low frequency energy. The problem could be a spring-mass resonance in the transducer housing or could be the lateral oscillations in the PZT crystals generating the low frequency large amplitude noise. A diameter of 8 in. would produce a near field at 16 in. for a transducer of 180 kHz in 15,000-ft/sec concrete. This should be ideal for measuring the thickness of a 9-in. slab or pavement as the two-way distance would be 18 in.

126. The OSU transducer represents the best in the pitch-catch measurements made in concrete. Probably, the high input energy of the OSU transducer overcomes many of the hindrances to pulse-echo measurements in concrete. Certainly credit should be given to the engineering team that persevered for a number of years to understand and record many of the concepts that influence pulse-echo measurements in concrete. Now that backwall echoes can be seen in concrete, it should be possible to improve the S/N ratio of the echo signal to detect reflections of much smaller energy from flaws and defects.

Ultrasonic pulse-
echo prototype system

127. Another transducer that incorporated most of the important principles in flaw detection was designed and constructed here at WES. Eight PZT-5H plates were bonded to a 1/4-in. thick-aluminum faceplate, as shown in Figure 40.

128. As shown in Table 2, PZT-5H has the best transmitting constant (d_{33}) and has the lowest mechanical Q for any of the PZT types. Both of these characteristics are highly desirable for an active transmitter with a minimum of ringing. The plates were 1-1/2 by 1 by 1/4 in. The total dimension of the mosaic was 3 by 4 in. It was hoped that the larger area of the transducer would collimate the beam enough to provide a strong echo with a minimum of surface waves. The acoustic impedance of aluminum is a good match between PZT and concrete, as already explained in paragraph 67. The top electrodes were connected by soldering a lead wire to each plate. The plates are coated at the factory by an evaporation process that deposits a thin layer of nickel on the plate elements. The bottom electrodes become part of the case ground for

Figure 40. 3- by 4-in. PZT-5H mosaic transducer

the aluminum housing. The plates were bonded to the aluminum with Loctite 326. The plates were then thinly coated with epoxy to provide electrical insulation for the backing. Tungsten mixed with epoxy was then placed over the mosaic to further damp the amplitude at resonance of the crystal. Mylar was used around the sides of the housing as an insulator to prevent electrical conduction between the backing and the aluminum ground.

129. The bandwidth of a single undamped element is shown in Figure 41. Mode conversion is significant and produces many unwanted modes. Although these elements are supposed to be the most active in the thickness mode, a much higher amplitude resonance is displayed in the 1-in. direction, or transverse direction. According to Vernitron, the frequency constant in the thickness direction is 78 kHz × in. This means that the resonant frequency for the 1/4-in. direction is as follows:

$$f \times th = 78 \text{ kHz} \times \text{in.}$$

$$f = \frac{78 \text{ kHz} \times \text{in.}}{0.25 \text{ in.}} \qquad (18)$$

$$f = 312 \text{ kHz}$$

This agrees with the 315-kHz resonance measured. In the transverse directions the frequency constant is 56 kHz × in. For the 1-in. direction this calculated to be 56 kHz x in. It measured about 60 kHz. This was the largest amplitude

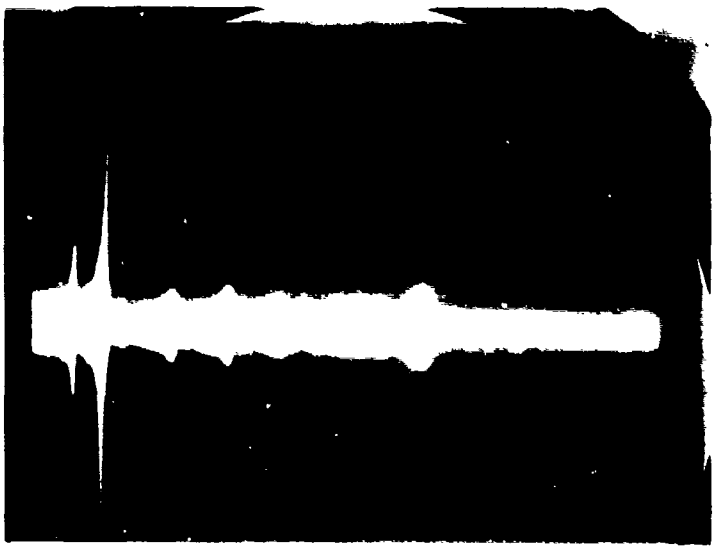

Figure 41. Bandwidth of an undamped PZT-5H piezoelectric plate element (0 to 500 kHz)

resonance shown. In the 1.5-in. direction the calculated frequency was 37 kHz. It measured about 32 kHz.

130. When the eight elements were installed in the aluminum housing before the tungsten-loaded epoxy was installed, the undamped bandwidth still looked like that in Figure 41. After the mosaic was damped with the loaded epoxy, the 312 kHz resonance was almost gone but a resonance with low amplitude occurred at 100 kHz (Figure 42). It may be that the tungsten in the backing could have been reduced without creating excessive ringing. About a 1-in. depth of loaded epoxy was placed over the mosaic. As the backing material also covered the edge of the plates, this may have been significant in reducing the transverse modes of oscillation.

131. The length of the near field, N , is calculated as follows:

$$N = \frac{D^2 - \lambda^2}{4\lambda} \qquad \text{(1 bis)}$$

$$N = \frac{(4 \text{ in.}/12)^2 - (0.15114 \text{ ft})^2}{4(0.15114) \text{ ft}} \qquad (19)$$

$$N = 0.146 \text{ ft} = 1.75 \text{ in.}$$

where

$$\lambda = \frac{v}{f}$$

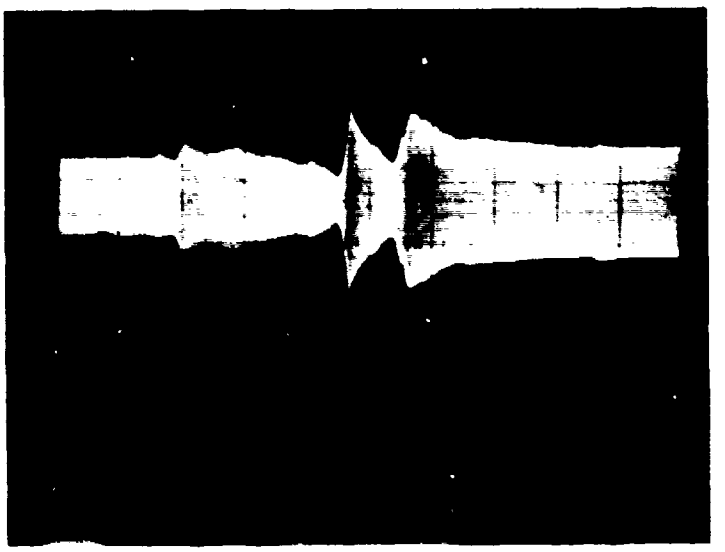

Figure 42. Bandwidth measurement of PZT-5H mosaic transducer damped with backing of tungsten-loaded epoxy (0 to 200 kHz)

$$\lambda = \frac{15,114}{100,000} = 0.151 \text{ ft}$$

$$\lambda = 1.81 \text{ in.}$$

The half angle of divergence in the far field would calculate as follows:

$$\sin \alpha = \frac{\lambda}{D} = \frac{1.81 \text{ in.}}{4 \text{ in.}} = 0.4525 \qquad (20)$$

(see paragraph 53)

$$\alpha = 26.9°$$

132. The area covered on the back surface of a 9.25-in. thick slab, measuring by the through transmission technique, would be as shown in Figure 43.

133. Although, ideally, one would need to make measurements in a water tank with a tiny receiver to map the correct sound field at a constant distance from the transmitter, it was noticed (by moving the receiver around on the flat surface) that the receiver detected a strong signal over roughly the same range as that calculated. Obviously, in the 3-in. direction of the transducer, the divergence would be greater than the 4-in. direction and a larger dimension would be illuminated in that direction. The near field would be shorter as calculated by Equation 1.

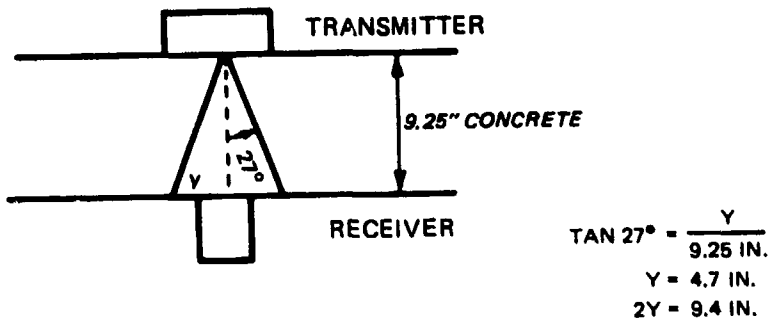

Figure 43. Area illuminated at bottom surface of concrete

134. The receiver used was a PZT-7A transducer built by a transducer manufacturing company. A broadband transducer was requested with a Q of 0.5. A bandwidth measurement revealed that the admittance was fairly flat over the range from 0 to 1 mHz. Four 1-in.-square piezoelectric elements of 9/16-in. thickness were stacked together for a total of 2-1/4-in. height. A cone-shaped backing of tungsten-loaded epoxy to damp the crystal and electrical filtering was used to produce a uniform bandwidth. Full details of the transducer are not known as it is proprietary information. The transmitter was excited by a 1400-V capacitor discharge pulser with a repetition rate of 100 pulses per second (pps). The presence of surface wave energy was too high to discern the pulse reflected from the base of the 9-1/4-in. slab. Later, calculations were performed to determine the angle required for some plexiglas wedges in order to direct the center of the beam toward the receiver. With the transmitter and receiver separated by about 5 in., the wedge angle calculated was 8.56°. Figure 44 shows the measurement configuration. Figure 45 shows the pulse-echo measurement. The system zero time plus the time through the wedges is 15 μsec. The arrival time of the reflected wave is about 120 μsec, leaving 105 μsec for the travel time through the slab. The one-way transmission time through the slab measured by other methods is about 51 μsec for a total of 102 μsec in the pulse-echo mode. Since the beam travels a longer path rather than straight down the back, this accounts for the other 3 μsec as shown in the following calculation and Figure 46.

$$(Z/2)^2 = (2.25)^2 + (9.25)^2 \qquad (21)$$

$$Z = 19.04 \text{ in.}$$

Figure 44. Pulse-echo measurement showing PZT-5H transmitter, 2.25-mHz lithium sulfate receiver, concrete slab, and Plexiglas wedges in foreground, OSU transmitter, and PZT-7A receiver in background

Since transmission time is directly related to path length of travel when the velocity is constant, a 2.92 percent increase in distance means a 2.92 percent increase in time, which is about 3 μsec for a slab with a round-trip time of 100 μsec, as this one is. The S/N ratio is about 2.

135. An undamped, lithium sulfate transducer was requested from another transducer manufacturer in an effort to improve the sensitivity of the received signal. Although the transducer was a resonant transducer at 2.25 mHz, it was still operated as a broadband receiver down at 100 kHz. Since it is difficult to damp low-frequency transducers, it was thought that the high receiving sensitivity of undamped lithium sulfate might exceed that of damped PZT. Although the sensitivity was about the same as the PZT-7A at the frequency of 100 kHz, the lithium sulfate receiver did not respond to surface waves as much as the PZT. As a result, the wedges could be eliminated, if desired. The measurement is shown in Figure 47.

136. The zero time was reduced to 2 μsec without the wedges, and of course the path length is now almost normal to the surface--reducing the arrival time. The arrival time is about 104 μsec making the time through the concrete to be 102 μsec. The S/N ratio is about 3.5, with the noise consisting of mainly surface wave energy or scattering. As shown in Table 1, interfering oscillations (coupling coefficient) in the transverse direction are much more pronounced with PZT and barium titanate than with lead metaniobate or lithium sulfate. This is apparently why the lithium sulfate receiver would work without the wedges while the PZT receiver would not. Therefore, a

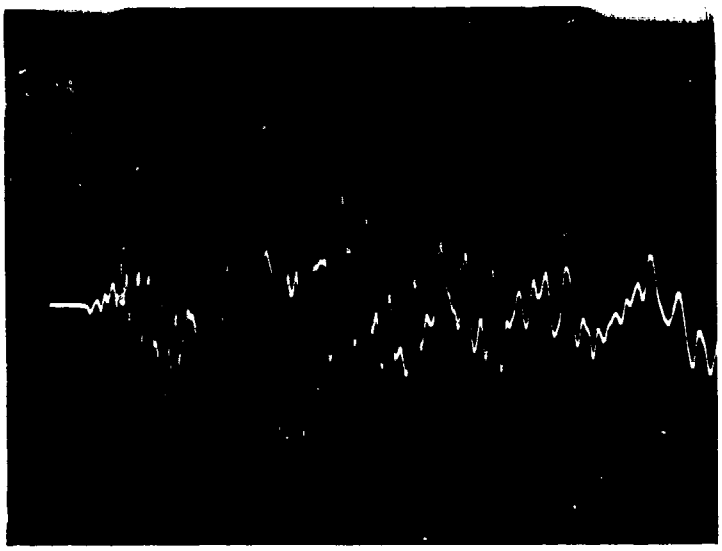

Figure 45. Ultrasonic pulse-echo measurement through 9-1/4-in.-concrete slab with PZT-5H as transmitter and broadband PZT-7A transducer as receiver, S/N ≈ 2 (0 - 500 μsec)

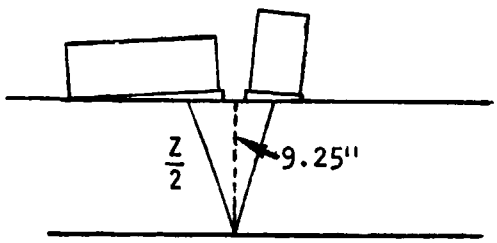

Figure 46. Percent increase in path length = $\frac{19.04 - 2(9.25)}{2(9.25)}$ = 2.92 percent

decision was made to build a transmitter with lead metaniobate and to risk sacrificing some output energy in an effort to reduce interfering transverse oscillations.

137. Meanwhile, a second lithium sulfate receiver constructed by the same transducer manufacturer was received by WES. The fragile nature of lithium sulfate to moisture required that someone skilled in the art build the transducer. A receiver resonant at 200 kHz and damped to a Q of 3-5 should be more sensitive at 200 kHz than the undamped 2-1/4-mHz resonant lithium sulfate receiver. The area of the receiver was about 2.35 $in.^2$ An S/N ratio of 3.6 was obtained when the PZT-5H transducer was used as the transmitter and the 200-kHz lithium sulfate as the receiver. There was no significant improvement of the latter receiver over the former (Figure 48).

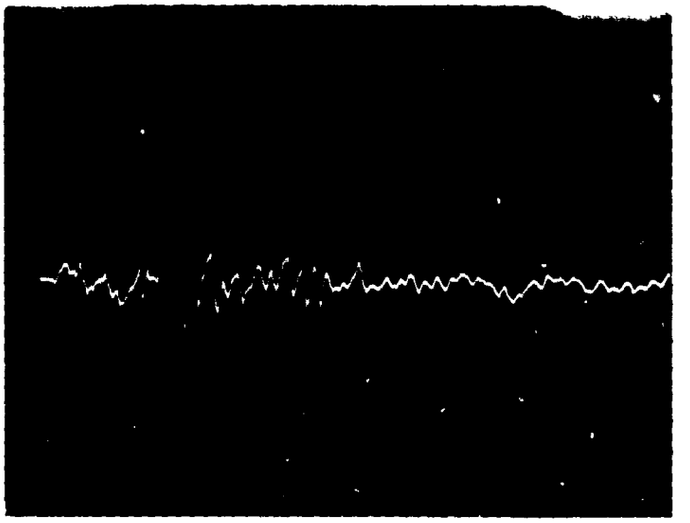

Figure 47. Ultrasonic pulse-echo measurement through 9-1/4-in.-concrete slab with PZT-5H transducer used as transmitter, and resonant 2.25-mHz lithium sulfate transducer used as receiver, S/N = 3.5 (0-500 μsec)

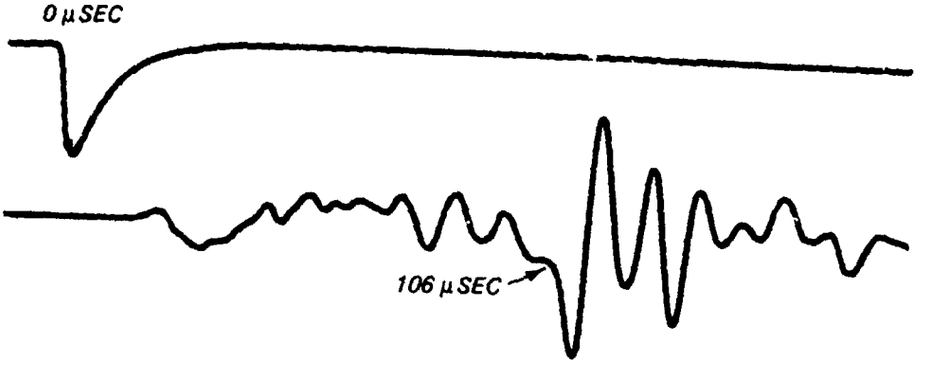

Figure 48. Echo signal through 9-1/4-in.-concrete slab using PZT-5H transducer as the transmitter and 200 kHz damped lithium sulfate transducer as the receiver, S/N = 3.6

138. The next transducer was constructed of four piezoelectric plates (2.35 by 2.35 by .28 in.) of lead metaniobate (EDO Western EC-82). The plates were connected in parallel electrically as shown in Figure 49. The total dimension were 4.7 by 4.7 in. The plates were polarized in the thickness direction to generate longitudinal waves like the previous PZT-5H transducer.

The undamped frequency was 200 kHz with a frequency constant of 56 kHz × in. The mechanical Q was 11 in air. After the plates were bonded with Loctite 326 to a 1/4-in.-thick plate of plexiglas, the resonant frequency dropped to 192 kHz. With a new Q of 2.6 no external damping was necessary on the back face. On the same 9-1/4-in.-thick control slab, the thickness measurement had a S/N ratio of 18 (Figure 50), when the lead metaniobate was used as the transmitter and the PZT-5H with the aluminum housing was used as the receiver in a pitch-catch configuration.

139. The PZT-5H receiver was terminated with 4 ft of 50-Ω coaxial cable

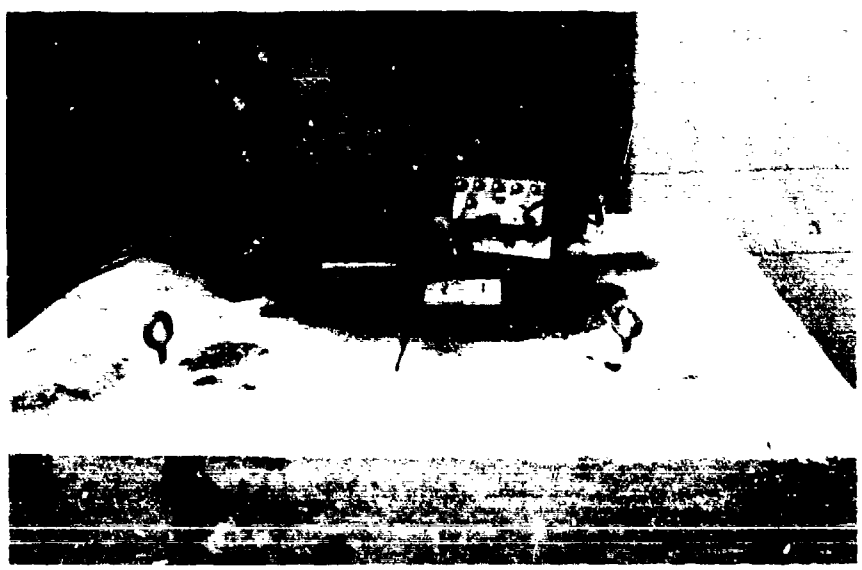

Figure 49. Lead metaniobate transmitter, PZT-5H receiver, pulser/receiver, and oscilloscope used to make ultrasonic pulse-echo measurement on concrete

with a 470 μh inductor shunted across the cable end of the 1 MΩ input impedance of the oscilloscope to tune out the static capacitive reactance of the PZT-5H transducer and cable. (The inductor could also be tied in parallel across the cable at the transducer end.) The inductor improved the S/N ratio by 50 percent and increased the level of the signal (see paragraph 74). Also, a series inductor was added to the transmitter which increased the output but did not improve the S/N ratio. The lead metaniobate was shock excited with a capacitor discharge pulse of -1390 V. It had a rise time of 150 μsec. The width of the pulse was 250 μsec at -768 V, 1 μsec at -492 V, and 2 μsec at -288 V as the pulse decayed. It was repeated at a rate of approximately 100 pulses/sec.

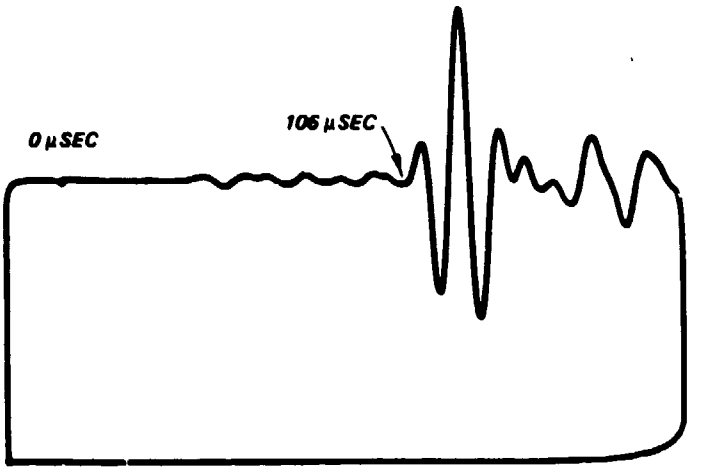

Figure 50. Echo signal through 9-1/4-in.-thick concrete slab using lead metaniobate transmitter and PZT-5H receiver in a pitch-catch configuration, S/N = 18

140. Although all the tests in this report (where the system was excited by a shock pulser) were done with a large, bulky, high voltage, tube-type, laboratory-built, capacitor discharge pulser (untuned pulser), it was decided that a smaller transistorized commercially available pulser would be more appropriate for field measurements and for technology transfer. Therefore, recent tests made with a Panametrics Model 5055 pulser/receiver (Figure 49) demonstrated that the system worked well for thickness measurements made on the same concrete slab mentioned in this report. Although this system only has an output of -350 V, it should suffice for shorter penetration distances. The calculated half angle spread for the transmitter is 11-1/2° and the near field length is 6 in. The noise in front of the back surface echo is not electrical as a through transmission measurement on the control slab verified that the S/N ratio was 300. A sawcut was made to test for surface waves between the transducers. The cut was made 1-3/4-in. deep (more than one Rayleigh wavelength) and 24 in. long. The cut failed to change the signal to any appreciable degree. Therefore, the noise is likely due to scattering as the wavelength (0.9 in.) of the ultrasonic pulse is comparable to the aggregate dimensions (3/4 in.-limestone).

141. It would seem that it might be possible to detect the presence of deteriorated concrete based on the degree of scattering. Microcracks and fractures should return a larger amplitude of "grass," although there has not been an opportunity to test this idea (see paragraph 44).

Summary

142. Many factors combine to make pulse-echo or pitch-catch measurements in concrete difficult. Obviously, before a system can detect flaws in thin sections, it first must be capable of measuring thicknesses. Back wall reflections contain much higher energy levels than those from cracks or flaws. Presently with a S/N ratio of about 18, the direction of our future effort should be at this stage to improve thickness measurements. But the basic design is now operative and the predominant problem hindering improvement in the S/N ratio now becomes easier to test. Every physical problem to be solved usually turns on a few critical principles, and it will be this way with ultrasonic pulse echo in concrete.

143. We know that 200 kHz is about the upper limit for making measurements in concrete. The grain size at that frequency is about the same dimension as the wavelength and the ensuing scattering becomes a problem for it at higher frequencies. Also, the high attenuation of concrete requires a higher wattage power supply for the transmitter pulses than is normally required in commercial metal pulse-echo units. Also, it is important that the diameter of the transducer be large enough to get directivity of the sound beam approaching that of commercial units used in metal flaw detection. Surface roughness of concrete is a problem but can be dealt with satisfactorily by using a good liquid couplant (castor oil, water, gylcerine) and maintaining a wavelength that is at least 10 times more than the peak-to-valley distance on the concrete surface. Ringing of the transmitter has been a real problem but can be reduced significantly by damping with tungsten-loaded epoxy and/or using a piezoceramic with a low mechanical Q. Also, the transmitter and receiver should be kept as separate units (pitch-catch mode). Since the two-transducer system works best, then angle probes may be an improvement over normal probes to get a directed beam. Also, both transducers can be tuned separately with electrical matching. Other important principles are that the transmitter should have a large d_{33} constant and the receiver a larger g_{33} constant. PZT for the transmitter and lithium sulfate for the receiver produce the largest loop gain although other piezoelectric properties may be more important factors. Finally, in the situation with the OSU transmitter, it has been necessary to use a high pass filter to reduce the effects of a low-frequency resonance due to the housing or due to the lateral oscillation of the PZT elements, or both.

144. The outstanding problem that still exists is the presence of surface waves. When the frequency is lowered below 200 kHz to reduce scattering, then surface waves appear. The following ideas are presented to show ways to increase the S/N ratio of a system. It is now known that the lateral ringing in PZT ceramics may be one of the main sources of unwanted surface wave energy for pulse-echo measurements in concrete. The electromechanical coefficient k_{33} for PZT-5h is 0.75 in the thickness direction, and the planar coupling coefficient (k_p) is 0.65 in the transverse direction. The interfering transverse oscillations are 87 percent of the desired longitudinal oscillation. However, lead metaniobate has a k_{33} of 0.38 and a k_p of 0.066. The unwanted oscillations are only 17 percent of the wanted energy. This could make a significant difference in pulse-echo measurements even though d_{33} (transmitter constant) is only about 14 percent of that for PZT. Less mechanical damping will be required for lead metaniobate, however, as the Q is only about 18 percent of that for PZT. Also, the acoustic impedance of lead metaniobate is closer to that of the concrete--resulting in less energy loss at interfaces. Lead metaniobate has a lower dielectric constant and will require a larger pulser voltage than PZT to obtain an equivalent output, but this is not a serious problem.

145. Another way to reduce the lateral ringing in the crystals is to use damping material around the edges of the ceramic (Krautkramer and Krautkramer 1977). Harisonics in Stamford, Connecticut, has drilled a hole in the middle of PZT discs and has provided plates to break up the interfering oscillations. Then, tungsten-loaded epoxy is placed in the hole. This only helps and is not totally effective.

146. Kossoff bonded a small rubber cube to the back face of a piezoceramic crystal which was then covered with backing material. The area underneath the cube was not plated with electrode material. This cube broke up the radial symmetry of the element and increased the dynamic range of the transducer 6 dB (factor of 2) (Kossoff, Robinson, and Garrett 1965). The dynamic range is the ratio of the main pulse to the interfering oscillations that "tails" behind the main pulse.

147. Bradfield suggests sectionalization of the transducer elements to reduce lateral ringing (Bradfield and Gatfield 1964). The authors assume he means to slice the ceramic elements in such a way as to break up the symmetry of the crystals. Also, "...square transducer plates, or transducers subdivided

into squares, do not radiate uniformly in all directions, but in the shape of a four-lobed direction pattern. By rotating this probe around the contact point interfacing, echoes can be distinguished from true echoes" (Krautkramer and Krautkramer 1977). Transducers with metal casings should have the ceramic elements isolated from the metal as the metal has a higher Q and will tend to ring unless isolated with an acoustic damping material. Materials such as Corprene, cork, rubber, nebar, and nylon can be used. Also, the profile of the metal casing can be broken up to reduce ringing (Wells 1977). Plexiglas housings can reduce this problem also.

148. Claytor used a unique idea to reduce surface wave interference. A surface wave will not radiate into a liquid if the longitudinal wave velocity in the liquid is greater than the Rayleigh wave velocity in the concrete. He used a liquid buffer of glycerin between the PZT-5A element and refractory concrete in both the transmitter and receiver. Although glycerin has a longitudinal velocity of 6,200 ft/sec and is less than Rayleigh wave velocity of concrete of about 7,800 ft/sec, still the angle of radiation into the liquid is more indirect and, therefore, the crystals are not excited as strongly from the Rayleigh wave interference. He obtained an S/N ratio of 8, the noise being primarily the surface wave energy (Claytor and Ellingson 1983). The S/N ratio may be better than what could be obtained in concrete as refractory concrete has less scattering due to smaller grain size. The frequency of operation was 250 kHz.

149. Transmitters that are pulsed with sharp high voltage pulses tend to excite all modes of oscillation in the crystal. This is because a short pulse contains energy over a wider range of frequencies unlike the energy from a gated sine wave. By incorporating a matching transformer that is tuned to the frequency of thickness expansion in the crystal, this may improve the amplitude of resonance as well as serve as a band pass filter to reject energy that excites the lower lateral frequency modes in the crystal element. In some cases, a plaster of cement paste can be placed over a concrete surface that is very rough. A piece of glass can be used during curing to maintain a flat surface. This will reduce surface wave interference (Bradfield and Woodroffe 1953). For transducers that have a spring-mass resonance, a filter can be used to reduce some surface wave interference. Ideally, the housing should be damped to dissipate the energy of resonance, but it is difficult to damp well at low frequencies. Most all materials increase in their damping as

the frequency goes up. Surface waves are more predominant at frequencies below 1 mHz (Krautkramer and Krautkramer 1977).

150. For measurements made by impact the following suggestions are made. The problem of ringing in the transmitter does not arise if the pulse produced by the impact is a one-shot pulse with no added aftershocks. The L-6 Schmidt hammer, for instance, continues to deliver impacts at a rate of about 17 impacts/sec with decreasing intensity, but this does not present a problem as the second impact comes about 60 msec after the first one. As an example, it only takes 100 μsec for the P-wave to make a round trip in a 9-in. thick slab. All measurements would be over with before the second impact occurred. However, energy immediately following the first pulse must be eliminated, or reduced. It could be that the hammer could be modified to prevent ringing in the housing--should any be present. This may be the source of confusion WES has had in the resonant measurements. Also, other waves are probably created by mode conversion which can complicate the echo trace. Although more tests are needed, it appears that impact measurements with a resonant receiver may have potential for quick and simple measurements. No hammer will produce a pulse as reproducible as a piezoelectric crystal, but a variation in amplitude of output is not too important when time separation measurements are the goal.

151. A number of suggestions are made here to improve the impact measurements with a resonant receiver.

a. Obtain signal-processing equipment that will allow averaging of a few impact measurements in situations where the received signal is weak.

b. Modify the Schmidt hammer by reducing the mass of the hammer head and thereby increase the energy output of the higher frequencies.

c. Use high-pass filtering with a sharp cutoff of 80 dB/octave to eliminate the low-frequency vibrations that will certainly be present on small structures. Vibration may not be a problem on massive structures such as a dam. Use a good low noise amplifier after the filter before going to the oscilloscope.

d. Damp the PZT receiver with epoxy-loaded tungsten. Use only enough epoxy to permit mixing and use pressure, if possible, to force out the excessive epoxy. Do not try to get a flat broadband receiver but only lower the Q to 1 to 3 according to how much ringing can be permitted. The transducer should remain a resonant receiver to maintain sensitivity. Have a transducer company build a lithium sulfate receiver if more sensitivity is required, or if it appears that lateral ringing is producing noise.

e. Make a receiver with a larger contact area (7 in. or so for a 9-in. slab) to obtain directivity. When fabricating a rectangular crystal element or array, the dimension perpendicular to the sagittal plane (focusing plane) may be smaller.

f. Use wedges to eliminate echoes from unwanted directions. Otherwise, since the energy spreads out in a large angle of divergence for a point source such as a hammer, echoes can come from horizontal directions and be interpreted as coming from directly below the hammer.

152. To illustrate further the idea of making impact-echo measurements at ultrasonic frequencies, consider using a Schmidt rebound hammer with a low Q (1-3) resonant receiver having a center frequency near 50 to 100 kHz. The energy introduced into the concrete would be broadband with energy from 0 to 200 kHz. Naturally, the energy would be low at 200 kHz. If a 1/8-in. crack was irradiated by the input energy, a reflection would take place probably with a ringing tail. Air-gap resonance could take place (Carlin 1960) as the energy reverberated across the gap until the energy was dissipated. Resonance takes place at 1/2 wavelength.

$$\lambda = 2\,\ell = 2 \times 1/8 \text{ in.} = 1/4 \text{ in.}$$

$$v = f\lambda \tag{22}$$

$$f = v/\lambda = \frac{1100 \text{ ft/sec}}{(1/4 \text{ in.}) \frac{1 \text{ ft}}{12 \text{ in.}}} = 53 \text{ kHz}$$

Since every defect would produce a different center frequency and a different decay rate, it would require that broadband energy be introduced into the concrete and received by a receiver with a broad bandwidth. Because the echo produced would be low-level energy, it would require signal processing to build it up for detection as well as good signal rejecting techniques to eliminate low-frequency energy caused by the impact. So measurement by impact may be possible if high-frequency energy (> 20 kHz) can be introduced into the concrete and the resulting low-level echoes properly detected.

153. The technique of sonic impact measurements using a broadband transducer is not recommended for thin sections of concrete even if the receiving transducer is perfect in sensitivity and reproduction. The rise time is simply not sharp enough with energy below 20 kHz. It could be that a shorter pulse

with sufficient intensity could be generated by some means such as a small explosion, or by laser generation, or some other means to generate energy around 100 kHz, or higher. If that is possible, then impact measurements with a nonresonant transducer might have potential. Also sonic measurements on large structures could have promise.

154. Also, if signal processing could be used to reject the sonic energy and possibly pull out small low level resonances from the main energy that may reverberate from a flaw or discontinuity, then a broadband measurement with hammer impact may be feasible. It should be emphasized that the equipment needed should be capable of high-powered signal rejection capabilities for some frequencies and considerable amplification factors for other frequencies. It should be capable of adding impact signals to further build up the small buried signal. Only then could this idea be tested sufficiently.

PART III: TASK II - UNDERWATER MAPPING AND PROFILING

155. The objective of Task II was to screen and investigate systems and technology presently available which might be applicable to the mapping and profiling of underwater concrete structures (such as stilling basin slabs and lock chamber floors). Systems and technology with developmental potential for application to this task were evaluated. The ultimate goal was to develop a field-testing system.

The Problem

156. The problem was to obtain rapid, accurate, bottom-contouring data on submerged structures while avoiding the expense of dewatering and the inaccuracies inherent in diver-obtained data. A survey of erosion/abrasion damage repairs indicates that dewatering accounts for over 40 percent of the total repair cost. Dewatering is often necessary since the extent and location of damage must be known to determine what steps should be taken to correct the damage and to prepare valid cost estimates. Task II of the joint CE-USBR NDT R&D program was initiated to produce a mapping system which would provide (without dewatering) an accurate and comprehensive evaluation of top surface wear on horizontal surfaces such as aprons, sills, lock chamber floors, and stilling basins, where turbulent waterflow (which carries rocks and debris) may have caused erosion/abrasion damage.

Underwater Inspection Techniques

157. The safety of a structure depends on the physical integrity of both the superstructure and substructure. The superstructure generally receives much more attention than those parts of the substructure located below the waterline. It is essential, from a safety standpoint, that the underwater portions of a structure be adequately inspected, maintained, and repaired as necessary (Stowe and Thornton 1984).

Divers

158. The syntheses by Lamberton et al. (1981) and Rissel et al. (1982), and the work by Brackett, Nordell and Rail (1982) are excellent references on the inspection, maintenance, and repair of substructures below the waterline.

Lamberton's synthesis is a survey of practices of a number of state highway agencies, selected railroads, and turnpike and bridge authorities. The report identifies the policies, procedures, and techniques currently used to inspect underwater bridge substructures.

159. All of the techniques presented require a diver to locate the area of the defect, make the measurements, and either record the results or relay them to the surface by means of a diver communications system. In every case, the diver must be knowledgeable about the "normal" condition of the structure and types of damage/defects which may be encountered. Experience requirements for the diver may be reduced in many instances by using an underwater video system. This allows both real time observation of the inspection by a facilities engineer and video tape documentation of severely damaged areas.

160. Visual inspection is usually the first test that is applied for underwater evaluation. Its purpose is to confirm the as-built condition of the structure and detect severe damage to the structural elements (Level I inspection), and to detect surface damage (Level II inspection). In certain cases, this can be done from above the water by using an underwater scope. At Chief Joseph Dam, engineers made underwater observations through the use of a 35-ft-long underwater scope equipped with a 6-in.-diam bottom glass and a high power telescope (McDonald 1980). Visual inspection is quick, easy, and nondestructive. However, there are numerous limitations to this type of inspection technique resulting from the environment, the diver, and defects which are not obvious on the surface of the structure. Visual inspection is qualitative in nature and does not provide information about concrete strength or other quantitative properties. Visual inspection by divers can provide much useful information and locate some defects, but there is much desirable information which cannot be provided by visual inspection.

161. Many substructures are in water so turbid that visibility is severely limited. In this type of environment the diver must touch and feel the substructure to detect flaws, damage, or deterioration. Divers may conduct an inspection using only tactile methods in zero visibility, but it is difficult, if not impossible, to accurately assess the condition of a structure using this technique. The task is even more difficult in cold water, or when there is a strong current, or where the structure is coated with marine deposits.

Ultrasonic pulse velocity

162. Ultrasonic pulse velocity (ASTM C597-71/CRD-C 51-72) is determined by measuring the time of transmission of an acoustic pulse of energy through a known distance of concrete. The velocity of the pulse is proportional to the dynamic modulus of elasticity which, in turn, infers concrete strength. The results can be affected by many factors including aggregate content and reinforcing steel location. The results obtained are quantitative, but they are only relative in nature. Pulse velocities need to be correlated with other tests such as corings, in order to obtain absolute values. That is, the test is not reliable enough in its present form for direct strength determination but evaluates homogeneity and crack location quite well. Underwater use of this method has been limited.

Echosounders

163. Echosounders (specially fathometers) are effective in checking scours in the streambed. However, when an echosounder is used very close to the structure erroneous returns from the structural elements underwater may occur. Consequently, undermining of piers or abutments cannot be adequately detected with an echosounder. Furthermore, the broad sonic beam and inadequate resolution make it unsuitable for mapping erosion damage to horizontal concrete surfaces.

Side-scan sonar

164. A side-scan sonar system is similar to the standard bottom-looking echosounder except that the signal from the transducer is directed laterally, producing two side-looking beams. The system consists of a pair of transducers mounted in an underwater housing, or "fish", and a dual channel recorder connected to the fish by a conductive cable. The recorder initiates the signal to be transmitted by the transducers and, after a period of time, depending on the distance the signal travels, the reflected return signal is received and appears as a darkened area on the chart recorder. The more reflective the object illuminated by the signal is, the darker the object appears on the record. Directly behind this return appears a shadow area the size of which is dependent upon the size of the object illuminated, the angle of the signal to the object, and the angle of the slope behind the object. The various shades of gray indicate changes in texture and relief on the bottom (Patterson and Pope 1983).

165. A major concern of the application of the side-scan sonar

technique in observing underwater structures along coastal slopes, is the resolution (the ability to distinguish one object from another) offered. Since the goal of the inspection work is to assess the condition, coverage, or damage, the highest degree of available resolution is sought. The problem of resolution is of greater concern with regard to mapping and profiling erosion damage to lock chamber floors, stilling basins, and other horizontal concrete structures where accuracies of ± 1 to 2 in. are desired.

166. In the past several years the side-scan technique has been used to map surfaces other than the ocean bottom. Successful trials have been conducted on the slopes of ice islands and breakwaters and on vertical pier structures (Mazel 1984). Although the side-scan sonar technique permits a broad-scale view of the underwater structure, the broad beam and lack of resolution make it unsuitable for obtaining the kind of data required from inspections of CE's horizontal concrete structures.

Radar

167. As previously noted (Task I) in this report, certain types of radar have been used to evaluate the condition of concrete up to 30 in. in depth. Radar can differentiate between serviceable concrete and deteriorated concrete. The deterioration can be in the form of delaminations, deteriorations, microcracks, and cracks up to and including small voids. Radar can also detect changes in material and locate where these changes occur. These types of evaluations have been performed on dry concrete, that is, concrete above water.

168. There are no references describing radar evaluation of underwater concrete. Members of the staff of the CRREL successfully used impulse radar to locate the "black box" which was lost in the Potomac River after the Air Florida jet hit the bridge near Washington, DC, in January 1982. In September 1985, WES and CRREL personnel worked together in an initial attempt to locate and determine the condition of underwater articulated concrete mattresses used for bank erosion control in the Mississippi River.

169. The tests mentioned above indicate that the use of radar as an underwater inspection tool may certainly be feasible. However, further research is needed in this area.

Laser mapping

170. The invention of the laser and subsequent advancements in measurement technology have made possible a promising new mapping technique

that has the potential to dramatically improve the capability to map topographic features. Previously it was impractical to acquire this information over large areas. Laser systems are capable of making extremely accurate distance measurements. Airborne laser mapping systems have been examined for applicability in terrain surface mapping, bathymetry, and water quality.

171. The ability to accomplish terrain bathymetric mapping (in reasonably clear water) has been demonstrated. Perhaps the most serious constraint to improving the performance of airborne laser mapping systems is the adaption of improved positioning technology. Improvements in laser systems can enhance current capabilities but to a lesser degree than improvements in positioning technology (Link, Krabill, and Swift 1982).

172. When the CE-USBR study was initiated, arrangements were made for the review of terrain surface data to be collected by the Environmental Laboratory, WES, with an airborne laser system. Tentative arrangements were made with the Naval Ocean Research and Development Activity to have access to pertinent data collected from tests of a laser system being developed for bathymetric measurements.

173. The information gathered from following the progress of these programs indicates that airborne laser systems could be applied to the detailed mapping of underwater structures. However, such an application was beyond the state of the art at the time and would have required more manpower and fiscal resources than were available in this work unit. There are also technical problems associated with laser systems in achieving the desired resolution for our purposes. Future developments in laser technology (as applied to bathymetric) may solve these problems and make the laser a technically and economically feasible tool for underwater evaluation applications.

Remotely operated vehicles

174. Remotely Operated Vehicles (ROVs) have been employed in underwater work since the mid-1900's. Since about 1975, the number and type of ROVs have greatly increased. Today, there are towed vehicles, bottom-crawlers, vehicles which carry their own power supply, and those which are controlled remotely from the surface. Needless to say, this list is not all-inclusive. There are at least six basic types of ROVs:

a. Tethered, free swimming.

b. Towed (midwater and bottom/structurally reliant).

c. Bottom-reliant.

d. Structurally reliant.

e. Untethered.

f. Hybrid vehicles.

The primary distinction between these groups is the means whereby they obtain power for operation (Marine Technology Society 1984). The ROV will almost always be equipped with closed circuit television (CCTV), and it is capable of accommodating some types of mechanical manipulators. Surface-cleaning equipment and selected types of nondestructive testing apparatus have been operated from ROVs.

175. The tethered, free-swimming ROV has been used for inspection of at least two CE projects. The US Army Engineer District, Omaha, contracted for ROV inspection of underwater tunnels at Fort Peck Dam in Montana and tunnels and trashracks at Oahe Dam in South Dakota. The tunnels which were approximately 20 ft in diameter ranged in length from 1,600 to 2,600 ft and were between 150 and 190 ft below the water's surface. Deterioration, major offsets, cracking, and spalling were the features to be identified in the tunnels. Material buildup and structural condition were the concerns for the trashracks. Except for minor amounts of debris near the bases of the trashracks, nothing was observed that would warrant any further investigation.

176. ROVs perform well in investigations of this nature where observance of general conditions and abnormal features of otherwise inaccessible structures is desired. However, at the present state of development, ROVs are not capable of delivering high-resolution, repeatable, erosion-damage data from underwater concrete structures such as aprons, lock chamber floors, and stilling basins.

Underwater acoustic profilers

177. In view of the inadequacies, lack of applicability, or resource requirements of the previously listed inspection techniques, and because of known prior developmental work on an experimental acoustic system, a decision was made to concentrate on acoustics in the initial effort to develop a mapping-profiling system for underwater structures.

178. Erosion and downfaulting of submerged structures have always been difficult to accurately map using standard acoustic (sonic) surveys because of limitations of the various systems. Sonic surveys, side-scan sonar, and other underwater mapping tools are designed primarily to see targets rising above the plane of the sea floor. As previously discussed, broad sonic beams

provide broad coverage. A narrow beam is needed to see into depressions and to use close to vertical surfaces.

179. In 1978, as a part of a program to look for alternatives to construction of new structures at Locks and Dams No. 26 (L&D No. 26) on the Mississippi River, Holosonics, Inc., did some work for the US Army Engineer District, St. Louis, with a "High Resolution Acoustic Mapping System" (HRAM). This work was the first attempt to develop within the CE an acoustic system suitable for mapping the surface contours of stilling basins, lock chamber floors, and other underwater structures. The results obtained with the HRAM system were very encouraging. The floor slabs of the main and auxiliary lock chambers were profiled and defects that had been previously located by divers were detected by the HRAM system. A portion of the stilling basin downstream of one gatebay in the dam was inspected with the system. Features of the stilling basin such as the concrete sill, the downstream diffusion baffles, and some abrasion-erosion holes were mapped and profiled. The accuracy of the system appeared to be adequate for defining bottom features in the field. There were some problems with the positioning and orientation of the work platform (boat) and with recording its location so that a permanent record of defects could be made and compared with results of future surveys.

180. Holosonics, Inc., went out of business in 1979. This fact plus the fact that the investigation at L&D No. 26 was part of a special, one-time funded program, precluded any immediate followup on development of the HRAM. After the initiation of the joint CE-USBR NDT R&D program, it was determined that the improvement of the accuracy and operational efficiency of the HRAM system would probably be the quickest and most economical approach to providing a suitable mapping and profiling system for field use in lock chambers, stilling basins, and other underwater structures. In December 1981, during a discussion of the general scope and direction of the NDT work, representatives of the Office, Chief of Engineers (OCE), the USBR, and the WES agreed that the accuracy and operational efficiency of the HRAM should be improved, and that the system should be improved and modified to facilitate underwater mapping and profiling of typical USBR and CE structures. They also recommended that a demonstration should be arranged to verify the accuracy and operational efficiency of the system.

181. In July 1982, a contract was awarded to SONEX, Ltd., of Richland, Washington, to write a detailed description and specifications for an acoustic

system which would meet the needs of the USBR and WES for mapping and profiling underwater structures. The description and specifications were delivered to WES in February 1983.*

182. The system which was subsequently built to these specification has unique capabilities which allow it to "see" objects rising above the plane of the bottom, extract data from narrow depressions and areas close to vertical surfaces (Figure 51), provide continuous real-time data on the elevation of the bottom surface, and record and store all data so that three different presentations of output may be produced.

183. The system contains an acoustic subsystem, a positioning subsystem, and a compute-and-record subsystem. The acoustic subsystem includes a transducer array (Figures 52 and 53) and a transceiver-signal processing module (Figure 54).

184. The functions of the acoustic subsystem are to (a) generate pulses to activate each of the transducers of the transducer array; (b) amplify, rectify, and detect the reflected acoustic signal received at the transducer array; (c) determine the time-of-flight for the acoustic signal from the transducer to the bottom surface and back; and (d) output the time-of-flight data to a computer.

185. The computer calculates the elevation of the bottom surface using the time-of-flight information and prerecorded water level data. This information is displayed on a video terminal on board the surveying boat, and the basic data are recorded on magnetic disks.

186. The primary interrogation transducers are designed to have a narrow cone transmission pattern. Their nominal operational frequency is 360 kHz, and the narrow pattern is achieved by using a piezoelectric ceramic element whose diameter equals several wavelengths. The resultant cone dispersion is 1 deg at 6 db. The transducers are classified as flat-piston radiators and transmit an essentially flat acoustic wave front. Their narrow beam design provides the capability for looking into a depression of 2 ft or larger in diameter and detecting the bottom elevation within ±2 in.

---

* The description and specifications are included in this report as Appendix A. Anyone needing further information should contact Henry Thornton at the following address: Commander and Director, US Army Engineer Waterways Experiment Station, ATTN: Henry Thornton, Jr. (CEWES-SC-A), PO Box 631, Vicksburg, MS 39180-0631; or call (601) 634-3797.

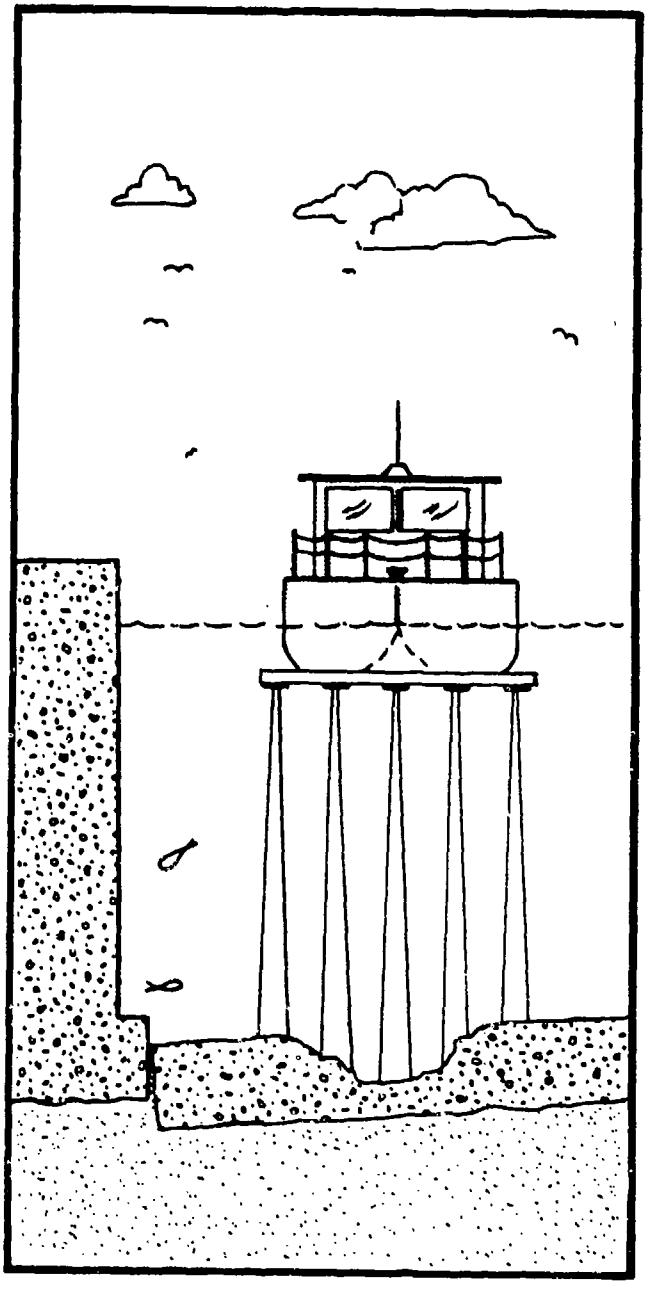

Figure 51. Artist's concept showing survey boat and narrow-beam transducers of underwater acoustic profiler

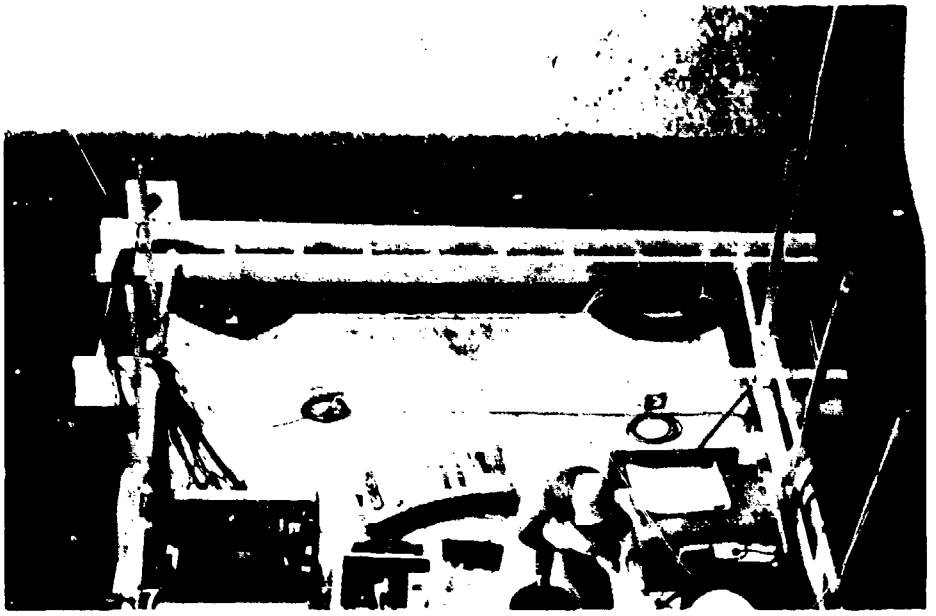

Figure 52. Transducer array bar prior to lowering into water

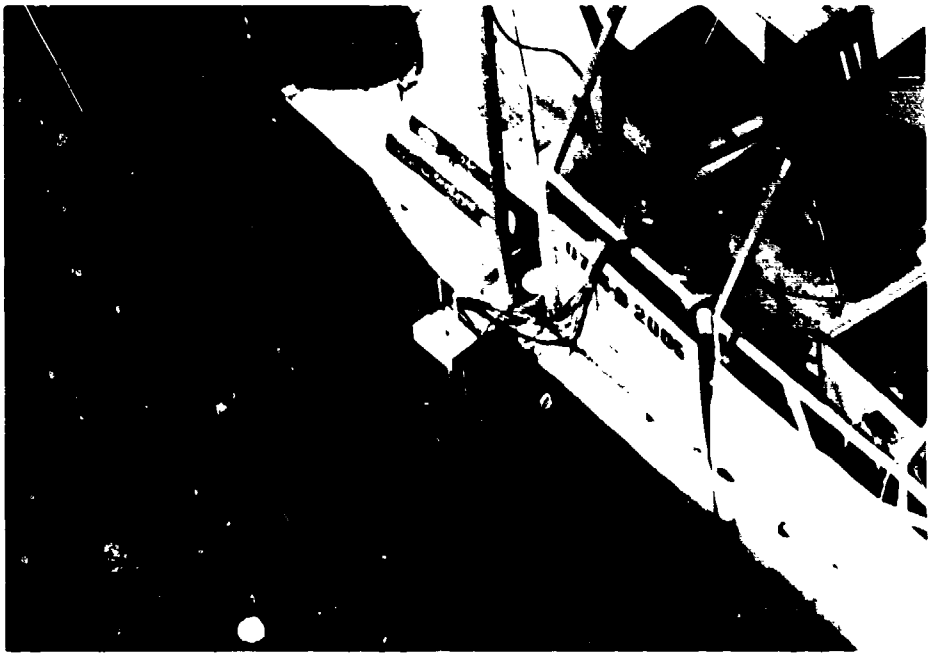

Figure 53. Transducer array bar lowered into survey position under survey boat

Figure 54. The transceiver-signal processing module calculates bottom elevations using data from acoustic transducer array

187. During a survey, as the boat-mounted array is moved forward, the multiple transducers are sequentially pulsed. The first signal returning to each transducer from the bottom is detected, and depth and location data are recorded.

188. The positioning subsystem keeps track of the position of the transducer array bar. Since the bar is mounted on a floating work platform, it is free to move in any direction and to rotate about any of three orthogonal axes; i.e., it has six degrees of freedom (Figure 55). The positioning subsystem is capable of controlling and determining the displacement of the bar in each of these six degrees of freedom. Because the system has excellent vertical resolution, the lateral position of the survey boat must be determined with greater accuracy than the 10- and 15-ft accuracy of standard ocean surveys to take full advantage of the system capabilities.

189. The lateral positioning network consists of a submerged sonic transmitter on the boat and two or more transponders in the water at known or surveyed locations (Figure 56). Boat position can be calculated from two known distances. As each transponder receives the sonic pulse through the water from the boat transmitter (Figure 57), it causes the time-of-detection

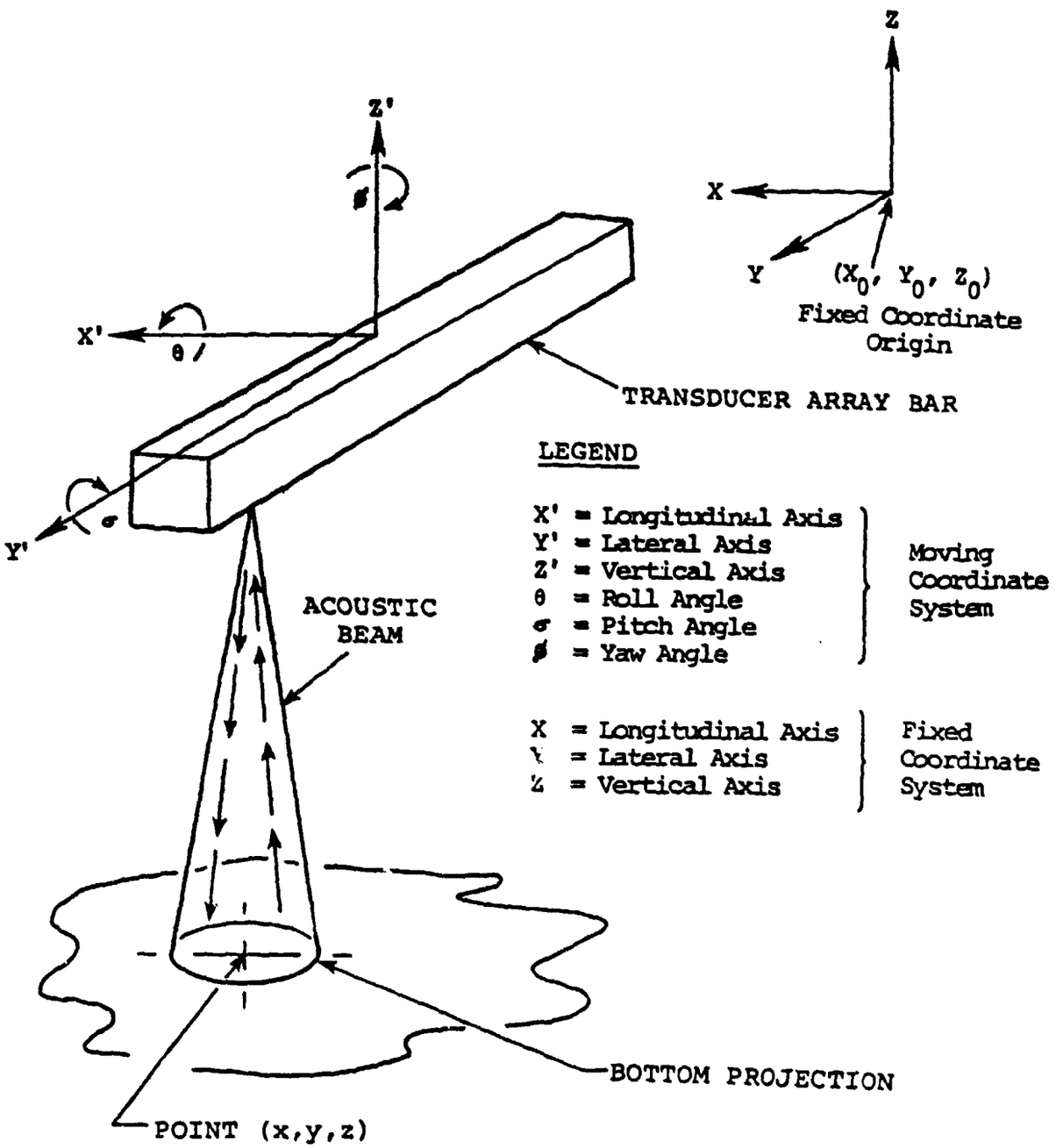

Figure 55. Definitions of coordinate systems and parameters

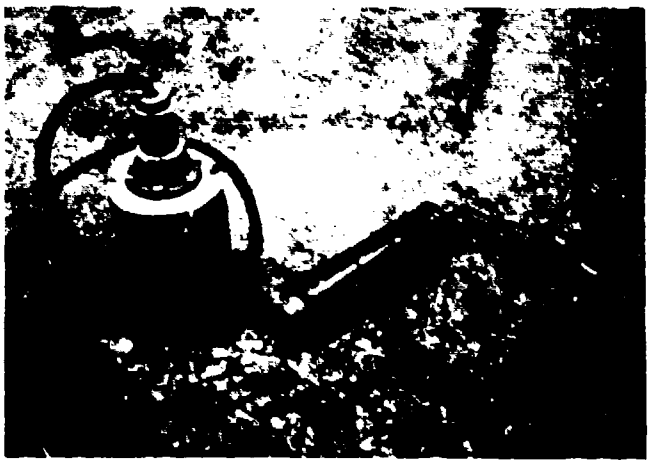

Figure 56. Underwater locator transponders; the remote transponder is on the right; the boat transponder is on the left

Figure 57. Radio transmitter

to be instantaneously radioed back to the survey boat. Distance from the boat to the transponder is then calculated from the time-of-flight, and the position is calculated and displayed by an onboard computer. The network can be easily reestablished for subsequent surveys, and the survey boat and transducer array bar can be returned to any location within the network with the same accuracy.

190. The compute-and-record subsystem provides for computer-controlled operation of the system, and for processing, display, and storage of data. Survey results are in the form of real-time strip charts showing absolute relief for each run, three-dimensional (3-D) surface relief plots showing composite data from the survey runs in each area, contour maps of selected areas, and data printouts of the individual data point values.

191. The high-resolution acoustic mapping system is designed to operate in water depths of 5 to 40 ft and produce accuracies of ±2 in. vertically and ±1 ft laterally. The system can be modified to do deeper surveys and can be adapted to large or small survey areas. An artist's concept of the system in operation is shown in Figure 58.

192. In September 1983, a contract was awarded to SONEX, Ltd., to provide high-resolution acoustic survey equipment and to perform a survey, in accordance with the specifications, at Folsom Dam, a USBR project on the American River near Sacramento, California (Figures 59 and 60). The structure inspected was the stilling basin which is approximately 242 ft wide and 350 ft long (Figure 61). Nearly 85,000 sq ft of stilling basin floor were surveyed in approximately two days, exclusive of setup time (SONEX 1984).

193. The purpose of this survey was to (a) demonstrate the ability of the system to perform in the field in accordance with the specifications, (b) determine the presence of erosion and deposition on the stilling basin floor, and (c) produce survey data which would be easy to read and would readily indicate the presence and extent of erosion and deposition in the stilling basin.

194. The results of the survey were presented as a contour map of the stilling basin area, and a 3-D surface plot of the stilling basin floor. These are included as Plates 1 and 2 which contain the contour map, and Plate 3, the 3-D plot of the stilling basin floor (SONEX 1984).

195. The final results are produced from the raw survey data. Two different presentations are given. These serve two different purposes:

a. The contour map can be easily read to determine the absolute elevation within the limits of the contour interval selected. The lateral and vertical extent of any changes in the bottom elevation can be measured.

b. The 3-D plot provides a more easily understood picture of the overall condition of the area. By accentuating the vertical scale, subtle elevation changes which may cover less than one contour interval, can be seen. The viewer can pick out features which might be overlooked on the contour map and determine the relationship between them.

196. Plate 1 is the contour map of the downstream half of the stilling basin. Plate 2 shows the upstream half. Scale for each plate is 20 ft/in. The contour interval for each plate is 0.2 ft. The numbers inside of each contour enclosure show the erosion (or deposition) for that enclosure, as indicated by the code at the bottom of the sheet. A "1" indicates erosion in the range from 0.2 to 0.4 ft deep; "2" indicates 0.4 to 0.6 ft, and so forth.

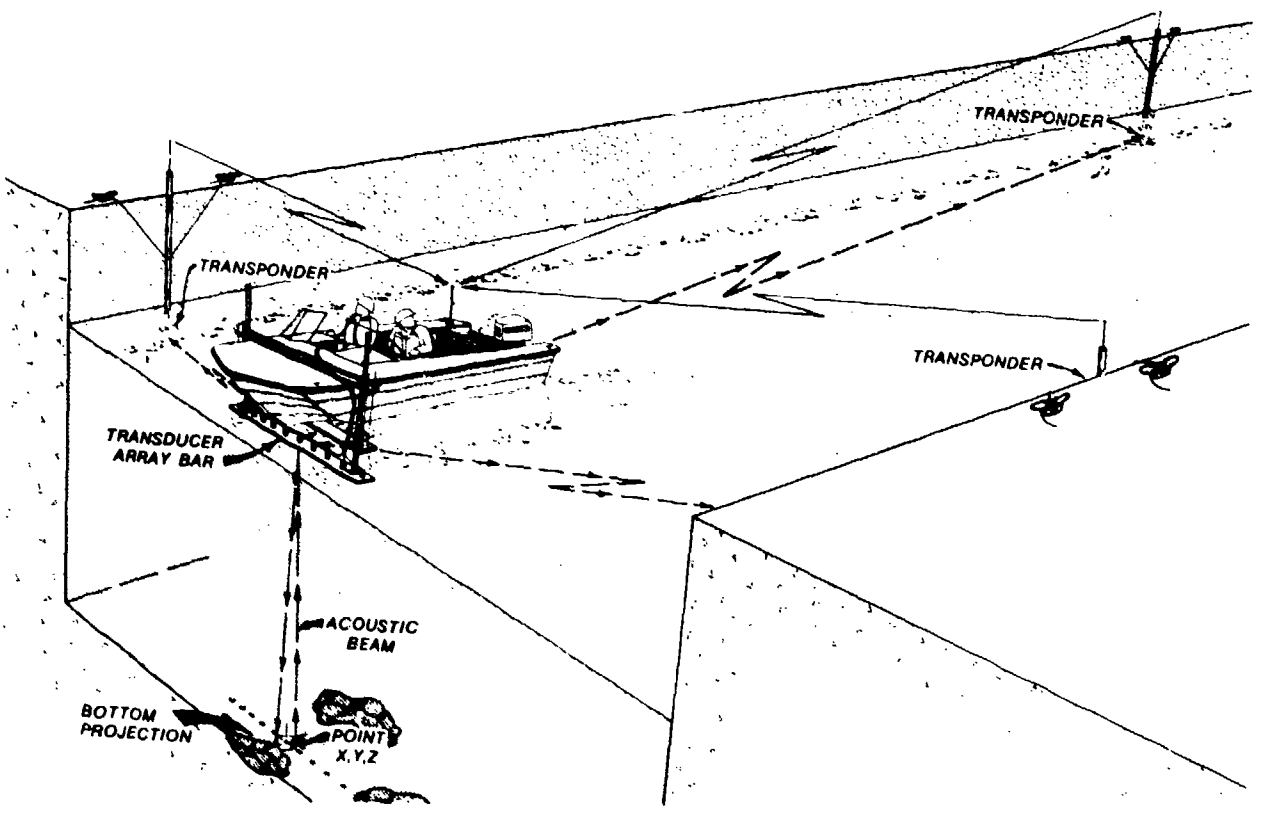

Figure 58. Artist's concept of the HRAM in operation

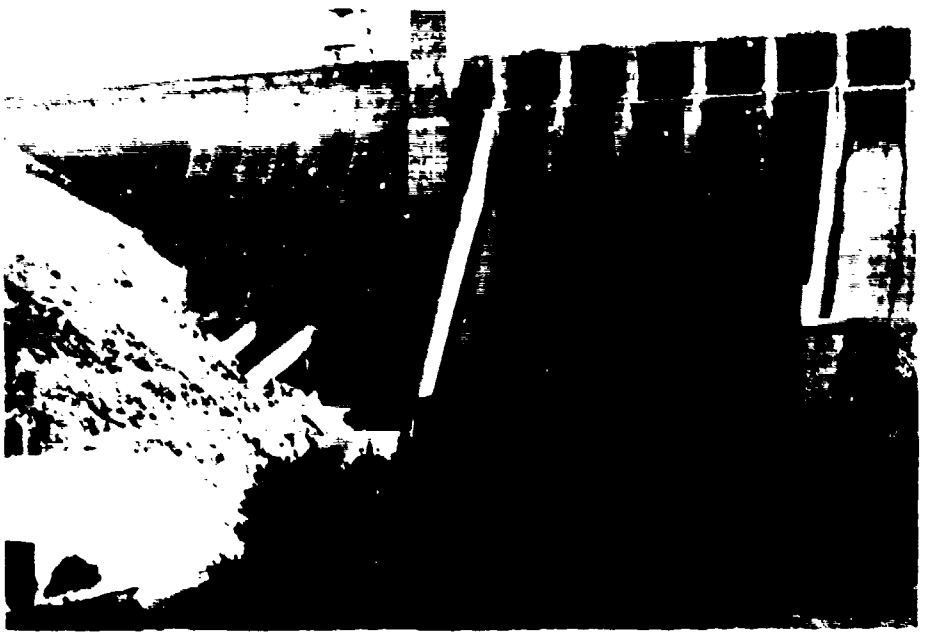

Figure 59. Folsom Dam, California

Figure 60. Boarding the survey platform at Folsom Dam

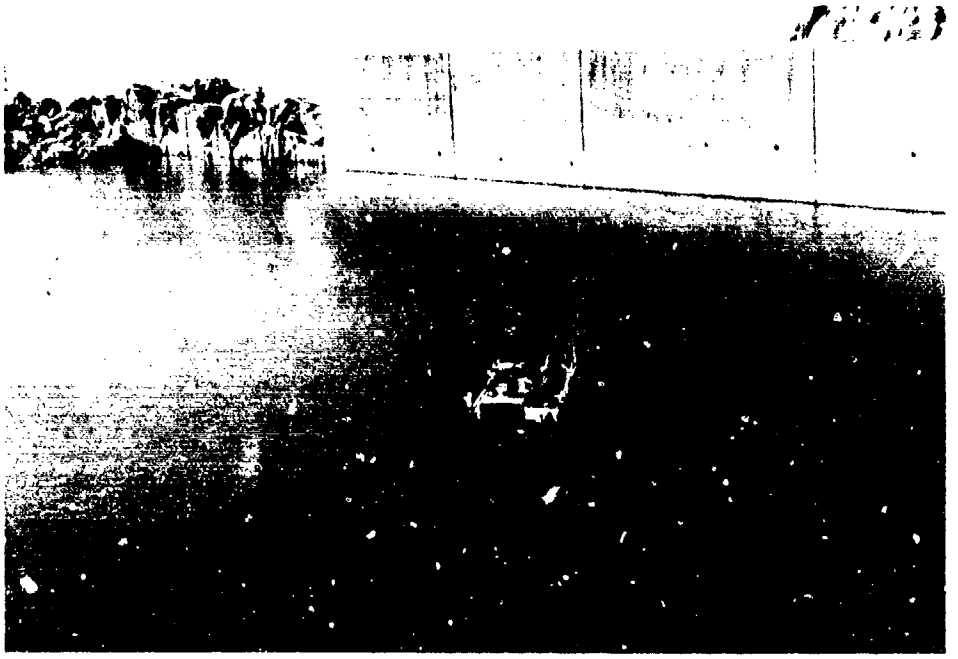

Figure 61. Survey of stilling basin in progress at Folsom Dam

A "+" indicates that the measured elevation was within 0.2 ft, plus or minus, of the calculated as-built elevation. Letters "A" or "B" indicate elevations above the calculated as-built elevation. Asterisks indicate that no-depth data were available at that point. The sonic signal was lost, probably due to signal scattering in a debris pile. Areas where erosion is more than 0.4 ft deep are shaded for clarity.

197. There are a few locations where over 1.0 to 1.2 ft of erosion was measured. These are marked with the number "5" on the contour map. If any deeper holes are present, they were too small to be detectable at a depth of 35 ft. (The sonic footprint of a 1-deg transducer at a depth of 35 ft is a circle about 1-1/2 ft in diameter.)

198. Near the top of Plate 1, the dashed line shows the position of the slope break. Below this line, the stilling basin floor is flat. The as-built elevation is 115 ft. Above the line the floor rises to the dam on a 12.5 percent slope. In preparing the contour map, the effects of the slope rise were removed. The contours shown in Plate 2, and in the upper strip of Plate 1, are relief above or below the calculated as-built elevation. Since this calculation was necessary, and because the accuracy of the calculation depends greatly on knowing the precise location, the absolute accuracy of the contours on the slope is not as good as the accuracy of the contours on the flat. A

1-ft error in boat position causes a 0.125-ft error in the calculated as-built, more than half of a contour interval.

199. Plate 3 shows a 3-D surface plot of the stilling basin. The horizontal scale is 40 ft/in., and the vertical scale is 8 ft/in.

200. The 3-D presentation gives an overall picture of the floor of the stilling basin as it would appear if it were dewatered. The observer is standing at the powerhouse, and looking toward the Folsom side of the basin. The dam is at the left of the picture. The flat-topped end sill can be seen at the right. The apparent superimposition of the end sill of the floor is a function of the viewing angle and the vertical scale exaggeration.

201. The general outline of the erosion and deposition can be readily seen. As expected, the worst erosion is seen at the downstream end near the end sill where the turbulence would be most severe. This confirms the data seen in Plate 1.

202. The smoothness of the end sill profile confirms the repeatability and accuracy of the system's depth measurements, and also indicates the stability of the boat as a survey platform. The slight variations may be boat motion, or they may be construction or erosion irregularities.

203. In contrast to the smooth end sill, most of the bottom is covered with ripples. These are more likely to be ripple patterns in the thin silt cover, than to be an effect of survey boat motion. The ripple marks tend to cross from boat-run to boat-run without breaking, and occasionally the ripple patterns are detected by all but one or two of the transducers.

204. An example of the ability to recognize subtle features using the 3-D plot is seen in Plate 3 along line A-A' (Sta 13+21). An erosional feature can be seen near Point A. Following across the line, several other depressions can be seen forming a linear trend across the stilling basin floor. On the contour map some of the same depressions are seen; some are too shallow to be seen. The linear trend could be overlooked.

205. Is this really a linear feature? Most probably it is. At Sta 13+21, there is a construction joint across the basin floor. Evidently, erosion is developing along the edges of the seam.

206. Furthermore, 50 ft downslope at Sta 13+71 another, even more subtle, linear trend can be seen (line B-B'). This corresponds to another construction seam. At Sta 12+71 (line C-C'), one can barely discern the trace of a third seam.

207. Certainly, these last two features are not important. Perhaps even the first example is not significant in terms of structure and dam safety. The maximum erosion measured near A is 0.48 ft. This does provide an excellent example of the subtle features that can be seen on a 3-D surface plot.

208. At Folsom Dam, it was important to have both methods of data presentation. As mentioned earlier, the sloping section of the stilling basin floor created some difficulties for contour plotting, particularly at the ends of the run, where the greatest error in positioning was experienced. In this section, it was easy to see the relative elevation, but difficult to see whether a shallow depression represented erosion or a section with less silt deposition. Typically, the variations in elevation were under 3 in. Contour plotting under these conditions is less accurate than usual.

209. It is easier to distinguish between erosion and deposition when the entire picture can be seen as in the 3-D plot. Area D in Plate 3 is an example of broad, low deposition. The maximum height of the silt buildup measures 0.24 ft (2.9 in.). Over most of the area, the buildup is less than 0.2 ft, one contour interval.

210. Area E is another area of deposition. In addition to silt deposition, there may be a buildup of debris including brush and logs. This is interpreted from the lack of sonic signal return in the three blank spots in Area E. As was seen at the end sill, the sonic signal can be deflected away from the transducer by sharply sloping surfaces. The signal can also be scattered by a rough surface such as a pile of brush would represent.

211. There is some deposition on the slope along the full length of the slope break at Sta 14+24.2. Accompanying this is some erosion on the flat directly below the break. This slope-break erosion appears worse in Area F, on the lower half of the plot where the maximum erosion measures 0.70 ft.

212. The greatest area of erosion occurs in the downstream half of the flat section of the stilling basin, Area G. Over 1 ft of material is missing in some spots. This can readily be seen in both the contour map and the 3-D plot. Interestingly, the evidence of erosion along the construction seams at Sta 14+71 and 15+21 can be seen along with the effects of general erosion.

213. Most of the sharp "spikes" on the 3-D plot are fish. Some appear to be bottom-feeders and some are near the surface.

214. The one spike which appears different is labelled "H" in Plate 3. The top of this feature is between 131 and 132 ft in elevation and covers an

area of 12 sq ft. The feature appears to be rectangular, 3 by 4 ft on the sides. It is separated from the wall by 2 ft, and extends from Sta 15+26 to 15+29. The uniformity of the elevations of the surface suggests that it is a manufactured artifact, but nothing was seen on the construction prints which would correspond to such an object.

215. Two runs at the bottom of the 3-D plot are shorter than the others. At the time the survey was run, water was being pumped out of a powerhouse sump and discharged in a heavy stream from a pipe high up the wall at the corner of the stilling basin. The runs were cut short to avoid the waterfall.

216. The contour maps in Plates 1 and 2 and the 3-D plot in Plate 3 are based on data from 83,260 individual depth measurements made during the survey. An additional 10,400 measurements were made to check specific areas and to confirm the results of the main survey. Furthermore, the existing survey data can be used to plot a variety of 3-D surfaces using different viewing angles and different vertical scales. Comparisons can be readily made between the current data and data which may be obtained in future surveys.

217. With the completion of the survey at Folsom Dam, two of the goals agreed upon by the representatives of OCE, USBR, and WES had been accomplished; i.e., that the accuracy and operational efficiency of the HRAM be improved, and that the system be improved and modified to facilitate underwater mapping and profiling of typical USBR/CE structures. The remaining goal was to verify the accuracy of the system.

218. The stilling basin at Folsom Dam was dewatered in August of 1980, and an examination of erosion and buildup of gravel and debris was performed. The stilling basin was again dewatered in September of 1982. Topographic data obtained in 1982 were compared with data obtained in 1980. No significant changes were noted at the scale used. For this reason, the drawings showing the features of the stilling basin in 1980 were considered to be accurate for describing the features existing in 1982. These drawings are shown in Plates 4 and 5. Plate 4 gives elevations and other data on the downstream half of the stilling basin. Plate 5 gives similar data on the upstream half.

219. If the acoustic profiler can produce the required accuracy, then Plates 1 and 2, which show the condition of the stilling basin as recorded in the survey performed with the acoustic profiler in 1983, should match reasonably well the condition shown in Plates 4 and 5, which show the condition recorded in 1982 at the time of dewatering. A comparison of Plates 1 and

2 with Plates 4 and 5 shows that this is the case. This can be confirmed most easily by noting the locations of the most severe erosion on each of the two sets of plates.

220. In Plate 1, there are two areas showing considerable erosion of depths up to 1 ft. One area is located predominately along a vertical line between Sta 14+71 and 15+21--about 80 ft from the left wall (looking downstream). The other area is located along a horizontal line about 40-ft long near to, and running parallel with the end sill. These areas are defined with vertical stripes and the figure "4," indicating erosion depths of 0.8 to 1.0 ft. There are smaller areas of erosion of up to 1.2 ft within these two areas.

221. In Plate 4, a vertical line of erosion of comparable depth is located between Sta 14+71 and 15+21, about 80 ft from the left wall. There are numerous elevations recorded near, or below, elevation 114.0, which is 1 ft below the design elevation of 115.0. Plate 4 also shows a horizontal line of severe erosion, similar to the one in Plate 1, near the end sill (about midway across the stilling basin).

222. There are not as many areas of erosion with which to make comparisons in Plates 2 and 5. However, the area on the match line in Plate 2, near the right wall (looking downstream), shows up in Plate 5 where elevations of 114.7 and 114.9 are recorded (the design elevation nearing 116.0).

223. The comparisons of Plates 1 and 2 with Plates 4 and 5 show a strong positive correlation between the data obtained with the acoustic profiler and the actual condition by survey of the stilling basin when dewatered.

224. The results of these tests and subsequent comparisons of data indicate that the underwater acoustic mapping system contains the accuracy and operational efficiency to provide, without dewatering, an accurate and comprehensive evaluation of top surface wear on horizontal surfaces (such as aprons, sills, lock chamber floors, and stilling basins).

PART IV: TASK III - ENGINEERING GUIDANCE FOR EVALUATION OF CONCRETE IN SERVICE

225. The objective of this task was to develop engineering guidance to establish a uniform method for evaluating the condition and safety of existing concrete structures.

226. The study was authorized by Headquarters, US Army Corps of Engineers (HQUSACE), under Civil Works Research Work Unit 31553, "Maintenance and Preservation of Civil Works Structures," and was under way at the time that Civil Works Research Work Unit 31753, "Development of Nondestructive Testing Systems for In Situ Evaluation of Concrete Structures," the cooperative effort of CE and USBR, was initiated. Although the task was shifted to Work Unit 31753, the work continued on separate funding provided by the Concrete Research Program. Funds for publication of the report were provided through the Repair, Evaluation, Maintenance, and Rehabilitation (REMR) Research Program. The results of the study were published in a report entitled, "Engineering Condition Survey of Concrete in Service" (Stowe and Thornton 1984), and is available from the National Technical Information Service, 5285 Port Royal Road, Springfield, Virginia 22161.

PART V: TASK IV - VIBRATION SIGNATURE MEASUREMENTS

227. The objective of Task IV was to assess the use of a structure's vibration signature as obtained by the impact-resonance technique as a field inspection tool.

228. A literature review revealed a number of sources containing the results of experimental work with vibration signatures of structures. Baldwin, Salane, and Duffield (1978) report on a three-span continuous composite bridge of modern design that was field tested under fatigue loading which produced stresses equal to, or greater than, design stresses. Both the primary fatigue loading and loading for dynamic-property tests were imposed by a moving-mass closed-loop electrohydraulic-actuator system. During the fatigue loading the bridge was inspected periodically by eight different inspection methods, including visual, ultrasonic, radiographic, acoustic emission, and dynamic-signature techniques.

229. Stiffness coefficients were calculated from the experimental mode shapes on the basis of a multidegree-of-freedom system with modified coupling. Mechanical impedance plots were made from frequency sweep tests which included five resonant modes. Changes in the bridge stiffness and vibration signatures in the form of mechanical impedance plots were indicators of structural deterioration due to the fatigue. Indications of the general location of structural damage were provided by changes in the vibration signatures of the bridge. The study showed that structural degradation can be detected by use of mechanical impedance and change-in-stiffness techniques. These techniques also showed promise as a comparative method for locating crack zones. The study found that additional research is needed to refine and further develop these techniques as a dynamic inspection method.

230. According to Pace and Alexander (1982), the investigation of a structures' vibrational characteristics--such as frequency, damping, and mode shape--is called modal analysis. Modal analysis is the process by which the dynamics of an elastic structure are characterized.

231. There are a number of factors that influence the modal properties. The relationship is complex. One can experimentally observe, however, broad changes in the modal characteristics by looking at three main factors: geometry, modulus, and boundary conditions.

232. Members of the WES staff routinely make resonant frequency measurements on concrete beams subjected to test for resistance to freezing and thawing (ASTM C215-60). By controlling the geometry and the boundary condition of the specimen, it is known that the resonant frequency of a particular mode will decrease as the modulus of elasticity of the specimen decreases.

233. It is known that a geometry change will affect the modal properties. If other parameters remain unchanged, an increase in length will decrease the resonant frequency of the fundamental flexural mode. If the thickness is increased, this will increase the frequency of vibration. It is evident, then, that many factors can influence changes in a structure's modal properties.

234. Richardson (1980) states (on detecting damage of structures by measuring changes in their modal properties):

> The underlying assumption of this survey is that changes in modal parameters are a reliable (and sensitive) indicator of changes in structural integrity. It is our contention, of course, based upon approximately 40 years of combined modal testing experiences, that this is indeed the case.

Numerous references are given in this survey that show how various forms of damage in a structure will also change the modal properties.

235. In 1980, resonance measurements were performed on a 14-ton concrete block in the laboratory using an impact technique. It was discovered that the dynamic modulus of the block could be determined, and, also, that the resonant frequency data could be indicative of cracking within a structure. Subsequently, the impact-resonant technique was used as an inspection tool to rank eight concrete piers on a dam structure in Lake Superior (Alexander 1981).

236. A fourier transform analyzer (Figure 62) was used to collect modal analysis data using transient methods. The metal A-frame with a manually operated winch that supports the impactor which was used is shown in Figure 63. The impactor was pulled back manually and allowed to swing over a 2- to 3-ft arc, striking the reaction block which was bolted to a metal plate. The plate was secured to the concrete structure to be tested by metal anchors and epoxy. A load cell secured to the front of the impactor measured the load pulse. The response of the structure was detected by an accelerometer placed at a suitable location. Thornton et al. (1980) gives a description of the piers.

237. The resonant frequencies of the eight piers were determined and

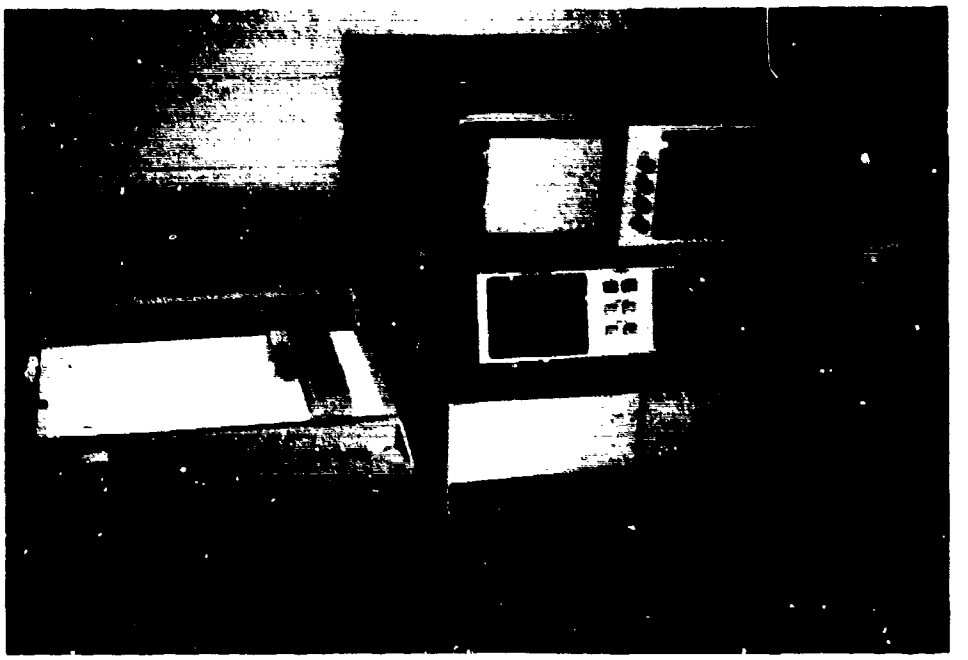

Figure 62. Real-time Fourier transform analyzer processes the load-pulse signal and the resulting free vibration of the structure

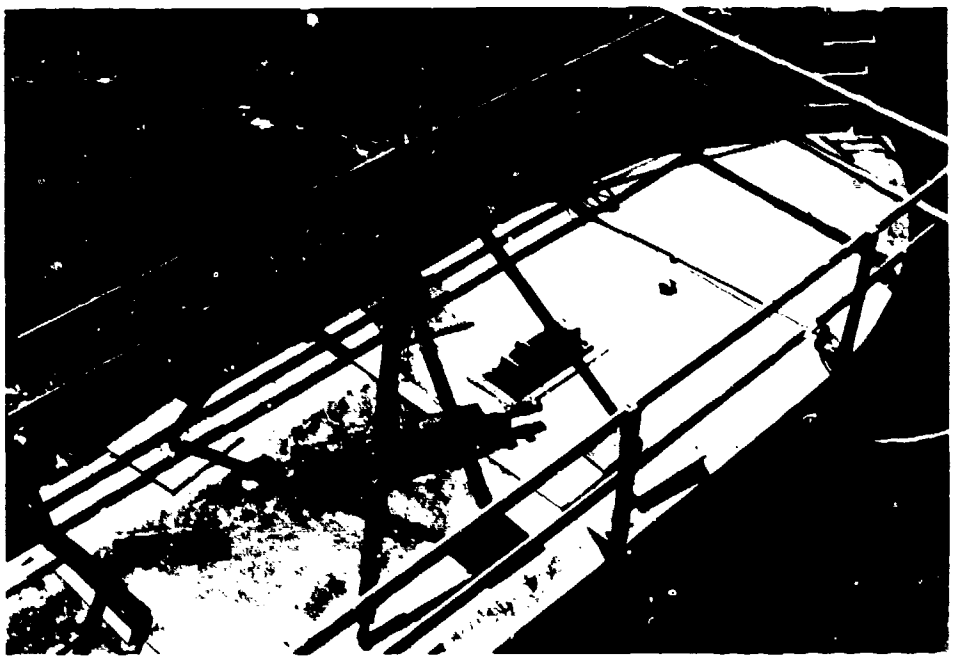

Figure 63. System to generate load pulse--A-frame, 550-lb impactor, load cell with impact pad, reaction block, and steel plate

found to be very close upon comparison. A calculated weight- and shape-factor was added to provide the parameters necessary to calculate the dynamic Young's modulus of each pier.

238. In another study to determine the state of deterioration and integrity of a structure, signature analysis measurements were made on a 4-mile supersonic naval ordnance research track (SNORT) (Sullivan, Pace, and Campbell 1984) in China Lake, California. The steel rail and concrete base were continuous for the total length of the structure. Vibration signatures were obtained at 100-ft intervals over the 4-mile length. The comparative analysis indicated that all the track was in the same general condition except where deteriorated concrete had been replaced. This structure was well suited for condition assessment by comparative signature analyses. The geometry and boundary conditions were constant over the entire length of the structure. Therefore, changes in signature could be attributed to changes in modulus, which is one of three parameters, that can significantly affect the response of the structure to dynamic loading.

239. Because resonant frequencies are directly related to the mechanical properties of a concrete structure, it appears that this technique can be a valuable inspection tool to indicate changes in the integrity of a structure (Baldwin, Salane, and Duffield 1978). The vibration signature of a structure can be determined at the time of construction and monitored over time for a change; or structures of like size, geometry, and construction (such as the Lake Superior piers) can be compared; or portions of a structure can be compared in a manner similar to that used on the SNORT structure. Because of the mentioned potential for making resonant frequency measurements on structures, we suggest that more work be done to develop the vibration signature-modal analysis technique for use as a field inspection tool for concrete structures.

PART VI: TASK V - MODAL ANALYSIS, FINITE-ELEMENT FEASIBILITY

240. The objective of Task V was to investigate the feasibility of using modal analysis in conjunction with a finite-element program as a method of assessing the deterioration, structural integrity, and stability of a concrete structure.

241. Although the resonant technique is presently available for use as a field inspection tool, it should be possible to determine the absolute integrity of a structure when resonant frequency measurements are used in conjunction with a mathematical model. By inputting into a finite-element program various parameters of geometry, restraint, and dynamic modulus of the total structure, the resonant frequencies and damping functions can be calculated. Then these numbers can be compared with actual measurement data from the structure to detect anomalous response of the structure. The finite-element program should be calibrated from measurements made soon after construction when the structure is known to be sound.

242. During FY 82, impact-resonance measurements were made on the walls of both a prototype and a model of a concrete building (Volz and Jones 1982). Mode shapes, resonant frequencies, and damping factors were measured. Measurements were made on the prototype before soil was moved against the outside walls, and afterward. Although damping increased (as expected) when the wall was covered, the significant finding was a 30 percent increase in the resonant frequency of the fundamental mode. After these measurements, the prototype wall was subjected to blast loading and sustained minor structural damage. The shock-absorbing soil was moved away from the wall and the impact-resonance measurements were repeated. Compared with the initial measurements (without soil), there was a slight decrease in the resonant frequency of the fundamental mode and a significant decrease in damping.

243. Modal analysis tests made on the Richard B. Russell Dam in Georgia (Chiarito and Mlakar 1983) showed that the damping was about 3 or 4 percent of critical. (Damping less than critical is oscillatory motion and damping greater than critical is non-oscillatory.) However, when cylinders (made from the concrete mixture used for the dam) were tested, it was found that the damping of the specimens was only about 0.37 percent of critical. The specimens were supported at the nodes with narrow supports which minimize the loss of energy to the base supports. Although size may have been a factor, the main

factor influencing the damping was the boundary conditions. By embedding a part of the cylinder into soil, the damping increased about 400 percent from that value made in air. With the specimen lying on the soil, the damping was 0.55 percent. When embedded in the soil about 2 in. deep, the damping was 0.86 percent of critical; however, when the specimen was 3 in. deep in the soil, the damping was 1.5 percent. In all cases, damping was determined from a measurement of the fundamental resonant frequency of the flexural mode. This test indicates the ability of the boundary conditions to influence damping. The frequency was not observed to change significantly.

244. Development of a system that is capable of determining the type and extent of deterioration taking place in a structure or in boundary conditions will entail the bringing together of two complex areas of technology, i.e., modal analysis and finite-element analysis. Such an undertaking was beyond the scope of this investigation. Development would be costly in manpower and fiscal resources. However, we are continuing to demonstrate that modal analysis parameters do correlate with structural damage and deterioration.

245. The best measurement that researchers have made in the past, to test the integrity of machinery and various equipment, has been to measure the vibration levels. Because modal analysis is a more complex measurement of the structural response of a structure, it holds promise for developing new techniques to evaluate structures in situ and nondestructively (Pace and Alexander 1982).

PART VII: CONCLUSIONS AND RECOMMENDATIONS

246. During the last three or four years, WES investigators and those outside WES who have been involved in the development of pulse-echo systems for measurements in portland cement concrete (PCC) have come to realize the complex nature of this endeavor. The heterogeneity of concrete and attendant problems of energy dispersion and attenuation of acoustic waves makes evaluation by ultrasonic pulse-echo a very illusive endeavor.

247. A literature review indicated:

a. That the development of an ultrasonic pulse-echo system would greatly enhance the capability to evaluate the condition of concrete structures.

b. There is no commercial equipment available for this type of testing in concrete.

c. The pulse-echo system developed by OSU researchers was state of the art for experimental systems at the time the WES-USBR effort began.

248. The prototype ultrasonic pulse-echo system for concrete developed by WES is a significant improvement over the system developed by the OSU team of researchers considering the 90 percent reduction of weight and dimensions, and an increase in signal to noise ratio of over 200 percent. Work on this system should be continued until an improved, field-worthy system is developed.

249. WES researchers developed an improved ultrasonic pulse-echo system for measurement in PCC having (1) the highest S/N ratio (18), (2) the highest resolution (Q = 2-1/2), and (3) 90 percent less area for the transducers than the previous state-of-the-art system; and recorded the first ultrasonic (200 kHz) impact-echo measurement in PCC. Impact-echo measurements have previously been done in the sonic range.

250. Investigations into the use of radar for inspection of interior PCC should continue.

251. A high resolution acoustic mapping system was developed which will provide, without dewatering, an accurate and comprehensive evaluation of top surface wear on horizontal surfaces such as aprons, sills, lock chamber floors, and stilling basins, where turbulent water flow carrying rocks and debris may have caused erosion/abrasion damage.

252. The results of the study to develop engineering guidance to establish a uniform method for evaluating the condition and safety of existing concrete structures were published in a WES report entitled, "Engineering Condition Survey of Concrete in Service" (Technical Report REMR-CS-1 by Stowe and Thornton (1984)). This report summarizes pertinent inspection procedures and methods of evaluation used by the Corps of Engineers in evaluating concrete civil works structures. Techniques are presented which have a potential for ascertaining the extent and cause of inadequacies in concrete structures. The report can be obtained from the National Technical Information Service, 5285 Port Royal Road, Springfield, VA 22161.

253. A structure's resonant frequencies are directly related to its mechanical properties. For this reason, it appears that the vibration signature can be a valuable inspection tool to indicate changes in the integrity of a structure. The vibration signature-modal analysis technique for use as a field inspection tool for concrete structures should be developed further in order to realize its full potential.

254. It appears that modal analysis parameters could be used in conjunction with a finite element program to determine the type and extent of deterioration taking place in a structure over a period of time. Development of such a system would entail bringing together two complex areas of technology, i.e., modal analysis and finite-element analysis.

REFERENCES

Alexander, A. M. 1980 (Apr). "Development of Procedures for Nondestructive Testing of Concrete Structures; Feasibility of Sonic-Pulse Echo Technique," Miscellaneous Paper C-77-11, Report 2, US Army Engineer Waterways Experiment Station, Vicksburg, Miss.

_____. 1981 (Nov). "Development of Procedures for Nondestructive Testing of Concrete Structures; Feasibility of Impact Technique for Making Resonant Frequency Measurements," Miscellaneous Paper C-77-11, Report 3, US Army Engineer Waterways Experiment Station, Vicksburg, Miss.

Alongi, A. V., Cantor, T. R., and Alongi, A., Jr. 1982. "Concrete Evaluation by Radar Theoretical Analysis," Transportation Research Board 853, Concrete Analysis and Deterioration, pp 31-37, Transportation Research Board, Washington, DC.

Acoustical Society of America. 1957. "American Standard Procedures for Calibration of Electroacoustic Transducers Particularly those for Use in Water," 31 December 1957, Z24.24-1957.

Bacon, J. P. 1961. "New Developments in Ultrasonic Transducers and Their Application to Nondestructive Testing," Nondestructive Testing, Vol 19, No. 3.

Baldwin, J. W., Jr., Salane, H. J., and Duffield, R. C. 1978 (Jun). Fatigue Test of a Three-Span Composite Highway Bridge," Study 73-1, Missouri Cooperative Highway Research Program.

Bowders, J. J., Jr., Koerner, R. M., and Lord, A. E., Jr. 1982. "Buried Container Detection Using Ground-Probing Radar," Journal of Hazardous Materials, Vol 7, pp 1-17.

Brackett, R. L., Nordell, W. J., and Rail, R. D. 1982 (Mar). "Underwater Inspection of Waterfront Facilities: Inspection Requirements Analysis and Nondestructive Testing Technique Assessment," Technical Note TN-1624, Naval Civil Engineering Laboratory, Port Hueneme, Calif.

Bradfield, G. 1948 (Mar). "New Electro-Acoustic Transducer Operating with Short Pulses," Electronic Engineering, Vol 20, No. 241, pp 74-78.

Bradfield, G., and Gatfield, E. N. 1964 (Mar). "Determining the Thickness of Concrete Pavements by Mechanical Waves: Directed-Beam Method," Magazine of Concrete Research, Vol 16, No. 46.

Bradfield, G., and Woodroffe, E. P. H. 1953 (Feb). "Determination of Thickness of Concrete Pavements Using Mechanical Waves," Report No. PHYS/U5, Teddington National Physical Laboratory, Dept. of Scientific and Industrial Research, Great Britain.

Bradfield, G., and Woodroffe, E. P. H. 1964 (Mar). "Determining the Thickness of Concrete Pavements by Mechanical Waves: Diverging-Beam Method," Magazine of Concrete Research, Vol 16, No. 46.

Canfield, J. R., and Moore, W. H. 1967 (Jun). "Development of Instrument for Nondestructive Measurement of Concrete Pavement Thickness," Research Project No. 1-9-63-61, Materials and Test Division, Texas Highway Department in Cooperation with the US Department of Transportation, Federal Highway Administration, Bureau of Public Roads.

Cantor, T. R. 1984. "Review of Penetrating Radar as Applied to Nondestructive Evaluation of Concrete," In-Situ/Nondestructive Testing of Concrete, V. M. Malhotra, ed., ACI Publication SP-82, pp 581-602, American Concrete Institute, Detroit, Mich.

Cantor, T. R., and Kneeter, C. P. 1982. "Radar as Applied to Evaluation of Bridge Decks," Transportation Research Record, pp 37-42, Transportation Research Board, Washington, DC.

Carlin, Benson. 1960. Ultrasonics, 2d ed., McGraw-Hill, New York.

Chiarito, P., and Mlakar, P. F. 1983 (May). "Vibration Test of Richard B. Russell Concrete Dam before Reservoir Impoundment," Technical Report SL-83-2, US Army Engineer Waterways Experiment Station, Vicksburg, Miss.

Claytor, T. N., and Ellingson, W. A. 1983 (Jul). "Development of Ultrasonic Methods for the Nondestructive Inspection of Concrete," Ultrasonics International Conference, Halifax, Nova Scotia.

Clifton, J. R., et al. 1982. "In-Place Nondestructive Evaluation Methods for Quality Assurance of Building Materials," Technical Report M-305, US Army Engineer Construction Engineering Research Laboratory, Champaign, Ill.

EDO Western. No Date. "Piezoelectric Ceramics Bulletin," EWC 02025-8302, Salt Lake City, Utah.

Gaynor, R. D. 1969. "In-Place Strength of Concrete, A Comparison of Two Test Systems," 39th Annual Convention of the National Ready Mixed Concrete Association, New York, 28 Jan 1969; published with NRMCA Technical Information Letter No. 272.

Golis, J. J. 1968. "Pavement Thickness Measuring Using Ultrasonic Pulses," Highway Research Record No. 218, pp 40-48, Highway Research Board, Washington, DC.

Golis, M. J., et al. 1966 (Dec). "The Development of Ultrasonic Nondestructive Testing Instrumentation to Measure Pavement Thickness," Report No 208-3, Engineering Experiment Station, Ohio State University, Columbus, Ohio.

Green, A. T. 1970 (Aug). "Stresswave Transmission and Fracture of Prestressed Concrete Reactor Vessel Materials," Proceedings, Second Inter-American Conference on Materials Technology, Mexico City, pp 635-649.

Grieb, W. E. 1958. "Use of Swiss Hammer for Estimating Compressive Strength of Hardened Concrete," Public Roads, Vol 30, No. 2, pp 45-52.

Gulton Industries, Inc. 1980. Bulletin, Fullerton, Calif.

Hewlett-Packard. 1981 (Nov). "The Fundamentals of Signal Analysis," Application Note 243.

Howkins, S. D. 1968. "Measurement of Pavement Thickness by Rapid and Nondestructive Methods," National Cooperative Highway Research Program Report 52.

Hueter, T. F., and Bolt, R. H. 1955. Sonics, Wiley, New York.

Jones, R. 1962. Nondestructive Testing of Concrete, Road Research Laboratory, University Press, Cambridge, Great Britain.

Kinsler, L. E., and Frey, A. R. 1962. Fundamentals of Acoustics, Wiley, New York.

Klotz, R. C. 1972. "Field Investigation of Concrete Quality Using the Windsor Probe Test System," Highway Research Record No. 378, pp 50-54, Highway Research Board, National Academy of Sciences--National Research Council, Washington, DC.

Kossoff, G. 1966. "The Effects of Backings and Matching on the Performance of Piezo-electric Ceramic Transducers," IEEE Transactions Sonics and Ultrasonics, SU-13, No. 1, pp 20-30.

Kossoff, G., Robinson, D. E., and Garrett, W. J. 1965. "Ultrasonic Two-Dimensional Visualization Techniques," IEEE Transactions on Sonics and Ultrasonics, SU-12, pp 31-37.

Kovacs, A., and Morey, M. 1983 (Jul). "Detection of Cavities Under Concrete Pavement," CRREL Report 83-18, US Army Cold Regions Research and Engineering Laboratory, Hanover, N. H.

Krautkramer, J., and Krautkramer, H. 1977. Ultrasonic Testing of Materials, 2nd ed., Springer-Verlag, New York.

Lamberton, H. C., et al. 1981 (Dec). "Underwater Inspection and Repair of Bridge Substructures," NCHRP Synthesis of Highway Practice 88, Transportation Research Board, Washington, DC.

L'Hermite, R. 1962. "Volume Changes of Concrete," Proceedings, Fourth International Symposium on the Chemistry of Cement, Washington, DC, 1960; Monograph No. 43, National Bureau of Standards, Washington, DC, pp 659-694.

Link, L. E., Krabill, W. B., and Swift, R. N. 1982. "A Prospectus on Airborne Laser Mapping Systems," Manuscript.

Lord, A. E., Jr., Koerner, R. M., and Freestone, F. J. 1982. "The Identification and Location of Buried Containers Via Non-Destructive Testing Methods," Journal of Hazardous Materials, Vol 5, pp 221-233.

Lundien, J. R. 1972. "Noncontact Measurements of Foundations and Pavements with Swept-Frequency Radar," Highway Research Record No. 378, pp 40-49, Nondestructive Testing of Concrete, Highway Research Board, Washington, DC.

Lutsch, A. 1961 (Sep). "Solid Mixtures with Specified Impedances and High Attenuation for Ultrasonic Waves," Journal of the Acoustical Society, Vol 34, 131-132.

Mailer, H., et al. 1970 (Jul). "The Development of Ultrasonic Nondestructive Testing Instrumentation to Measure Pavement Thickness," Final Report EES 208, Engineering Experiment Station, Ohio State University, Columbus, Ohio.

Mailer, H. 1972. "Pavement Thickness Measurement Using Ultrasonic Techniques," Highway Research Record No. 378, pp 20-28, Highway Research Record, Washington, DC.

Malhotra, V. M. 1970. "Preliminary Evaluation of Windsor Probe Equipment for Estimating the Compressive Strength of Concrete," Mines Branch Investigation Report IR 71-1, Department of Energy, Mines, and Resources, Ottawa.

_____. 1971. "Evaluation of the Windsor Probe Test for Estimating Compressive Strength of Concrete," Mines Branch Investigation Report IR 71-50, Department of Energy, Mines, and Resources, Ottawa.

Malhotra, V. M. 1972. "Canadian Mines Branch Unpublished Data Dealing with the Use of Acoustic Emission for Investigation in Concrete," Department of Energy, Mines, and Resources, Ottawa.

_____. 1976. "Testing Hardened Concrete: Nondestructive Methods," ACI Monograph No. 9, American Concrete Institute, Detroit, Mich.

Marine Technology Society. 1984. Operational Guidelines for Remotely Operated Vehicles, Washington, DC.

_____. 1985. Rov. '85, San Diego, Calif.

Mazel, C. H. 1984 (14-17 May). "Inspection of Surfaces by Side Scan Sonar," ROV '84, Marine Technology Society.

McDonald, J. E. 1980 (Apr). "Maintenance and Preservation of Concrete Structures; Repair of Erosion-Damaged Structures," Technical Report C-78-4, Report 2, US Army Engineer Waterways Experiment Station, Vicksburg, Miss.

McMaster, R. C. 1959. Nondestructive Testing Handbook, Vol II, Section 44, p 20, Ronald Press, New York.

Mlakar, P. F., Walker, R. E., and Sullivan, B. R. 1981 (Sep). "Acoustic Emission from Concrete Specimens," Miscellaneous Paper SL-81-26, US Army Engineer Waterways Experiment Station, Vicksburg, Miss.

Moore, W. A. 1973. "Detection of Bridge Deck Deterioration," Highway Research Record No. 451, pp 53-61, Highway Research Board, National Academy of Sciences--National Research Council, Washington, DC.

Muenow, P. 1963. "A Sonic Method to Determine Pavement Thickness," Journal of the Portland Cement Association Research.

Pace, C. E., and Alexander, A. M. 1982. "In-place Stability and Deterioration of Structures," Miscellaneous Paper SL-82-20, US Army Engineer Waterways Experiment Station, Vicksburg, Miss.

Patterson, D. R., and Pope, J. 1983. "Coastal Applications of Side Scan Sonar," Coastal Structures '83, J. R. Weggel, ed., pp 902-910, American Society of Civil Engineers.

Richardson, M. H. 1980 (Apr). "Detection of Damage in Structures from Changes in Their Dynamic (Modal) Properties--A Survey," Designation NUREG/CR-1431 UCRL-15103, Lawrence Livermore Laboratory and Structural Measurement Systems, Incorporated; prepared for US Nuclear Regulatory Commission.

Rissel, M. C., et al. 1982 (Oct). "Assessment of Deficiencies and Preservation of Bridge Substructures Below the Waterline," National Cooperative Highway Research Program Report 251, Transportation Research Board, Washington, DC.

Sears, F. W., and Zemansky, M. W. 1957. University Physics, Addison-Wesley Publishing Co., Inc., Reading, Mass.

Stein, P. K. 1964. "Measurement Engineering; Vol 1, Basic Principles," Stein Engineering Services, Inc., Phoenix, Ariz.

SONEX Ltd. 1984 (Jan). "High Resolution Acoustic Survey, Folsom Dam Stilling Basin Floor," Final Report, SONEX LTD., Richland, Wash.

Stowe, R. L. 1974 (Jul). "Low-Strength Concrete in the New Walter Reed Hospital, Washington, DC," Miscellaneous Paper C-74-14, US Army Engineer Waterways Experiment Station, Vicksburg, Miss.

Stowe, R. L., and Thornton, H. T., Jr. 1981 (Aug). "Condition Survey, Repair and Rehabilitation Lock and Dam No. 24, Mississippi River," Miscellaneous Paper SL-81-21, US Army Engineer Waterways Experiment Station, Vicksburg, Miss.

_____. 1984 (Sep). "Engineering Condition Survey of Concrete in Service," Technical Report REMR-CS-1, US Army Engineer Waterways Experiment Station, Vicksburg, Miss.

Stowe, R. L., et al. 1980 (Apr). "Concrete and Rock Tests, Major Rehabilitation and Compliance, Lockport Lock, Illinois Waterways, Chicago District," Miscellaneous Paper SL-80-4, US Army Engineer Waterways Experiment Station, Vicksburg, Miss.

Sullivan, B. R., Pace, C. E., and Campbell, R. L. 1984 (Feb). "Condition Evaluation of Supersonic Naval Ordnance Research Track (Snort)," Miscellaneous Paper SL-84-1, US Army Engineer Waterways Experiment Station, Vicksburg, Miss.

Thornton, H. T., Jr. 1977 (Sep). "Development Procedures for Nondestructive Testing of Concrete Structures; Present Practices," Miscellaneous Paper C-77-11, Report 1, US Army Engineer Waterways Experiment Station, Vicksburg, Miss.

Thornton, H. T., Jr., and Glass, D. 1980 (Apr). "Ultrasonic Velocity Measurements in Concrete, Lock and Dam No. 24, Mississippi River," Miscellaneous Paper SL-80-2, US Army Engineer Waterways Experiment Station, Vicksburg, Miss.

Thornton, H. T., Jr., Pace, Carl E., Stowe, Richard L., Pavlov, Barbara A., Campbell, Roy L., and Alexander, A. Michel. 1981. "Evaluation of Condition of Lake Superior Regulatory Structure, Sault Ste. Marie, Michigan," Miscellaneous Paper SL-81-14, US Army Engineer Waterways Experiment Station, Vicksburg, Miss.

Vernitron Piezoelectric Division. "Modern Piezoelectric Ceramics," Bulletin PD-9247, Bedford, Ohio.

Victor, D. J. 1963. "Evaluation of Hardened Field Concrete with Rebound Hammer," Indian Concrete Journal (Bombay), Vol 37, No. 11, pp 407-411.

Volz, R. D., and Jones, P. 1982 (May). "Post Test Data Report for Blast Resistance Capacity of Dept. of Energy Building 12-64, Phase 1," US Army Engineer Waterways Experiment Station, Vicksburg, Miss.

Walker, D. C. B., and Lumb, R. F. 1964 (Jul). "Piezoelectric Probes for Immersion Ultrasonic Testing," Applied Materials Research, pp 176-183.

Washington, A. B. G. 1961. "The Design of Piezoelectric Ultrasonic Probes," British Journal of Nondestructive Testing, Vol 3, pp 56-63.

Wells, P. N. T. 1977. Biomedical Ultrasonics, Academic Press, New York.

Willetts, C. H. 1958 (Jun). "Investigation of the Schmidt Concrete Test Hammer," Miscellaneous Paper No. 6-267, US Army Engineer Waterways Experiment Station, Vicksburg, Miss.

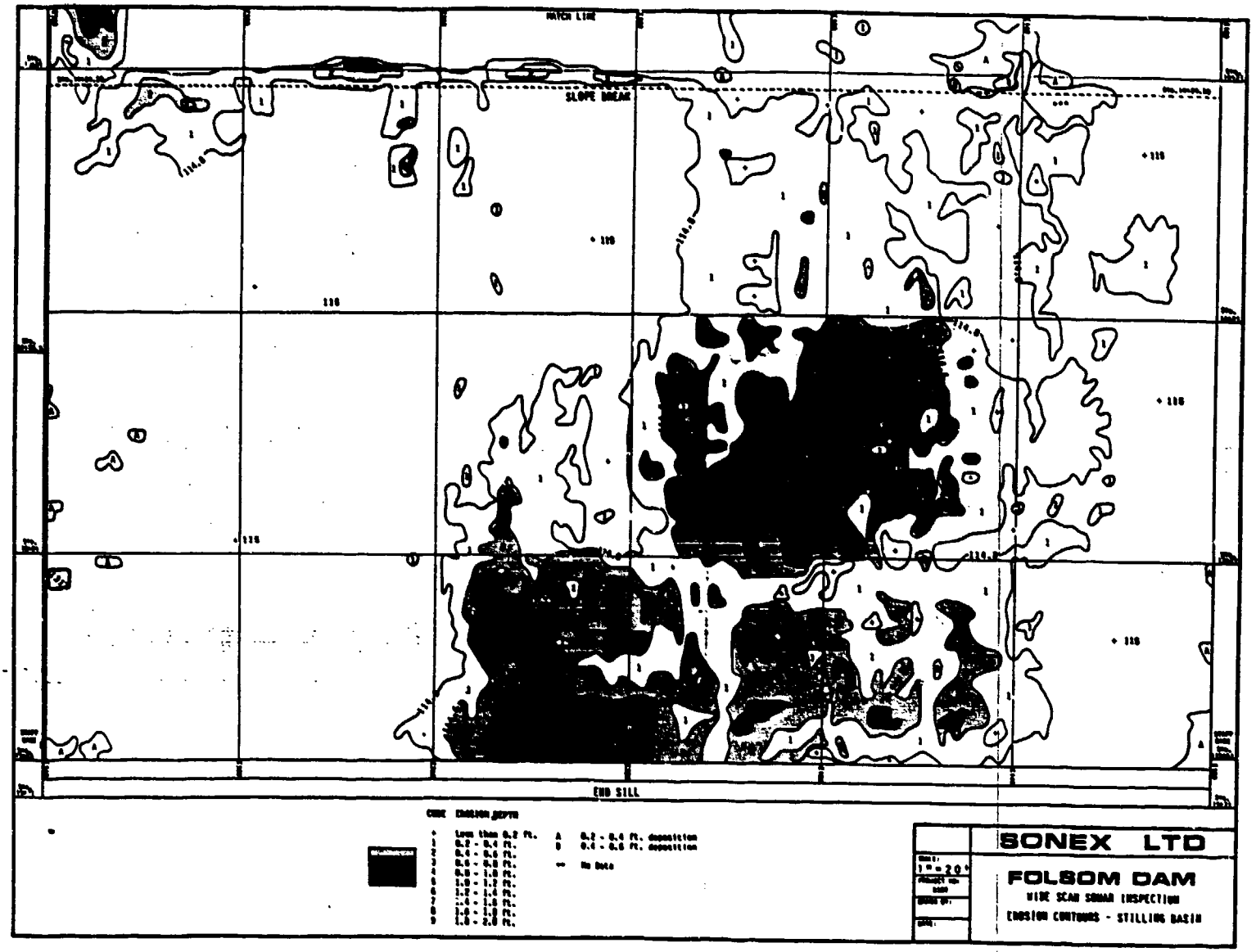

SONEX LTD

FOLSOM DAM

SIDE SCAN SONAR INSPECTION

EROSION CONTOURS - STILLING BASIN

PLATE 1

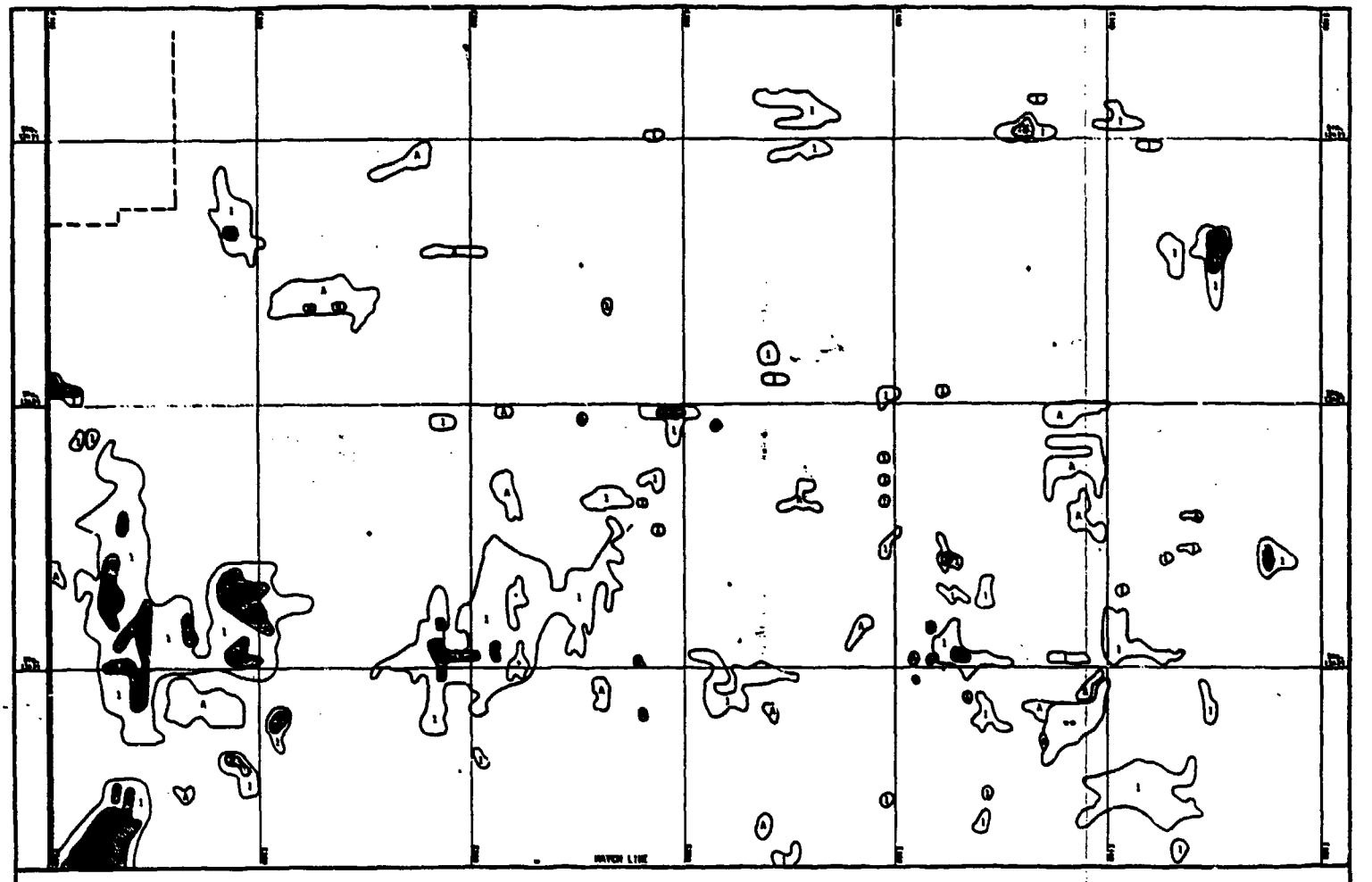

SONEX LTD

FOLSOM DAM

SIDE SCAN SONAR INSPECTION

EROSION CONTOURS - STILLING BASIN

PLATE 2

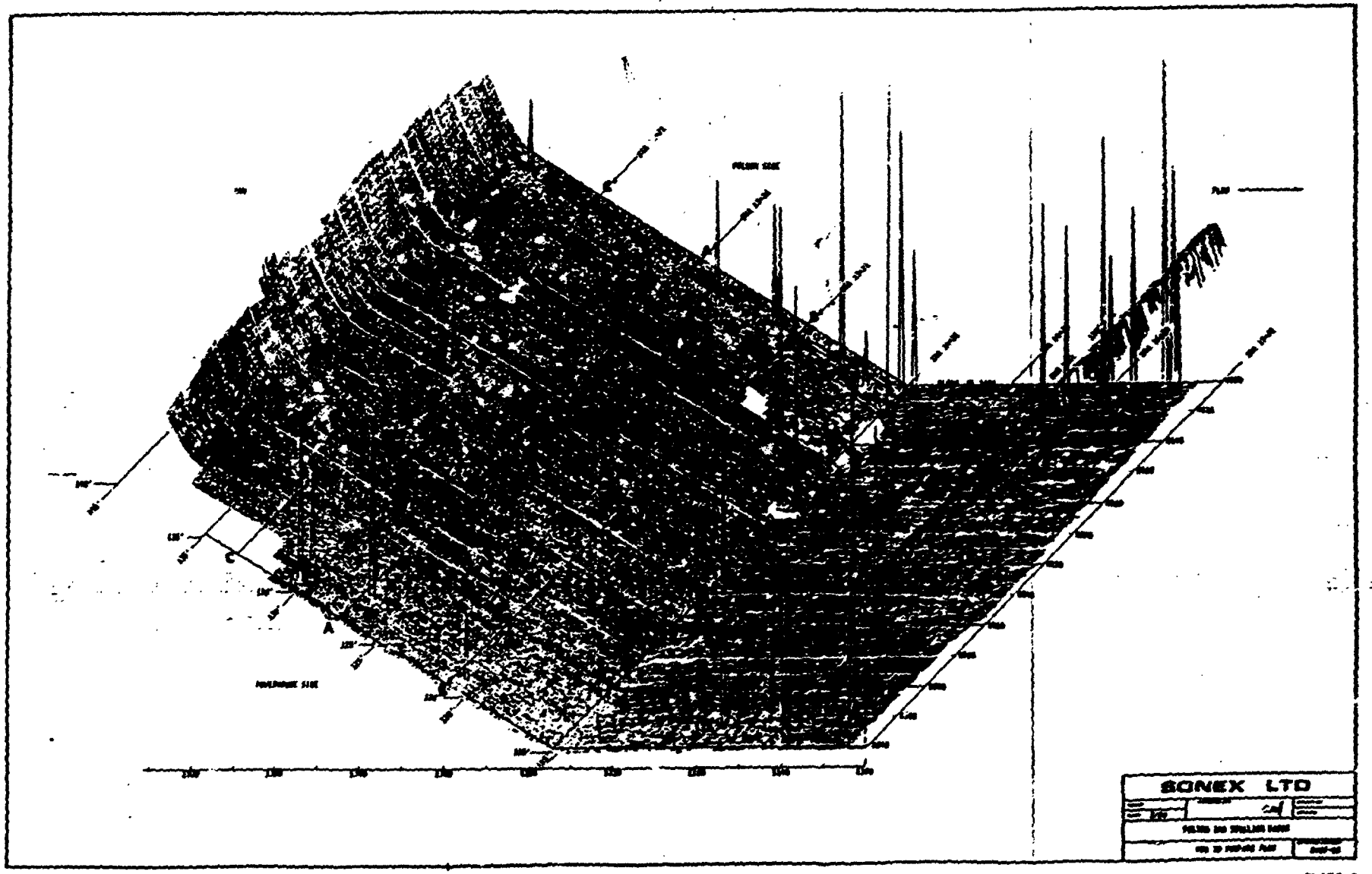

PLATE 3

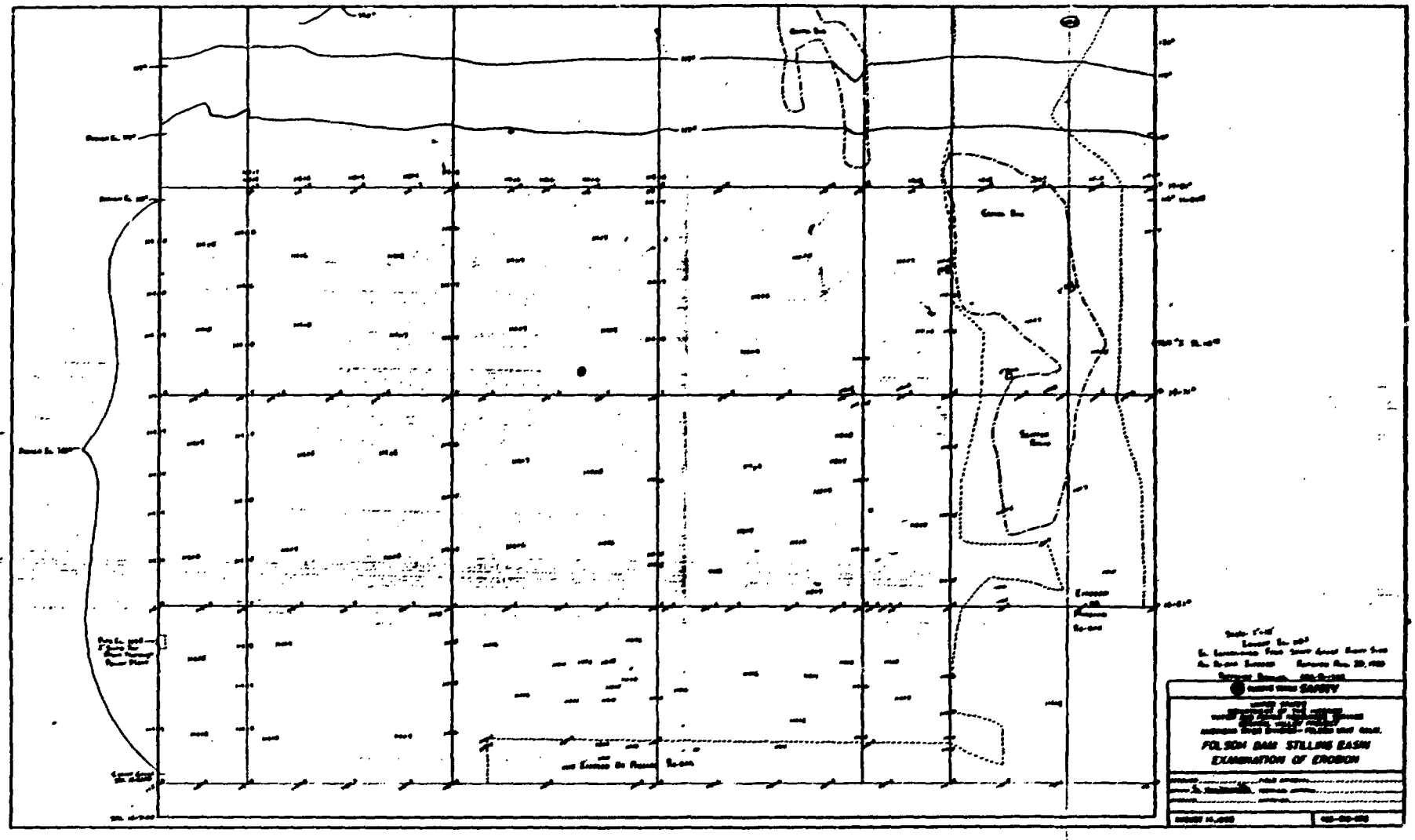

PLATE 4

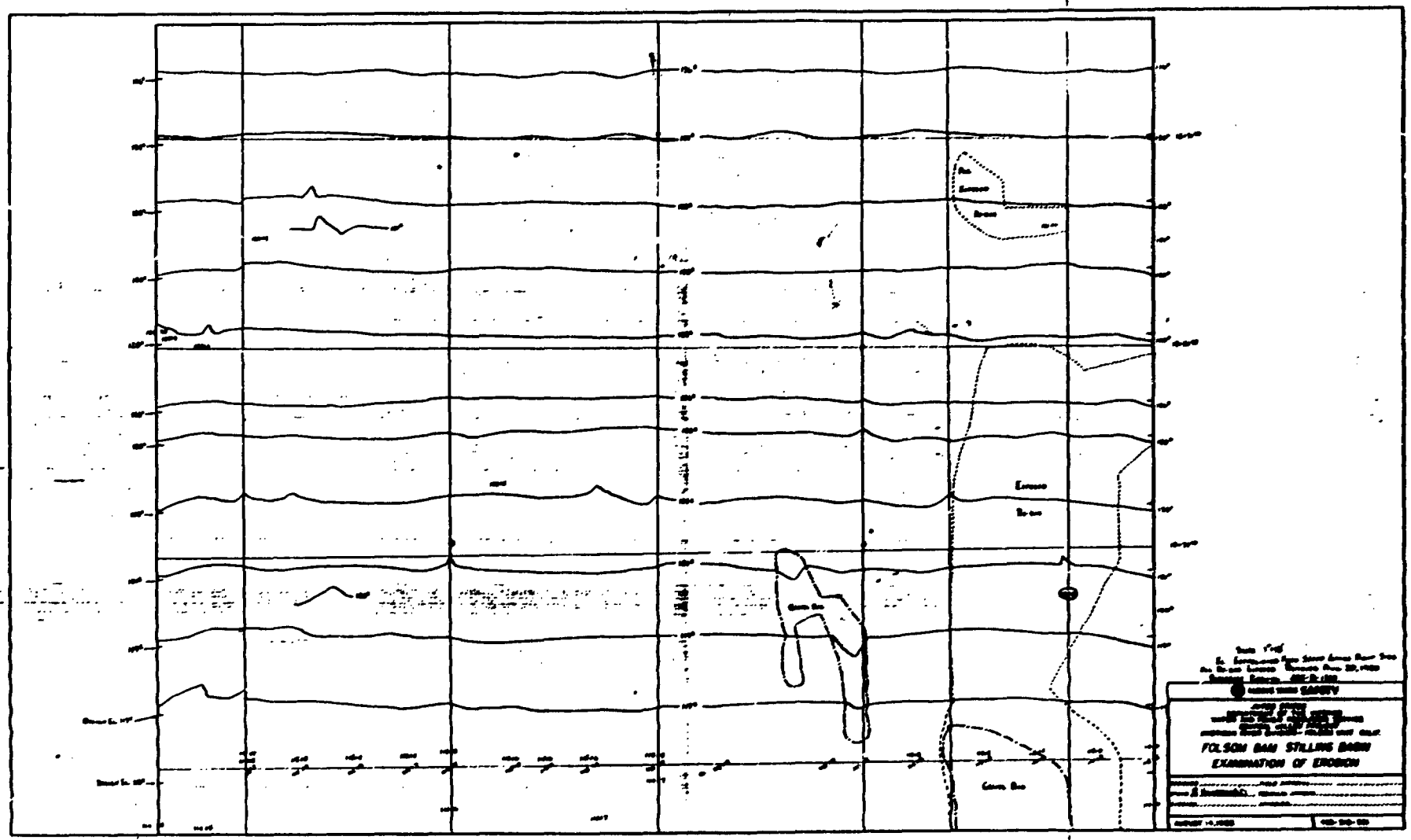

PLATE 5

APPENDIX A
HIGH-RESOLUTION ACOUSTIC SURVEYS; DESCRIPTIONS AND SPECIFICATIONS

Note: This appendix reproduces a section of a contract; in this case, it is Section F.

SECTION F
DESCRIPTIONS AND SPECIFICATIONS

F.1. Description of Work

Provide high resolution acoustic survey equipment and services to the government at the site specified in Paragraph F.2. Data from the survey will be used to evaluate the physical conditions of the underwater portions of large civil engineering structures. The requirements of this procurement differ from standard hydrological survey requirements in: the levels of vertical and horizontal accuracy, the ability to detect and measure negative surface anomalies (depressions), and the need to provide full coverage of broad areas in minimal time. Data shall be taken in such a manner that successive inspections, in following years,can be made with the assurance that the inspection data from the various surveys can be directly compared. Sufficient data shall be recorded so that the x,y,and z coordinates of each surveyed point can be recalculated from the stored data. Measurement accuracy shall conform to the specifications supplied in Paragraph F.4.

F.2. Project Location

[This section to be completed by the contracting agency for each specific site.]

F.2.1. Name of Dam or Structure:

F.2.2. Location:

F.2.3. Nearby Towns, Access:

[Include a location map or sketch]

F.3. Site Specific Information

[This section to be completed by the contracting agency for each specific structure. The area of the structure to be surveyed, and any pertinent physical parameters should be included.]

F.3.1. Description of structure: dam, spillway, lock, etc.

F.3.2. Approximate area in square feet:

F.3.3. Map or diagram of the areas to be covered by the reconnaissance survey.

F.3.4. Range of water depths to be encountered:
Minimum = Five feet; Maximum = Thirty feet

F.3.4.1. Water level gauges at the survey site continuously read water levels to 0.1 foot accuracy or better.

OR

F.3.4.1. Contractor must provide water level gauges which meet the required accuracy specifications.

F.3.5. Anticipated minimum and maximum flow rates:

F.3.6. Traffic conditions:

F.3.7. Restrictions on working hours:

F.3.8. Desired inspection period (dates):

F.3.9. Survey support boat

F.3.9.1. Description of the boat which the government can make available for mounting the survey equipment.

OR

F.3.9.1. The contractor will be expected to supply the survey boat.

[Any other site specific data which would help the contractor can be included.]

F.4. Survey Specifications

The acoustic survey will be conducted at a rate which will provide a minimum of 2,000 square feet of reconnaissance inspection coverage per hour, exclusive of mobilization and setup time. Government analysis requirements dictate that the survey system be capable of determining the X, Y, and Z coordinates of a boundary-defined underwater surface under static conditions within the following minimum limits.

F.4.1.	Vertical accuracy (Z)----------	± two inches
F.4.2.	Lateral accuracy (X, Y) --------	± one foot
F.4.3.	Roll Angle (0) _____	± 0.5 degree
F.4.4.	Yaw Angle (0) _____	± 1.0 degree
F.4.5.	Survey coverage:	
F.4.5.1.	Reconnaissance_____	One sample per two square feet
F.4.5.2.	Detailed Inspection --------	Two samples per one square foot
F.4.6.	Flaw Resolution: (Size of a detectable hole - X x Y)	
F.4.4.1.	Reconnaissance _____	2 ft. x 4 ft.
F.4.4.2.	Detailed Inspection _____	2 ft. diameter

F.4.7 Data to be recorded are the X and Y coordinates and 0 and 0 angles for each sample station, and the Z data (time-of-flight) for each transducer at that sample station; together with sufficient descriptive information to define the survey mode, location, and time period.

F.5. Work to be performed by the Contractor

F.5.1. Contractor shall furnish all professional and technical labor and suitable technical and support equipment to perform the required acoustical survey at the specified site. The crew and equipment shall be capable of acquiring data meeting the specifications of Paragraph F.4.

F.5.2. Contractor will conduct a high-resolution acoustic survey to fully cover the area of interest as defined in Paragraph F.3. Provisions will be made for providing a first-look capability as the acoustic data is acquired.

F.5.3. All data acquired during the survey will be recorded on 5 1/4 inch diskettes, in ASCII format.

F.5.4. Upon completion of the field survey, the Contractor shall process the survey data to provide two output formats.

F.5.4.1. 3-D graphic plot showing underwater surface relief to the detail shown in Paragraph F.7.

F.5.4.2. Contour map of the underwater surface to the detail shown in Paragraph F.7.

F.5.5 Contractor shall furnish data relating the coordinates of the survey to coordinates or recognizable, stable features of the structure being surveyed. Location accuracy shall be within ± one foot.

F.6.1.2. Wide Scan Sonar Controller

Associated electronics shall acquire and process the pulse-echo sonic data collected over the surveyed areas. Figure 3 shows a block diagram of the electronic section of a controller which has been used successfully for this type of work. Timing signals are transmitted by the WSS computer. The signals activate the transmit-pulse generator and the multiplex-demultiplex network which selects the proper transducer and amplifier. The transducer pulser and pre-amplifier circuits shall be individually tuned to the optimum frequency of each transducer.

The WSS controller shall perform the following functions:

1. Activate the appropriate transmitter/preamplifier/transducer as addressed by the computer.(Plate I)
2. Send a transmit pulse to each of the acoustic transducers in sequence and start a time-of-flight clock. (Plate II)
3. Pre-amplify the return echo from each of the acoustic transducers. (Plate II)
4. Detect the first-return echo above a preset detector level, following a transmit pulse. (Plate IV)
5. Stop the time-of flight clock to measure the time interval from the beginning of the transmit pulse to the detection of the first return signal. (Plate III)
6. Store the time-of-flight data in digital format for access by the WSS computer.
7. Notify the WSS computer when data is ready for transfer.

F.6.1.3. Display and Record

The WSS controller shall be interfaced to an ACE # 1000 6502-based computer or to other computers with speed and processing capabilities equal to or greater than this unit. This computer shall access the timing module after every data acquisition cycle and transfer the time-of-flight data into memory for processing.

A real-time video display controlled by the main WSS computer shall be provided. This shall be a columnar display of the depth (Z) data from each transducer. The software shall provide sreen scrolling capability so that several sets of data are available for the operator to view at any time. It is necessary that the operator be provided the capability of seeing the results in real time so that he can note anomalous areas for further study.

All raw data from the main WSS computer are stored on magnetic format for replay and printout after the survey. These include X and Y coordinates from the LOCATOR, and yaw angle and roll angle readings as well as the time-of-flight data.

These basic data fully describe the information available from any one survey and can be processed for printed or graphic output.

F.6.2. Location Subsystem

The location subsystem keeps track of the position of the transducer array bar. Since the array bar is mounted on a floating work platform, it is free to move in any direction, and to rotate about any of three orthogonal axes, i.e., it has six degrees of freedom as seen in Figure 4. The positioning subsystem of the WSS must be capable of controlling, or determining, the displacement of each of these six degrees of freedom. The positioning subsystem must also provide measurement of the position of the moving coordinate set (X', Y' and Z') relative to a fixed coordinate system (X, Y and Z).

F.6.2.1 Vertical

The vertical displacement and position of the transducers shall be controlled by precise placement of the transducers on the floating platform, and the floating level with respect to surface of the water.

Vertical displacement shall be determined in reference to a major structural benchmark. The instantaneous water level shall be measured during all data taking times. Water-level gauges already installed at the structure can be read to obtain this information if the resolution is 0.01 foot or better. Fluctuations of water level during the survey period must be taken into consideration when calculating the final results.

When the array bar is attached to the boat the distance from the water level to the transducer face is carefully measured to 0.01 foot. This transducer draft shall be subtracted from the water level measurement to give the absolute, or relative, elevation of the transducer face which will not change unless the water level changes.

F.6.2.2 Lateral

Lateral positioning shall be accomplished by triangulation using an RF-acoustic ranging system. The system shall measure the boat position at all times to better than one foot of lateral (X,Y) accuracy, with ranging resolution of ± two inches.

The LOCATOR system shown in Figure 5 is one example of a short range, high accuracy positioning system suitable for the specified application. Effective range of the system shall be not less than 350 feet. Range resolution shall be better than ± 2 inches. Boat location is immediately displayed on a video monitor during survey operatons so that it can be used for steering to targets or around obstacles.

The acoustic ranging network shall consist of three, or more, omnidirectional sonic receivers in stationary positions which can be precisely located in relation to the structure to be surveyed and one omnidirectional sonic transmitter mounted on the survey boat. Figure 5 shows the typical use of an RF-acoustic network in a confined area.

Figure 6 shows a block diagram of the functions of an RF-acoustic network. The transmitter is pulsed whenever location data is needed - typically once a second (Plate VI). When the pulse is triggered, three time-of-flight clocks are started, one for each of the receivers. As the sonic pulse is detected by each of the receivers, the receiver electronics triggers a frequency-coded RF transmitter. The three RF signals are received by a RF receiver aboard the boat and the appropriate time-of-flight clock is turned off (Plate

V). The block diagram of a suitable sonic beacon (Plate VII) is shown in Figure 7.

The three time-of-flight clocks are read by the position computer to calculate the distances from the boat to each of the three receiver beacons. These distances, and the surveyed location of the beacons, shall be used to define the location of the boat-mounted transmitter in terms of the base survey.

The boat coordinates are calculated from the fixed acoustic- beacon coordinates and the measured distance from the boat to each beacon. With three beacons, three pairs of distances are possible. The computer shall be programmed to calculate the boat location using each of the three pairs. Ideally the three calculated boat locations would be identical. The computer shall be programmed to select the most likely location by rejecting false data, averaging good data, and projecting the probable limits of boat movement.

An example of calculations for one set of X,Y coordinates is shown in Figure 8. The position computer shall plot these calculated X,Y coordinates as a point on the operator's videoscreen. All preceding locations within the range of the screen shall also be shown. The locations of the acoustic beacons shall be shown if within screen range. The course of the boat shall be displayed as a line traversing the screen. Software shall provide that the scale on the screen can be easily changed for large area, or for detailed, surveying.

The heading of the boat at any point in time shall be calculated as the forward vector for the present location from the most recent preceding location.

F.6.2.3. Rotational

The rotational degrees of freedom of the boat and array bar are pitch, roll and yaw. These are shown in Figure 4.

F.6.2.3.1. Pitch

Pitch is not a significant factor if proper boat selection is made. For this application wave action will be minimal and it is acceptable to assume that pitch will be less than 1 degree and will not require distance corrections.

F.6.2.3.2. Roll

The roll angle transducer shall be rigidly attached to the transducer array bar. This device shall measure the longitudinal tilt, or roll, of the transducer bar, transform this angle into digital format and transmit the data to the computer when interrogated at the start and finish of each array firing sequence. The roll angle encoder shall measure roll with resolution of 0.36 degree (21 minutes) or better.

A roll angle of one degree moves the center of the transducer beam about one-half foot laterally at the bottom of thirty feet of water. For smaller angles no lateral position correction is required. For angles of one to five degrees lateral corrections shall be applied for beam position correction. Vertical corrections of depth readings are not necessary when roll angle is less than five degrees.

F.6.2.3.3. Yaw

Yaw is the horizontal rotation of the boat around the Z axis. This shall be measured with a digital magnetic compass which provides digital data to the computer. The yaw compass shall have 1.4 degree resolution and ± 0.7 degree repeatability.

The yaw angle and the X,Y coordinates of the center of the array bar shall be used to calculate the X,Y positions of all depth measuring transducers. Figure 9 shows the relationship between yaw and course of the boat.

The X,Y coordinates of the center of the array bar and the yaw angle shall be recorded. These data define the position of the acoustic transducers.

F.6.2.4. Display

The video display showing boat location and progress is part of the LOCATOR system and is controlled by the LOCATOR computer. The basic data used by the computer is the coordinate data for the array bar and the yaw angle.

The boat-mounted computer shall calculate and keep a running record of the X and Y coordinates, yaw, and the boat course. On a video screen in front of the boat operator the transducer bar shall be shown as a moving white line, scaled to the length of the bar. As the boat moves forward, the transducer-bar location line shall sweep across the screen "painting" a white swath. To insure full coverage of the area to be surveyed the operator shall paint the screen white with consecutive traverses of the boat. In the example shown in Figure 10, the boat has just started across the survey area and turned for the first traverse.

The computer program shall provide means for the operator to return to any area of interest for subsequent surveys. After the operator enters the coordinates of the area into the computer, the target location shall be displayed on the screen, and the boat steered to the area (see Figure 11).

The video display scale shall be adjustable by the operator to fit whatever area is being surveyed. The screen display shall have at least 44,800 pixels, arranged 280 x 160. Screen resolution shall be at least one square foot per pixel.

F.6.3. Boat Requirements

The selection of a proper boat affects the reliability and accuracy of the WSS inspection survey. The amount of pitch and roll are affected by the length and beam of the boat respectively: the longer and wider the boat, the less the pitch and roll.

Another required characteristic is the ability of the boat to retain heading at very slow speeds. The boat used in the contract shall have twin screws, either inboard or outboard to aid in steering. The survey boat used for this survey shall be capable of maintaining a steady course, and keeping a speed of not less than ten knots with one engine disabled.

The boat should have a load capacity of at least 2500 pounds. The total estimated load for the WSS equipment together with the crew and an observer is about 2000 pounds.

Transducer Array Bar and Hardware -------	up to	500#
WSS Equipment ----------	"	150#
Peripheral Equipment ----------	"	100#
Generator ----------	"	150#
Twin Outboard Motors ----------	"	150#
Up to Four People ----------	"	800#
Total Estimated Load ----------	"	1850#

In addition to the above basic safety requirements, other features are desirable for ease of operation, and for instrument protection and operation.

The survey boat used for this contract shall have a flat,open work-area at the bow to facilitate assembling and installing the array bar. A square bow is useful for the same reason, and allows the array bar to be placed nearer the front of the boat so that data can be taken up close to walls.

An enclosed cabin, large enough for two men and the WSS equipment, is a necessity for this survey application. Flat sides, and a broad beam, are required for roll stability and to facilitate array installation. Flat sides also facilitate loading and unloading.

Several boat manufacturers make boats suitable for the inspection survey requirements of this contract. One example of a suitable boat is the MonArk 21 foot Little Giant. With a 20.5 foot length and a 7.75 foot beam, this is the smallest boat acceptable for a survey. MonArk also makes a 22 foot Workboat with an 8 foot beam which would be ideal for this survey. Specifications for these two boats are attached. Survey boats by other manufacturer will be acceptable if size and handling characteristics are similar or superior to the above boats.

The stability of the larger boats is an advantage, but this can be offset by the difficulty of finding berths, transporting, and launching the larger boats. In general, the largest available boat which will fit into the areas to be surveyed should be supplied.

F.7. Equipment and Services Provided by the Government

The Government will have the responsibility to supply, or arrange for the following equipment and services.

F.7.1. Access to the inspection site during the period of the inspection, together with and necessary licenses, permits, or rights-of-way required for such access.

F.7.2. Maps and drawings of the structures to be inspected.

F.8 Field Operations

F.8.1. Contractor shall perform a calibration check of depth and ranging equipment at the start of the day, midway through the day, and at the end of the day. The check shall be for the purpose of determining the factor for converting time-of-flight data into distance data. The depth check shall consist of lowering a suitable target beneath one of the 300 kHz depth-measuring transducers, and reading the time-of-flight to the target and back as the target is lowered to successive one- foot increments. The depth calibration factor shall be derived from the morning readings, and shall be used until midday. The midday reading shall be used for the remainder of the day. If the midday and evening calibration readings vary from the morning reading by more than 0.02 foot, then the second half of the morning readings shall be recomputed based on the midday calibration factor. If the evening calibration factor varies from the midday faactor, a similar afternoon correction shall be made.

F.8.2. Following the morning calibration procedure, the contractor shall perform a static check of the complete electronic system. Readings from the roll angle detector shall be observed on the video screen. These readings should be "0 degrees". If they are not zero, then one end of the transducer array bar should be raised or lowered until the desired zero reading of the roll angle detector is seen. Holding the boat stable, the system shall be used to acquire and record depth data for a period not less than two minutes. Data from any one transducer shall not vary more than ± two inches; ninety percent of the data shall be within ± one inch for the system to be considered acceptable.

F.8.3. Once these calibration and checkout procedures are satisfactorily completed, the contractor shall proceed with the daily acoustic survey operation in the reconnaissance inspection mode.

F.8.4. At the conclusion of each day of reconnaissance survey, the contractor shall provide a printout of the reconnaissance data for the day, either in the form of a contour map of the areas surveyed, or in the form of individual distances for each transducer shown to 0.1 foot or better.

F.8.5 The technical representative of the government at the site may request that specific areas of the structure may be resurveyed in the Detailed Inspection mode. These areas shall be resurveyed by the Contractor at the earliest practicable time, and the printed data delivered to the Government representative. This survey work will be charged on an hourly basis, with a minimum charge of two hours for each such request.

F.8.6. If, in the best judgment of either the Contractor or the Government representative, it is necessary to delay the survey operation because of traffic, weather, high water, or any other conditions which would interfere with the survey operation, the crew and equipment shall go on standby until such conditions change. If it is determined by the Government representative that the conditions will not change within a reasonable period of time then the crew and equipment will be demobilized. The Contractor will be paid the standby rate for each full hour in standby status, but not less than two hours for each standby occurrence. If the Government representative determines that demobilization is necessary before the survey is completed, then the Contractor will be paid a re-mobilization fee when the contract is restarted.

F.8.7. In the event that excessive turbulence seems to be present, the Government representative at the site may request a repeat of step F.8.2 to determine the effect of the turbulence on the data. If the effects of turbulence are such that the data from the survey would not be useful to the government, the Government representative may request that the crew and equipment go on standby status until conditions become better. Each such test

of the turbulence shall be considered as one hour of additional survey work for payment purposes.

F.8.8. At the beginning of the first survey, the Contractor may be requested to demonstrate the resolution and the accuracy of the system by surveying above a target prepared and positioned by the Government. The target will replicate the resolution and accuracy limits specified in Paragraphs F.4.1, F.4.2, and F.4.6.

F.9 Documentation

F.9.1. The Contractor shall submit to the Contracting Officer within thirty days after the completion of the survey, a typewritten report which shall contain all the findings, conclusion and recommendations pertinent to the survey activity. The report shall include, but not be limited to, identification of all procedures, equipment, field activities, and factors which affect the data results. The report shall include copies of the contour maps of the areas surveyed, and reduced scale copies of the 3D plots of the areas surveyed. Survey stations shall be identified, and tied to recognizable stations or points on the surveyed structure.

F.9.1.1. The report shall be copied on 8 1/2" x 11" paper,and bound with plastic binders.

F.9.1.2. Twenty copies of the bound report, including contour maps and 3D plots shall be delivered.

F.9.2. A composite contour map shall be provided of the contiguous areas surveyed. The map scale shall be 1 to 100 (1 inch = 8 feet 4 inches). The map shall be divided so that each segment of the map shall fit on an 11" x 17" sheet for reproduction and binding into the report.

F.9.2.1. The contour interval for the map shall be selected with consideration of the amount of relief detected in the area surveyed. Contour intervals shall not be less than two inches, and not more than one foot.

F.9.3. A 3D plot of the survey data for the entire contiguous area surveyed shall be provided. This presentation is to be similar to that shown in Figure 13. The scale shall be selected

so that the overall relief is easily seen, and so that the entire area can be drawn on one sheet, not to exceed 24" x 36" in size. Typically the vertical scale will be 10 to 20 times the horizontal scale. This 3D plot will be reduced to fit an 11" x 17" sheet for reproduction and binding into the report.

F.9.4. In addition to the report, the documentation shall include all of the raw survey data which was recorded on diskette. This shall be provided in a form which is useable by the Government in its computer facility. Data shall be provided in the following format.

F.9.4.1. Medium: [Tape, diskette, disk, cassette, etc]
F.9.4.2. Format: [ASCII or other code]
F.9.4.3. Other specifications

F.10. Payment Schedules

F.10.1. Payment for the survey and the related tasks shall be calculated in accordance with the following schedule.

F.10.1.1. Preparation, Mobilization, and Setup	Sum Job
F.10.1.2. Reconnaissance Survey	Sum Job
F.10.1.3. Detailed Inspection as Requested (Two Hour Minimum)	Per Hour
F.10.1.4. Additional Calibration Checks (One Hour per Event)	Per Hour
F.10.1.5. Standby Time as Required	Per Hour
F.10.1.6. Documentation	Sum Job

F.10.2. Invoices for payment shall be submitted within thirty days after the completion of each of the above tasks. Invoices may be submitted at the end of each calendar month for partial completion of any of the above tasks with the exception of F.10.1.6. (Documentation), which must be completed before the work is invoiced.

TABLE I

EQUIPMENT LIST

SUBSYSTEM - ITEM	SIZE (CF)	WEIGHT (LBS)
ACOUSTIC		
WSS Computer 6502 microcomputer w/64 K RAM, one disk drive, high-resolution video monitor, and multifunction series/ parallel I/O card.	2	~25
Interface Card	na	na
WSS Controller Pulser/Amplifiers T.O.F. Detectors Roll Ang. Reader HV Power Supply Multiplex Control	3	~50
Transducer Array	variable (Up to ten feet long, up to 500 pounds in air)	
LOCATOR		
Computer 6502 microcomputer w/ 48K RAM, one disk drive, video monitor and multifunction I/O card.	2	~23
Controller	na	na
Compass Digicourse #218 w/ #259 Interrogator	1	~10
Interface	2	~25
Transmitter Sonar transmitter, 25-50 kHz		
Sonic Beacons (3 Req'd) 25-50 kHz sonar recivers with auto-triggered RF transmitters, selectable transmit frequency		~50
RF Receivers (3 Req'd) Selectable frequencies to match the above transmitters.		~10

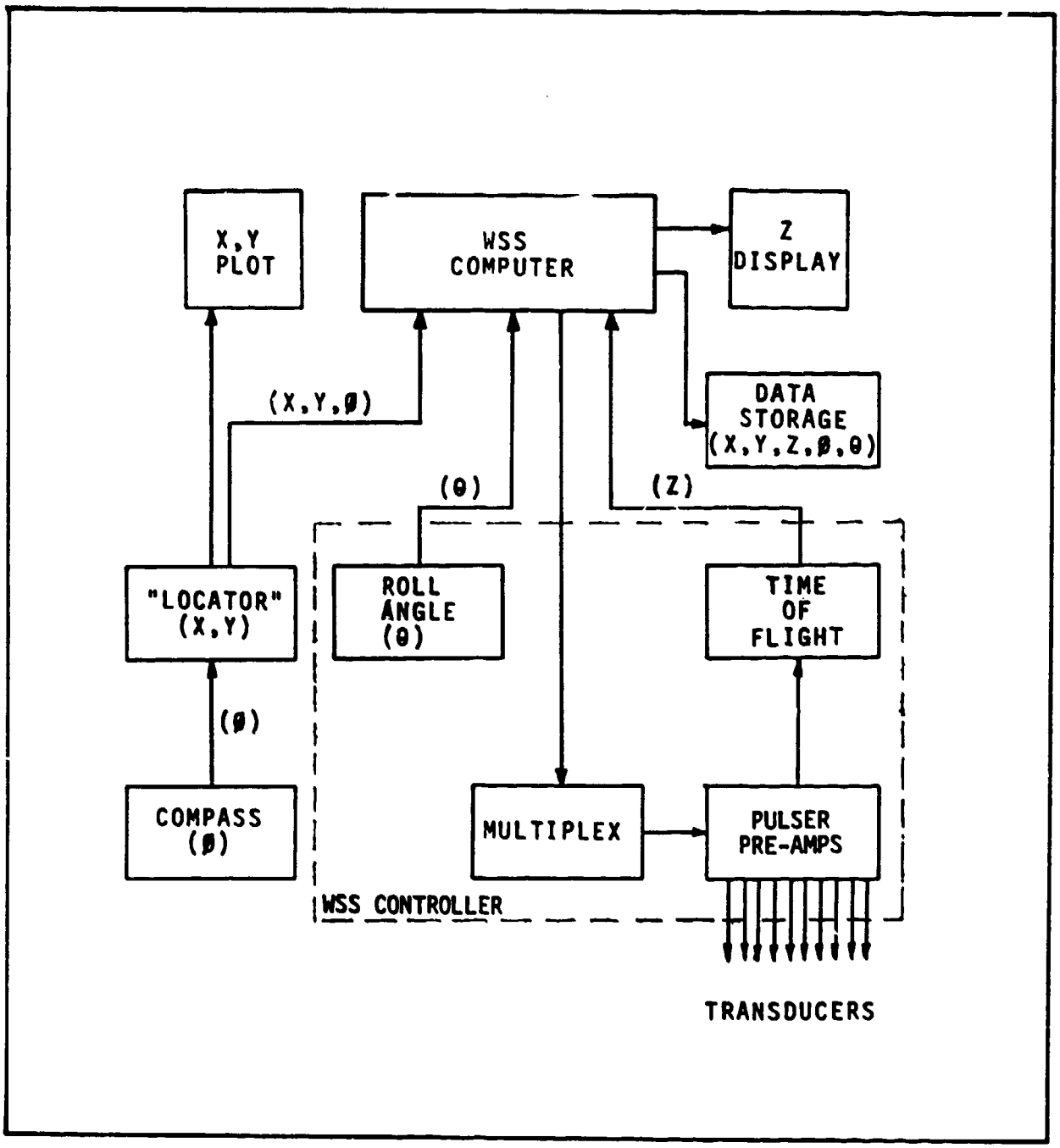

Figure 1. Wide Scan Sonar (WSS) - Functional Block Diagram
The WSS computer collects data from position and time-of-flight sensors, and then processes the data for display and storage. The array location is shown on the "X,Y PLOT", upper left. The bottom elevation (Z) data for each transducer is shown on the "Z DISPLAY", upper right.

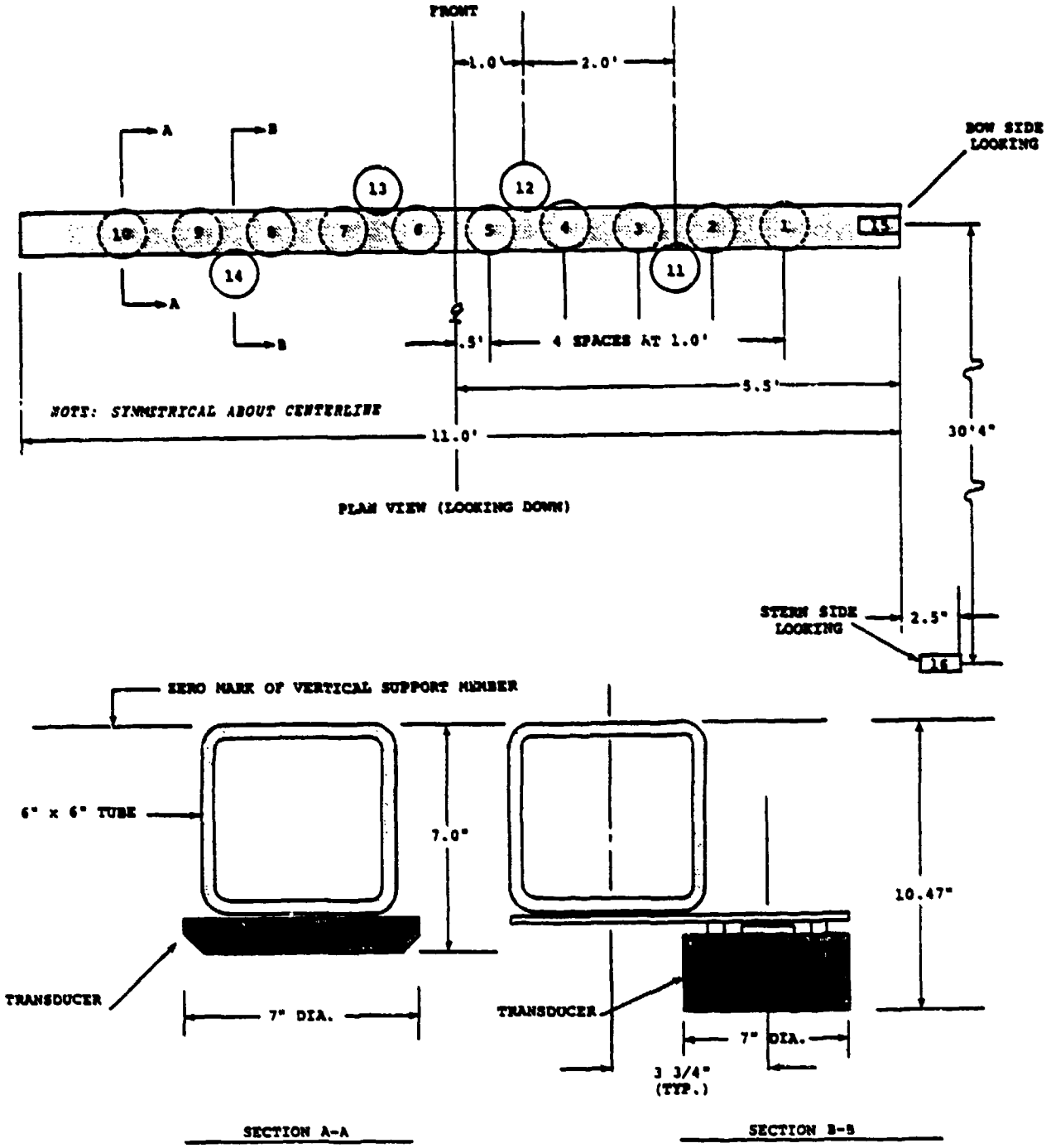

Figure 2. Transducer Array Layout
This is one possible arrangement of transducers for a large-area survey. Any number of transducers, up to 16, may be used. The array bar may be smaller for use in restricted areas.

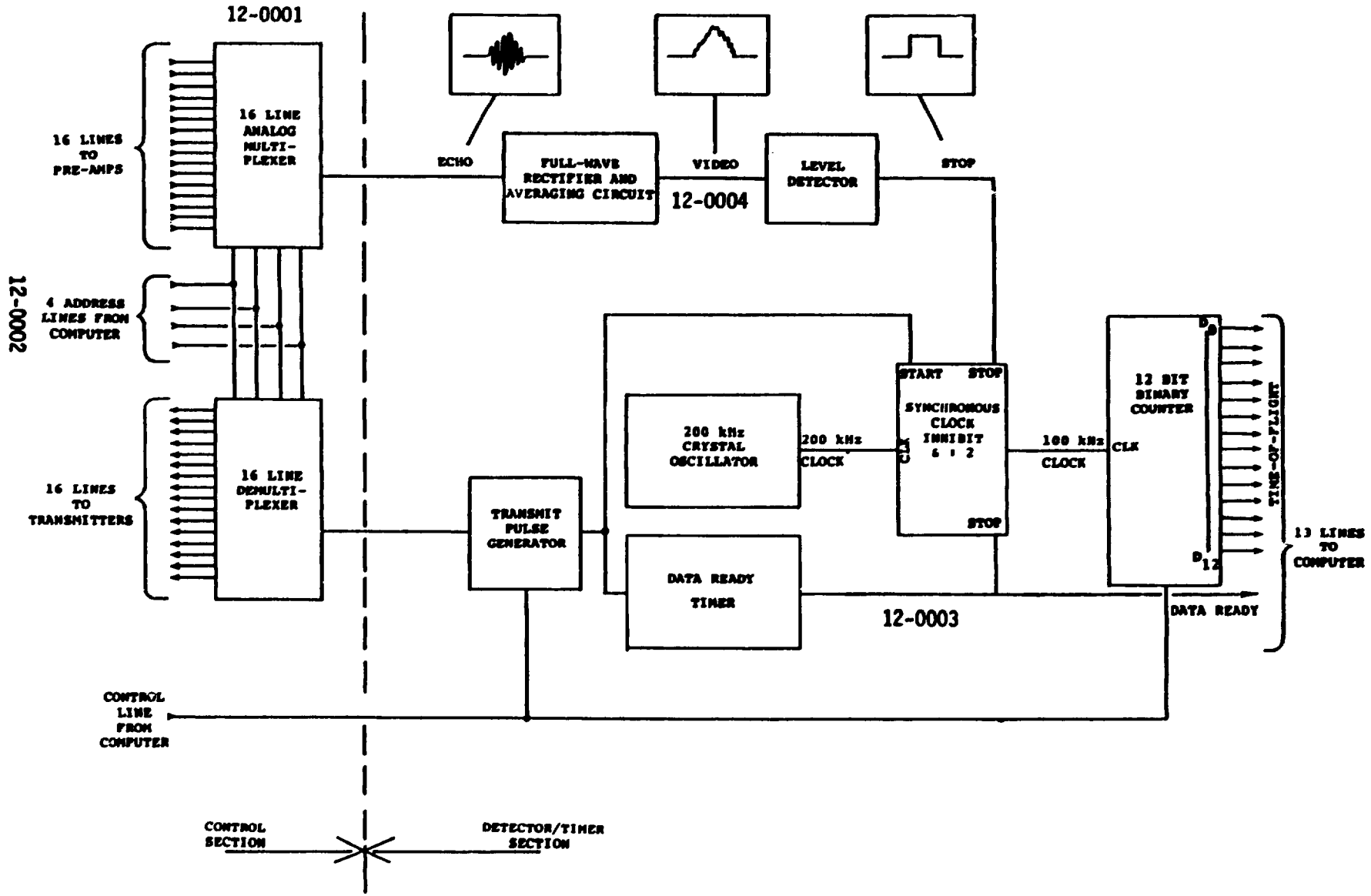

Figure 3. Wide Scan Sonar Controller - Block Diagram

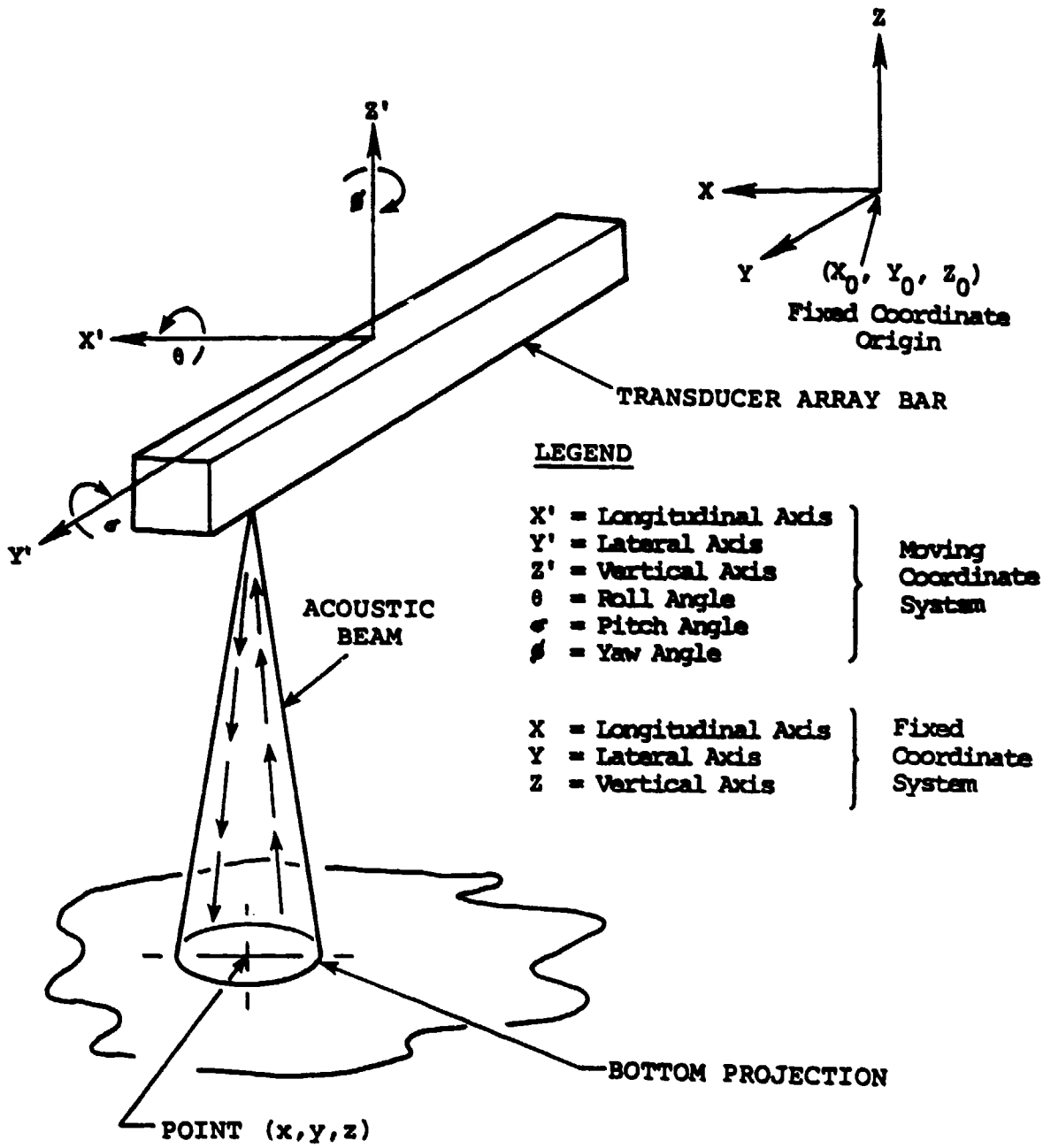

Figure 4. Definitions of Coordinate Systems and Parameters.

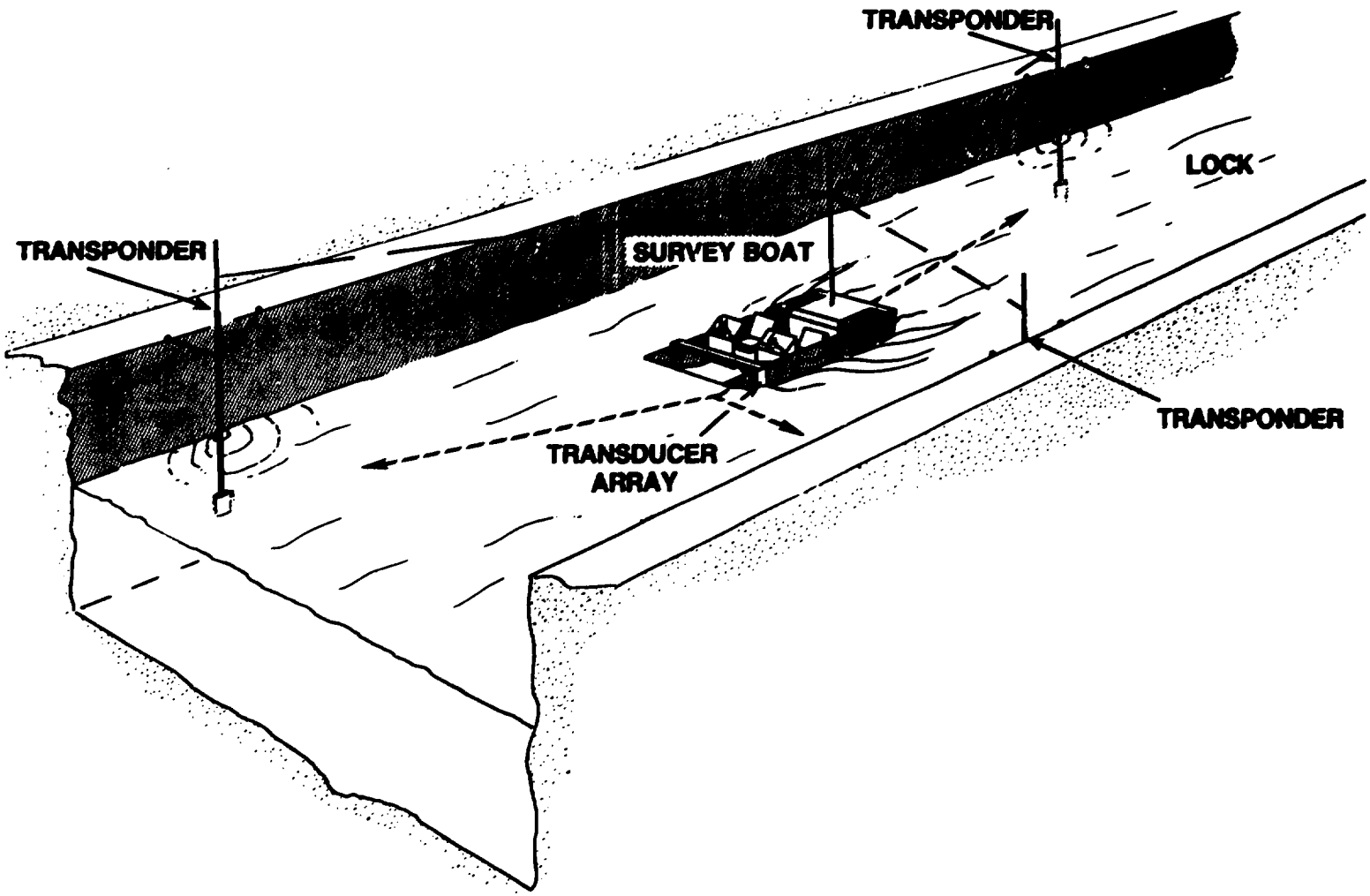

Figure 5. LOCATOR Network - Typical Operation
Acoustic/RF transponders are placed in the area to be inspected, and are located by survey. The WSS boat will triangulate its position in reference to the transponder beacons using the time-of-flight to each one. As these data are updated, the course of the boat can be computed and plotted on a video screen.

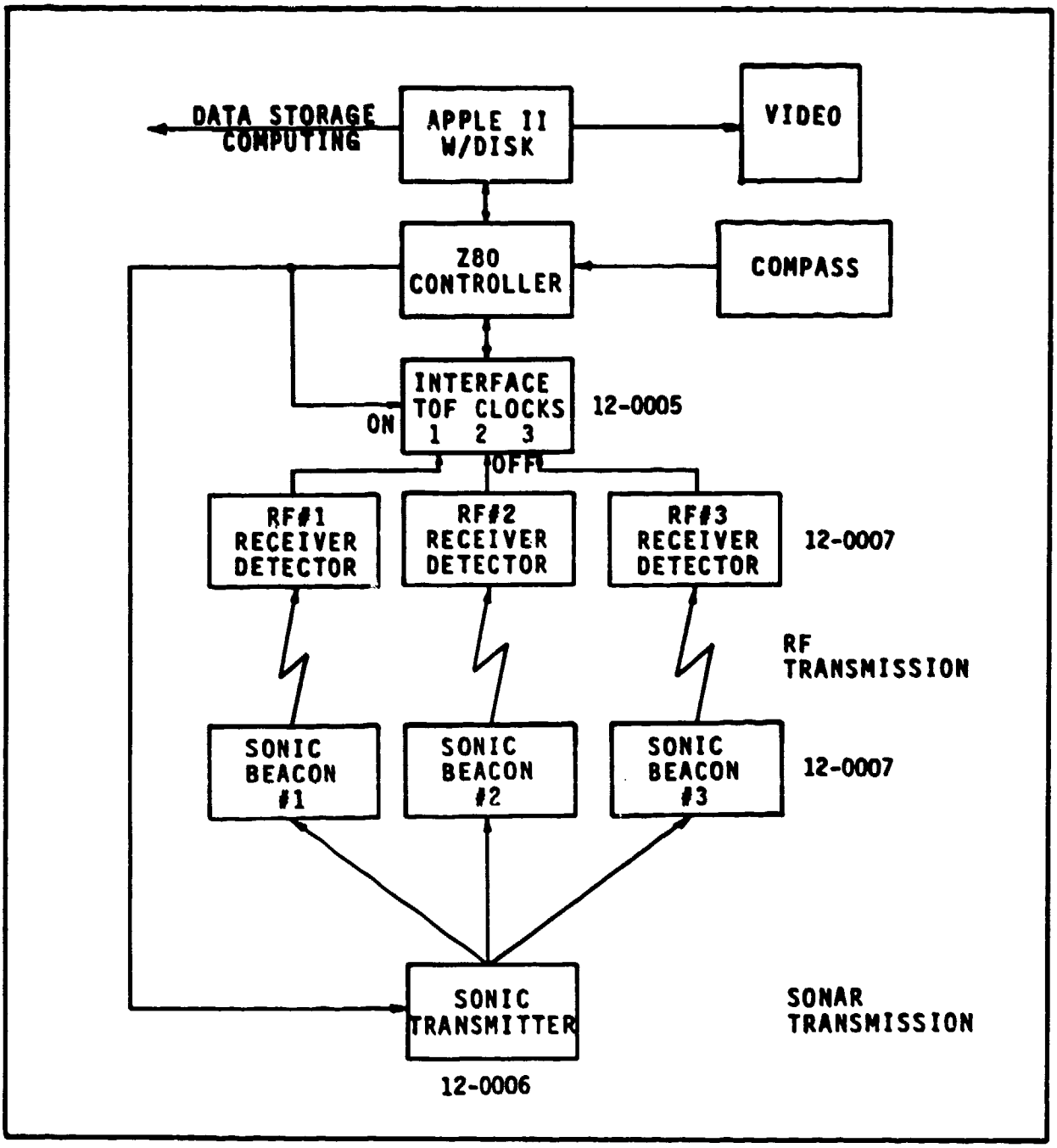

Figure 6. LOCATOR - Block Diagram
The controller initiates three time-of-flight clocks at the same time that the sonic transmitter is fired. When the sonic signal is detected at each of the beacons, that beacon sends a coded RF pulse to the controller interface, and that beacon's clock is stopped. The three clock readings are converted to distances (D=V*T), and the three distances used to triangulate the boat position.

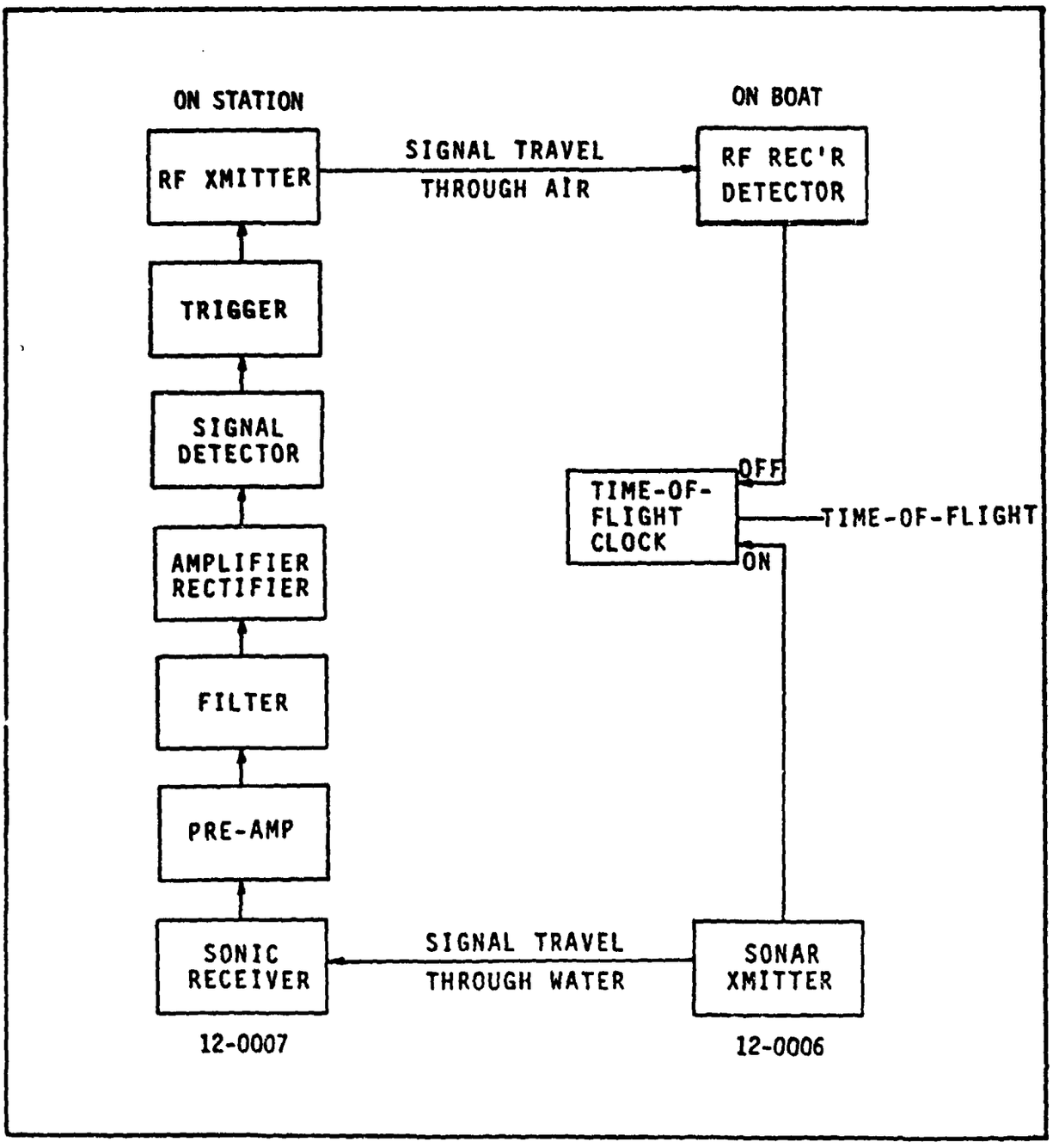

Figure 7. LOCATOR Sonic Beacon - Block Diagram
The pulse from the sonic transmitter, lowwer right, travels through water (V=4.9 ft/msec) to the beacon. The received signal is amplified, filtered and level detected. Signal detection triggers an RF signal which travels through air to the RF receiver. Each RF transmit-receive pair operates on a separate frequency. RF travel time is negligible in relation to the sonic travel time.

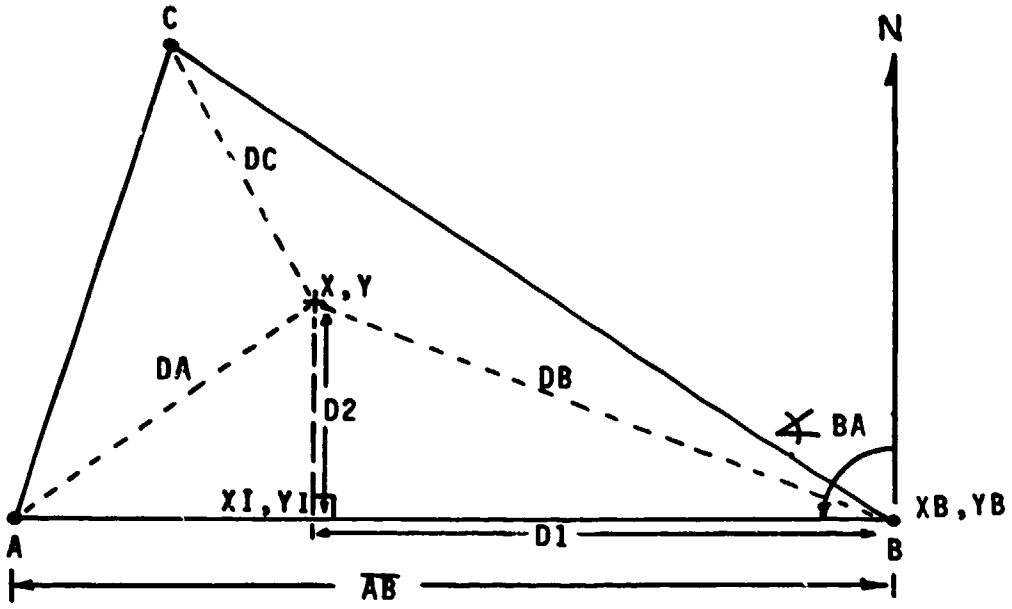

TO FIND BOAT POSITION (X,Y);
GIVEN COORDINATES OF A AND B, AND ANGLE BA:

1. $D1=(\overline{AB}^2+DB^2-DA^2)/2\overline{AB}$
2. $D2=\sqrt{DB^2-D1^2}$
3. XI= XB+(D1*SIN BA)
4. YI= YB+(D1*COS BA)
5. X = XI+(D2*COS BA)
6. Y = YI+(D2*SIN BA)

Figure 8. Calculation of Boat Coordinates
The LOCATOR computer performs this set of calculations using three pairs of distance readings: DA and DB; DB and DC; and DC and DA. The three sets of X,Y coordingates for the boat are compared and averaged to derive the final X,Y, coordinates for processing and storage.

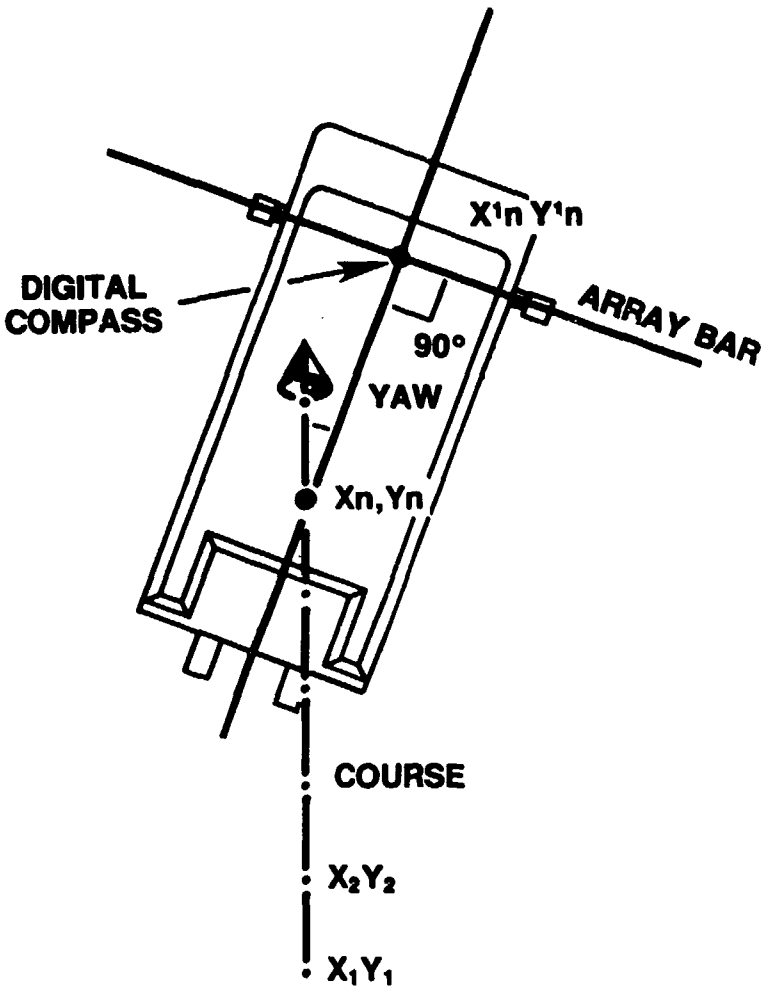

Figure 9. Course and Yaw. Course is calculated as the vector between X and Y locations, converted to magnetic bearing. Yaw is the angular difference between the course bearing and the compass reading of the array bar.

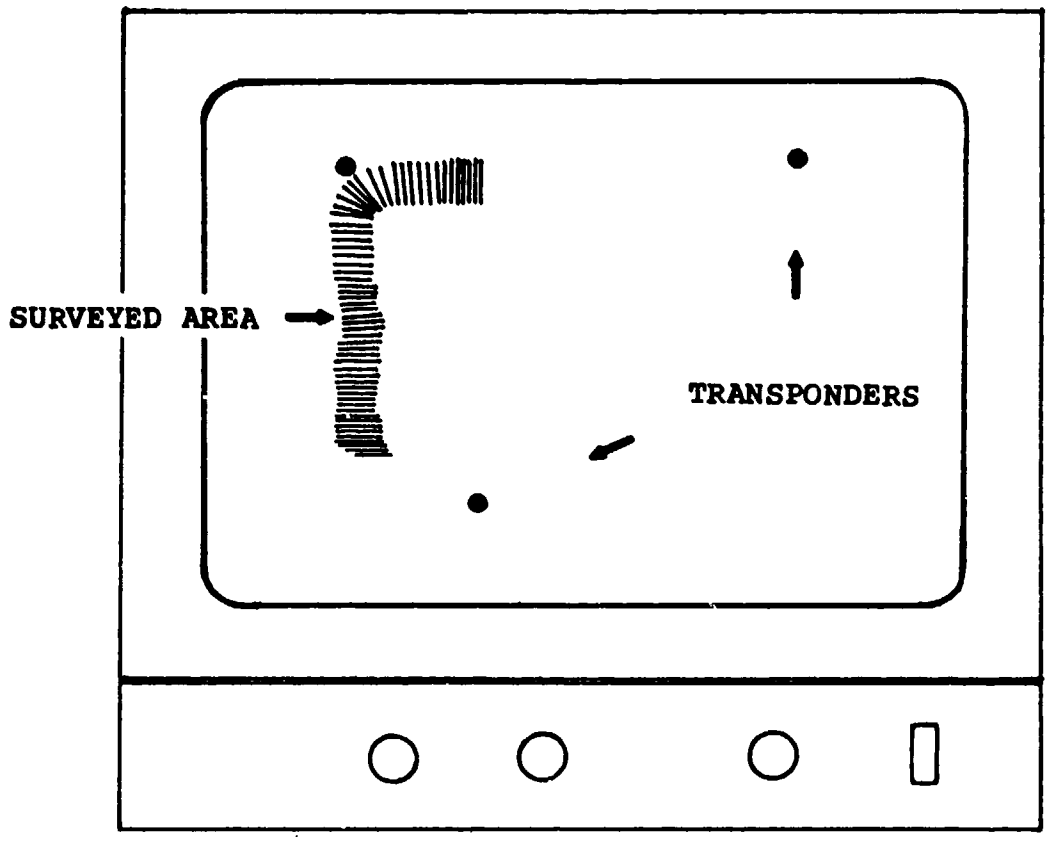

Figure 10. Position Computer Display - Survey Positions. This sketch shows the survey boat having made one traverse across the survey area, and turning to start a longitudinal traverse. For full coverage the boat would be maneuvered until the screen has been completely filled in.

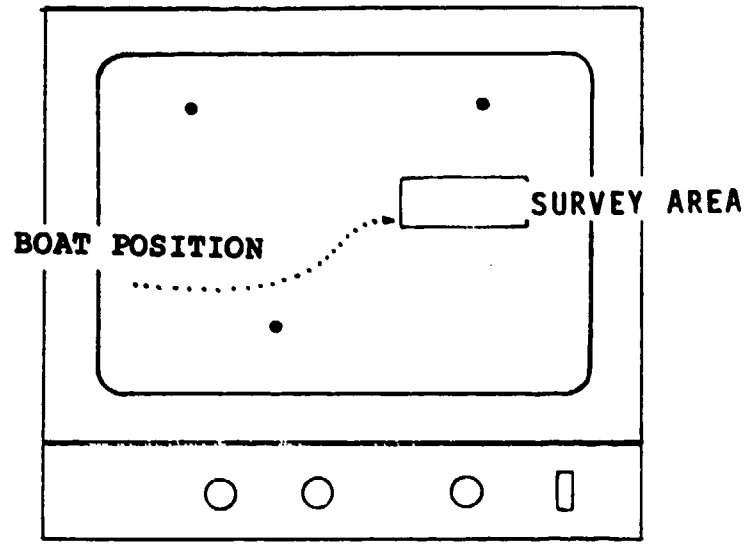

Figure 11. Steering the Boat to a Selected Target Area. The area in which subbottom profiles are to be run is outlined on the screen. Boat progress is shown as a line of points calculated by the position computer.

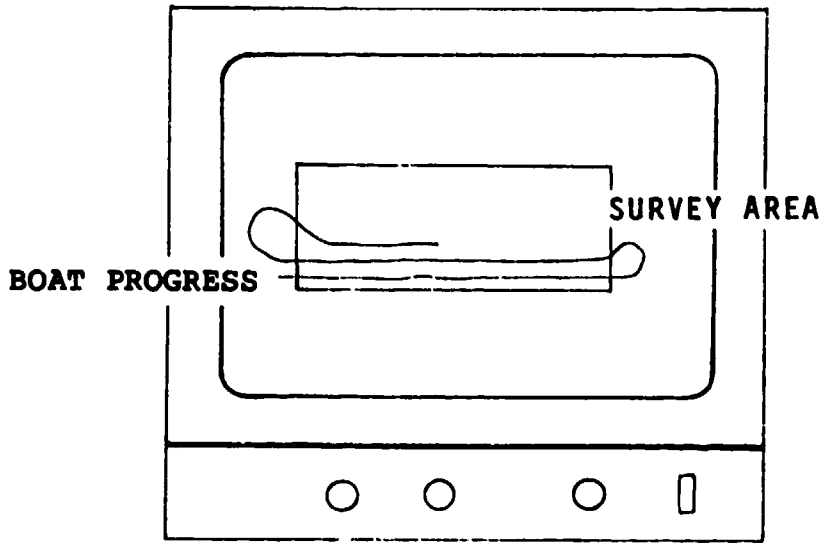

Figure 12. Traversing the Target Area. Subbottom profiles are run over the target area. The course of the boat is traced on the video display.

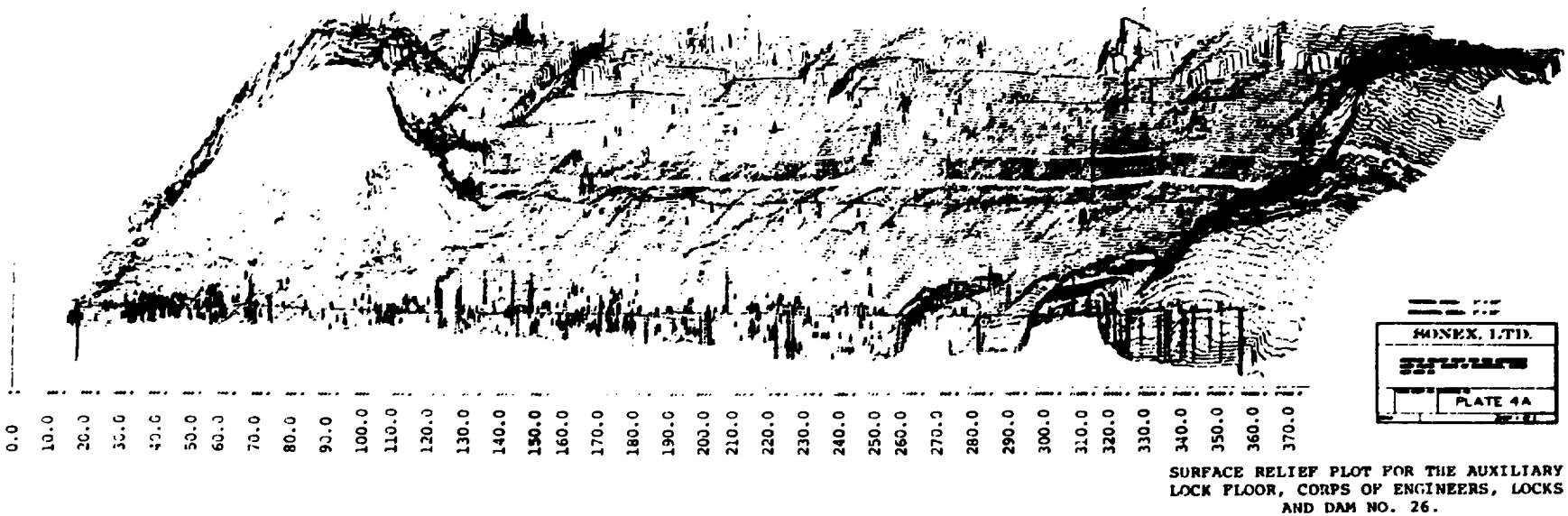

Figure 13. 3-D Bottom Plot. X, Y and Z data have been plotted to provide a easily visualized relief map of the bottom. This map is the bottom of Lock 26. Slab settling and cracking can be easily seen.

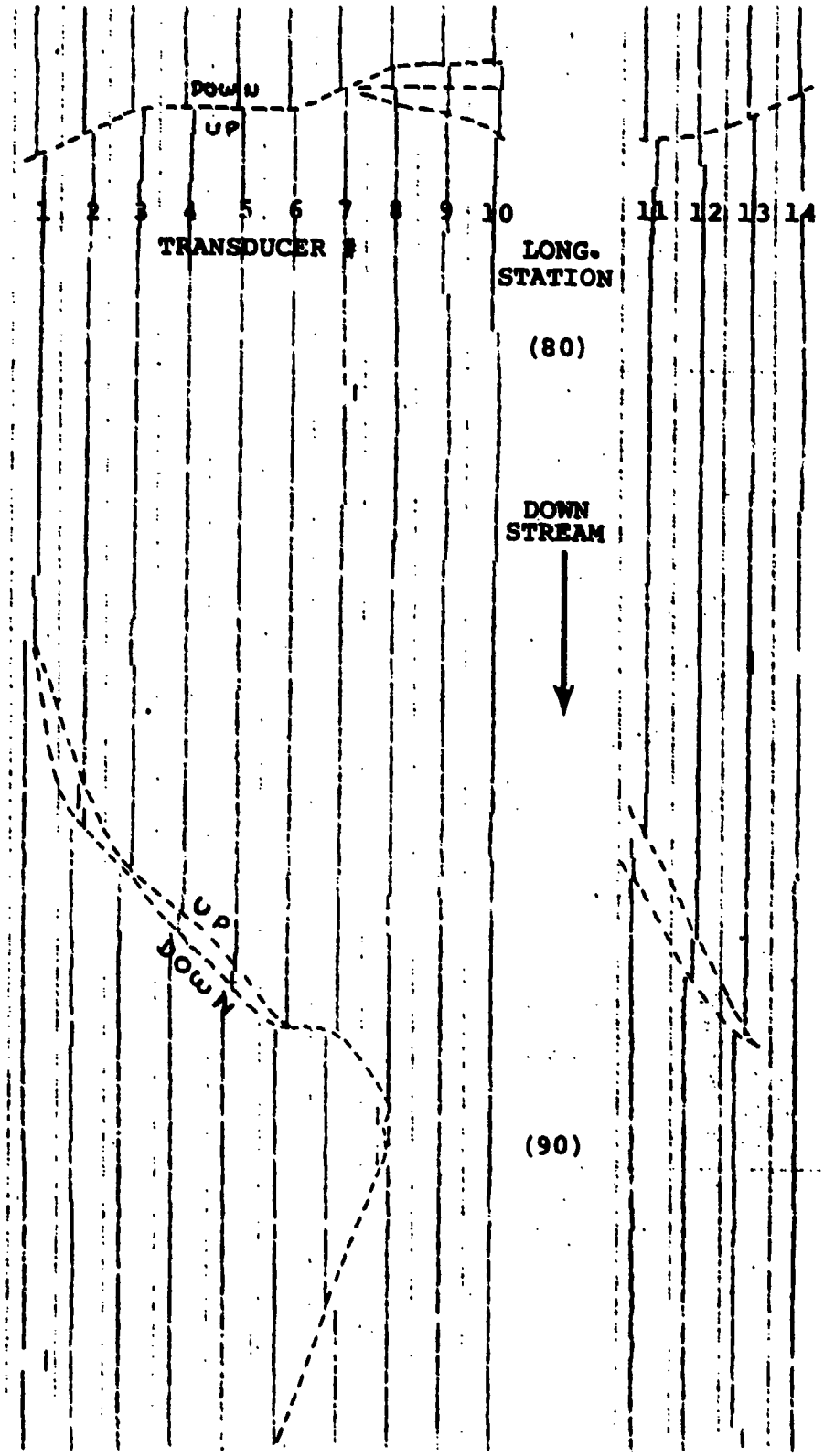

Figure 14. Real-time data display, Run 3 (File 04) in the auxiliary lock. Dashed line added to point out some major lineations.

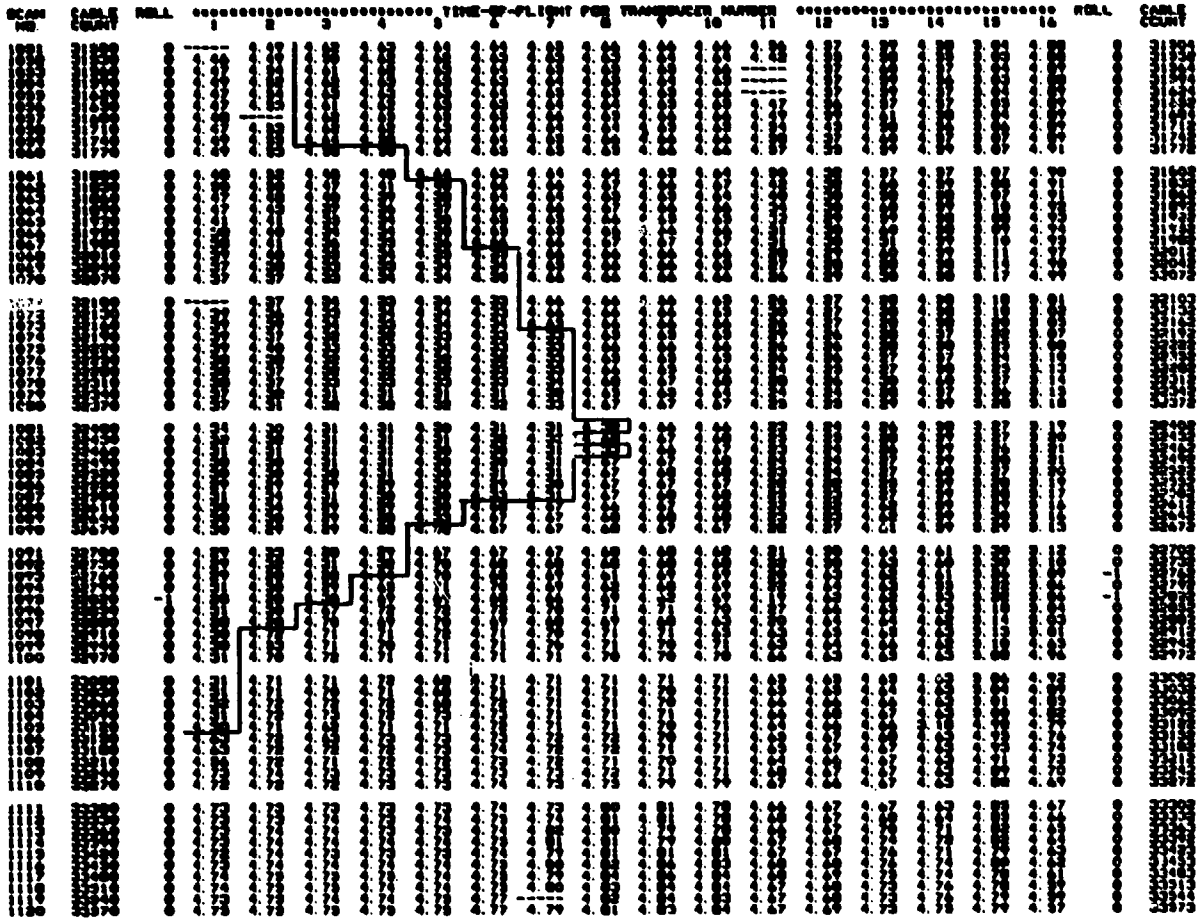

Figure 15. Typical original field data printout, a section of Run 3 corresponding to the lower half of the data display in Figure 14. Note the uplifted cracked slab.

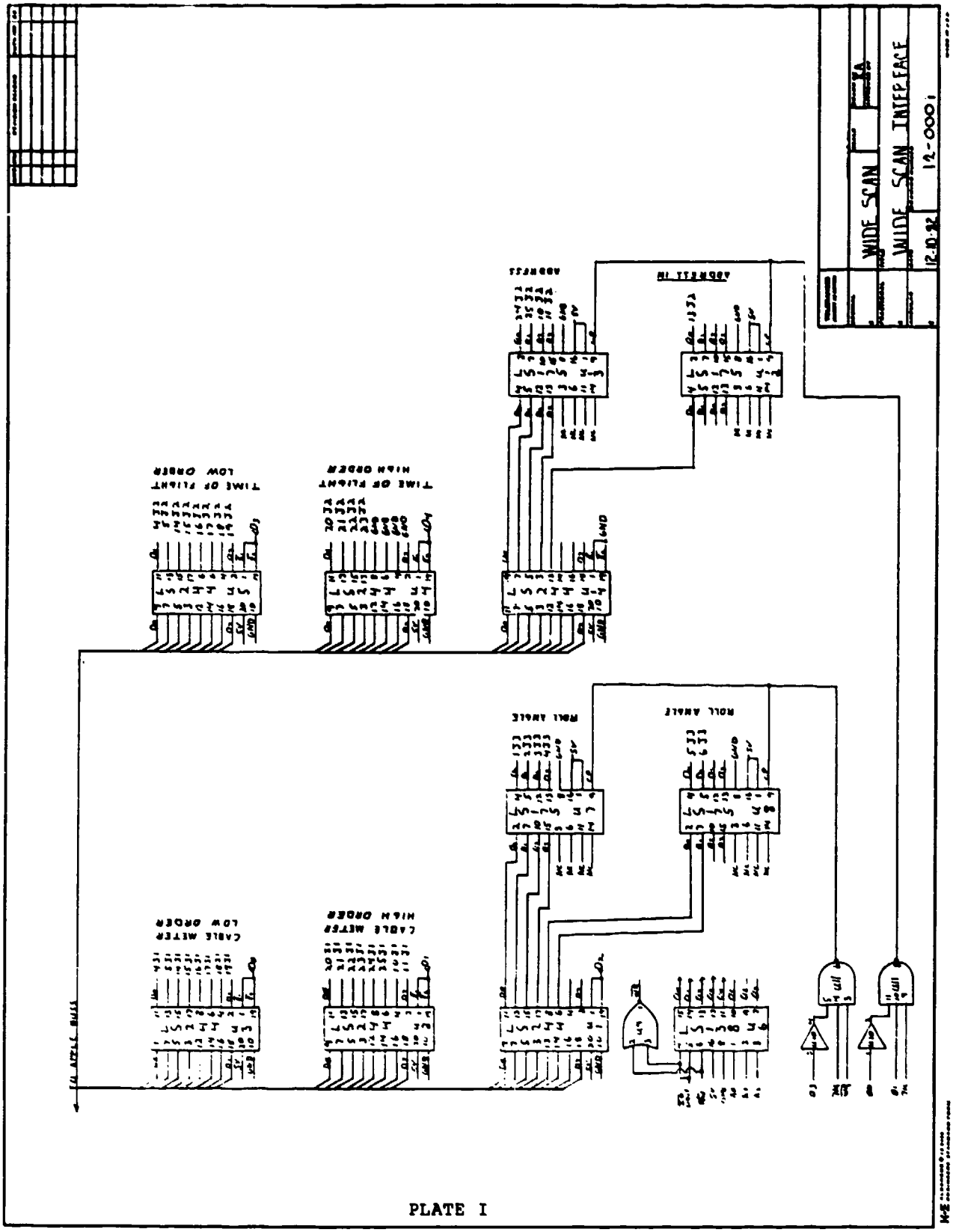
WIDE SCAN
WIDE SCAN INTERFACE
12-0000
12-0-82
XA
ROLL ANGLE
TIME OF FLIGHT
HIGH ORDER
LOW ORDER
CABLE METER
ROLL ANGLE BUS

PLATE I

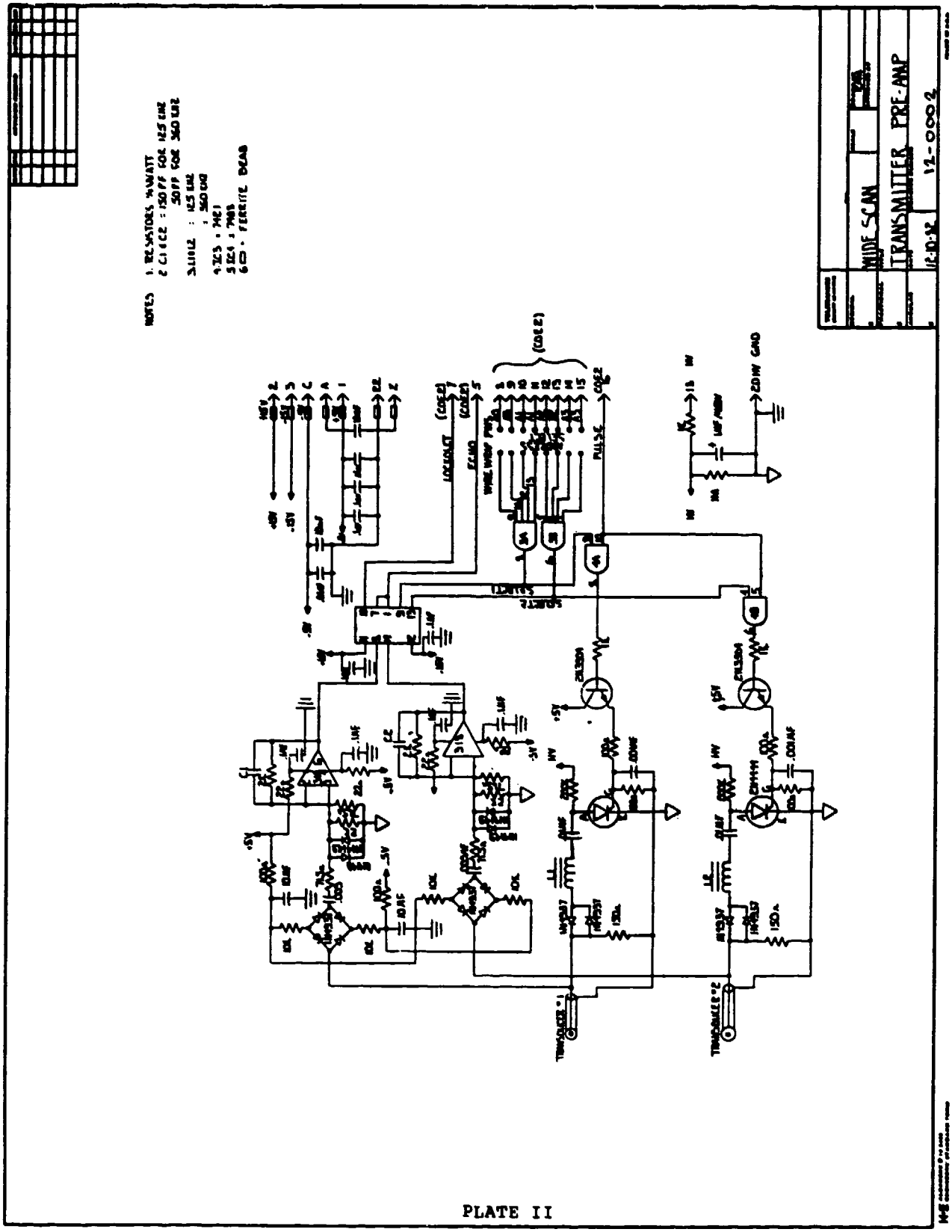

PLATE II

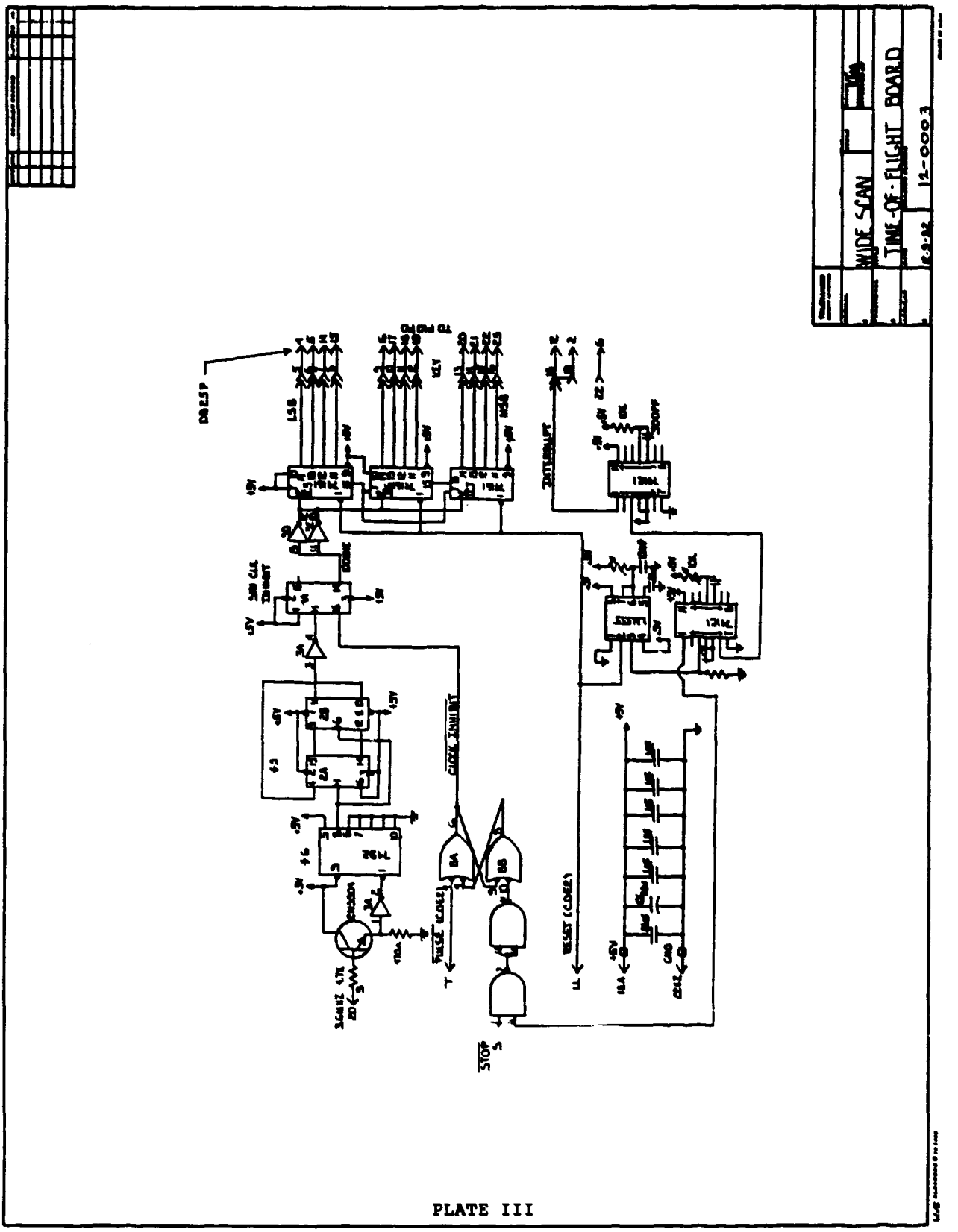

PLATE III

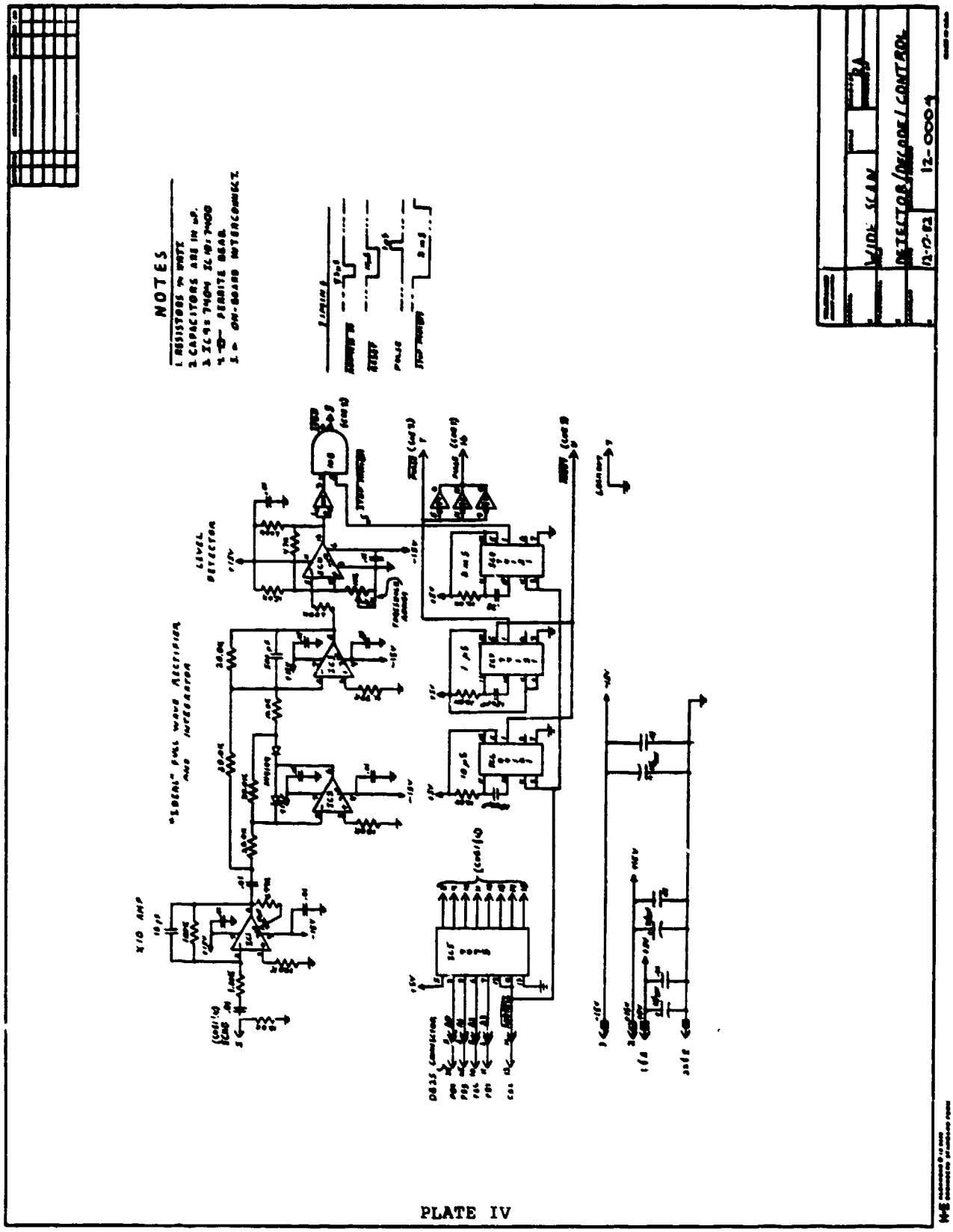

PLATE IV

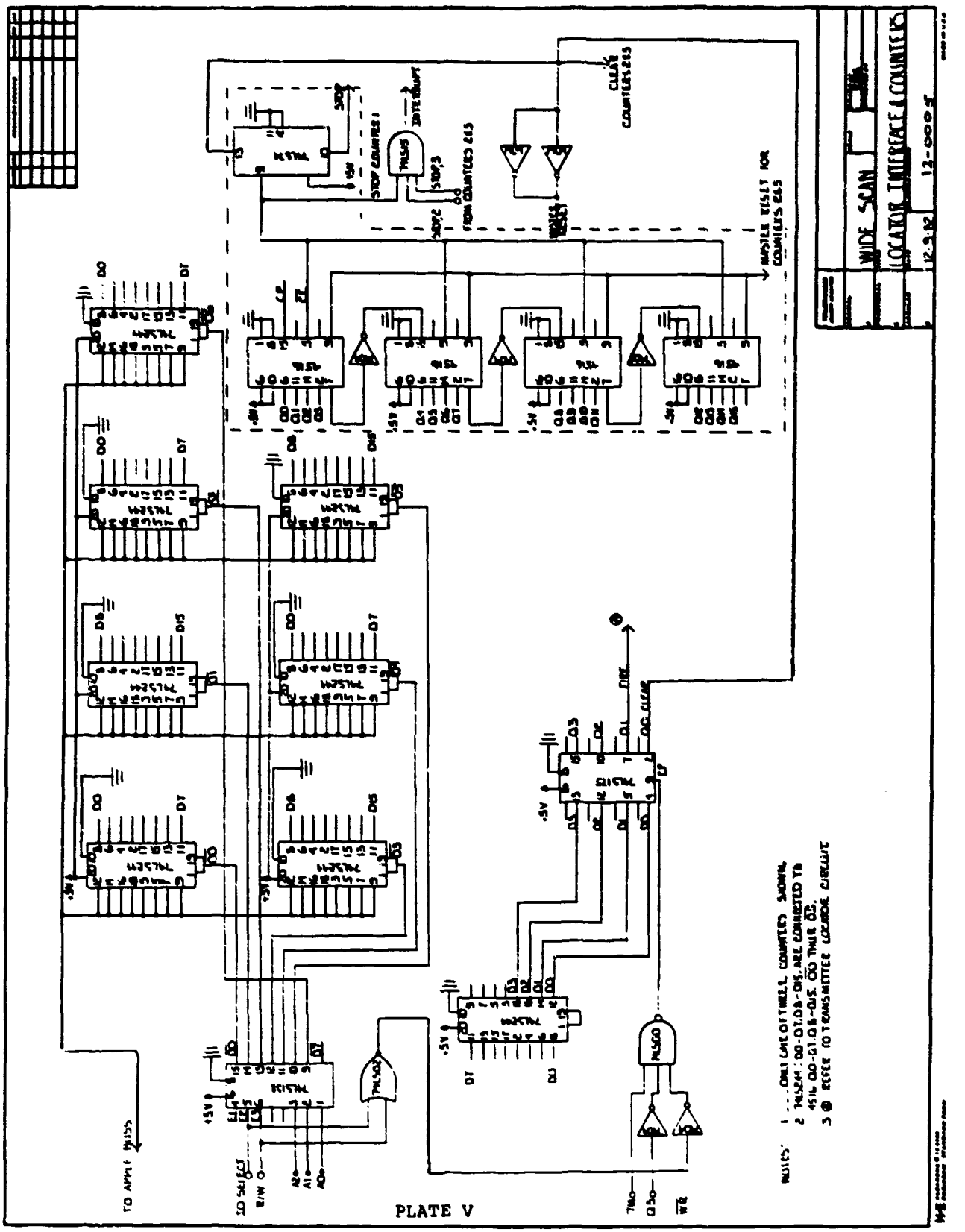
WIDE SCAN
LOCATOR INTERFACE & COUNTERS
12-9-92
12-000-5
PLATE V

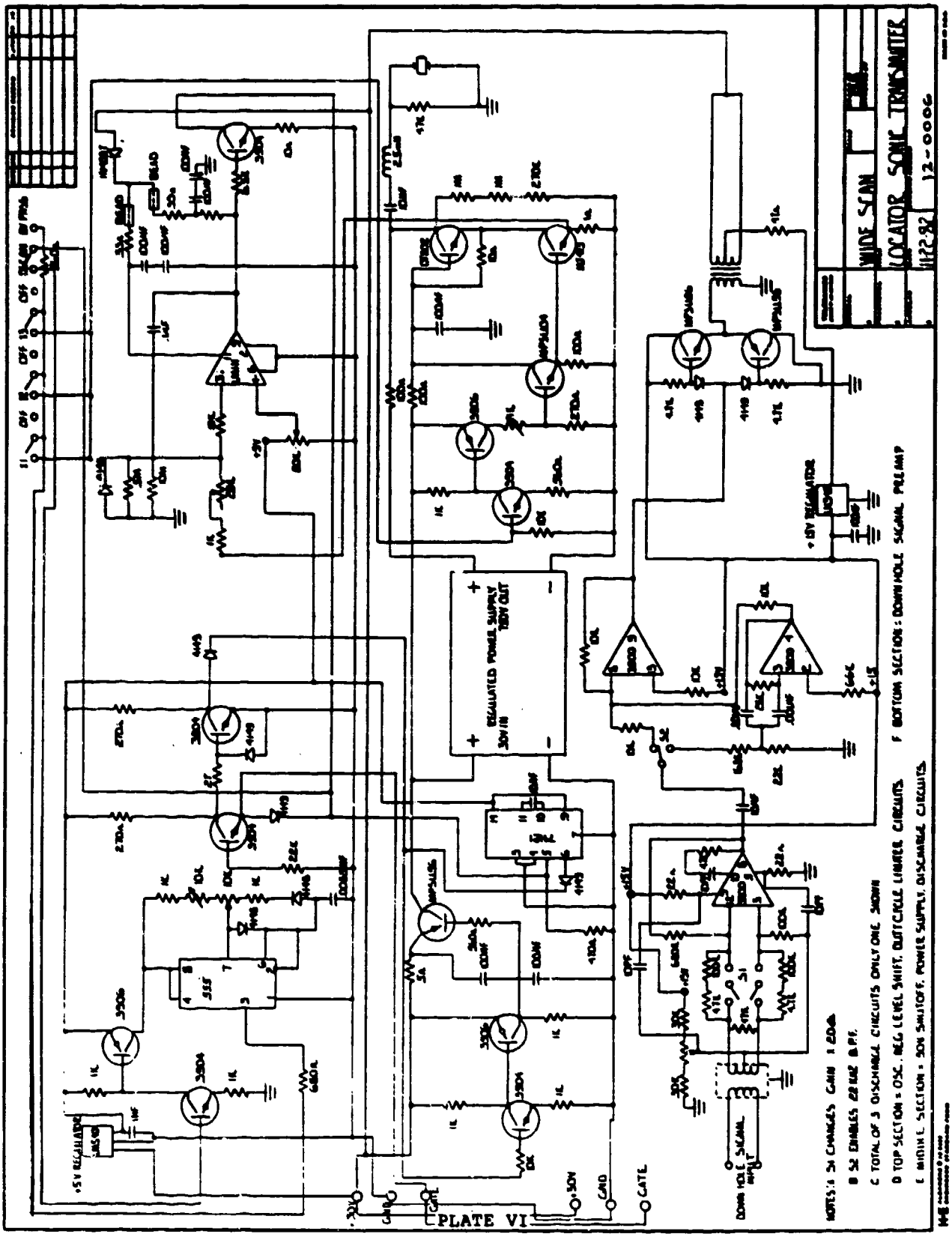
LOCATOR SONIC TRANSMITTER
WIDE SCAN
12-0006
PLATE VI

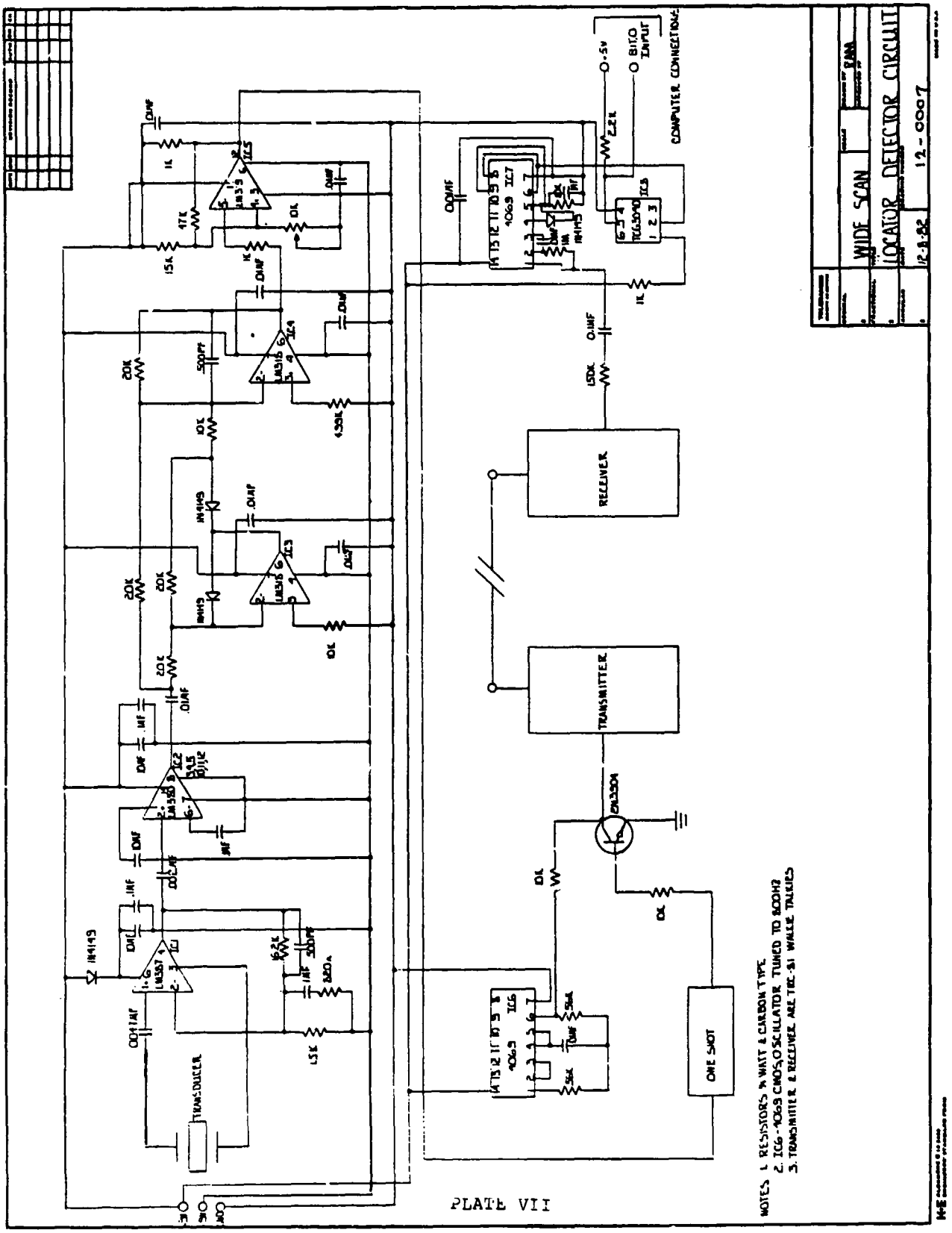
WIDE SCAN
LOCATOR DETECTOR CIRCUIT
12-9007
12-8-82
COMPUTER CONNECTIONS
0-5V
BITO INPUT
RECEIVER
TRANSMITTER
TRANSDUCER
ONE SHOT
NOTES 1. RESISTORS ¼ WATT 5% CARBON TYPE
2. IC6-4069 CMOS OSCILLATOR TUNED TO 80KHZ
3. TRANSMITTER & RECEIVER ARE TRC-81 WALKIE TALKIES

PLATE VII

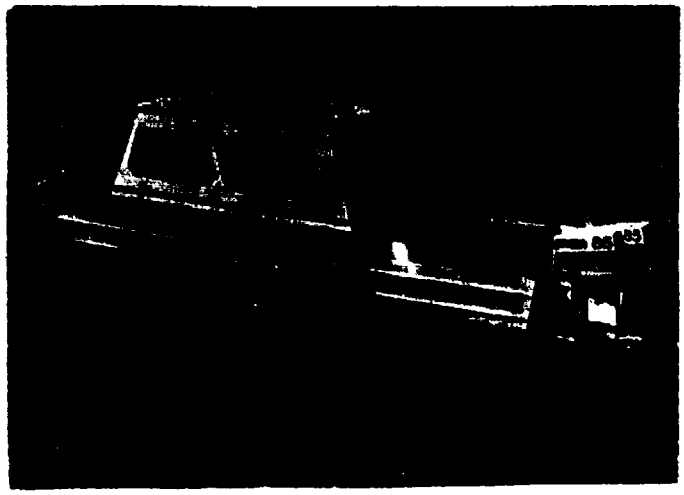

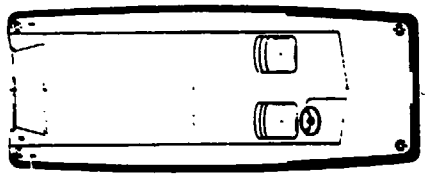

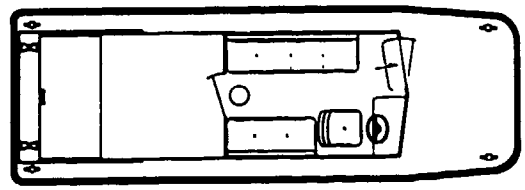

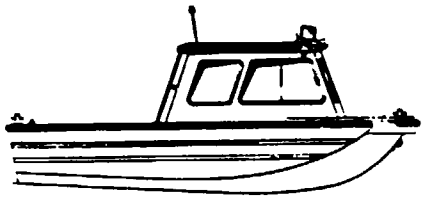

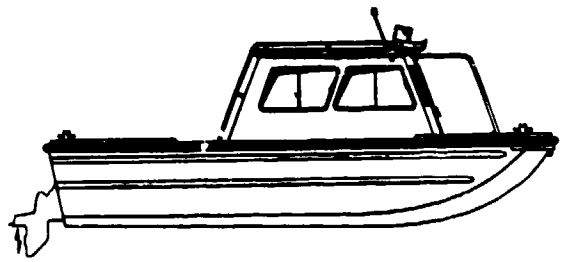

LITTLE GIANT

	21'	23'
Length Overall	20'6"	22'9"
Beam Overall	7'9"	7'9"
Depth Midship	3'2"	3'2"
Displacement	2,000 lbs.	2,400 lbs.
Draft (Hull)	1'1"	1'3"
Load Capacity	2,800 lbs.	3,400 lbs.
Standard Power	Outboard	Outboard
Cabin Dimensions		
Length	8'4"	8'4"
Width	5'4"	5'4"
Height	5'0"	5'0"

	2308-C
Length Overall	22'10"
Beam Overall	8'0"
Depth Midship	3'8"
Displacement	4,300 lbs.
Draft (Hull)	1'3"
Load Capacity	4,000 lbs.
Standard Power	Inboard/Outboard
Cabin Dimensions	
Length	8'6"
Width	5'8"
Height	6'0"